Functional characterisation of the Sterile 20 like kinase Slik in tracheal morphogenesis in *Drosophila melanogaster*

Inaugural-Dissertation

zur

Erlangung des Doktorgrades
der Mathematisch-Naturwissenschaftlichen Fakultät

der Universität zu Köln

vorgelegt von

Fiona Paul Ukken

aus Cochin, Indien

Köln, Februar 2011

1. Berichterstatter: Prof. Dr. Maria Leptin

2. Berichterstatter: Prof. Dr. Siegfried Roth

Tag der mündlichen Prüfung: 3 Februar, 2011

1. INTRODUCTION

1.1 Tubular organs - an overview

Tubular structures are a recurring anatomic feature in all multicellular life forms. The branched and hierarchal nature of tubes is common among several organs in the vertebrates. Among higher vertebrates, organs with tubular composition include the vascular, pulmonary, digestive and excretory systems, as well as the secretory organs such as the mammary, pancreatic and salivary glands. The *Drosophila melanogaster* tracheal system, the equivalent of the vertebrate lung is a prototypical model for studying molecular mechanisms governing tubular network development owing to the relatively simple structure of the respiratory system.

1.2 Tracheal morphogenesis in *Drosophila*

Tracheal branches are monolayer epithelial cells wrapped into tubes surrounding a central lumen through which gases flow (CASANOVA 2007). The tracheal system is bilaterally symmetric and segmentally repeated in its organisation, which reflects its developmental origin. The tracheal system comprises of three kinds of branches; the primary, secondary and the tertiary (terminal) branches, each established according to the sequence of migration and tube formation. During embryonic development (5hr After Egg Lay), 10 bilaterally symmetrical ectodermal cell clusters consisting of ~ 80 cells invaginate into an epithelial sac called the tracheal placode. The tracheal placode develops into interconnected tubes through a series of events including cell migration, intercalation and fusion (Fig.1). Over the course of the next few hours, six primary tracheal branches migrate out from each tracheal placode at stage 12 (Fig.1b, e). The branches bud out with a pair of leading cells followed by a small number of cells that organise into a tube during the migration process. At stage 15, the primary branches are ensued by the two-dozen secondary branches (Fig.1d, e). During further stages of development, the secondary branches sprout terminal branches. Much of the development of terminal cells takes place during larval phases in response to physiological oxygen demands.
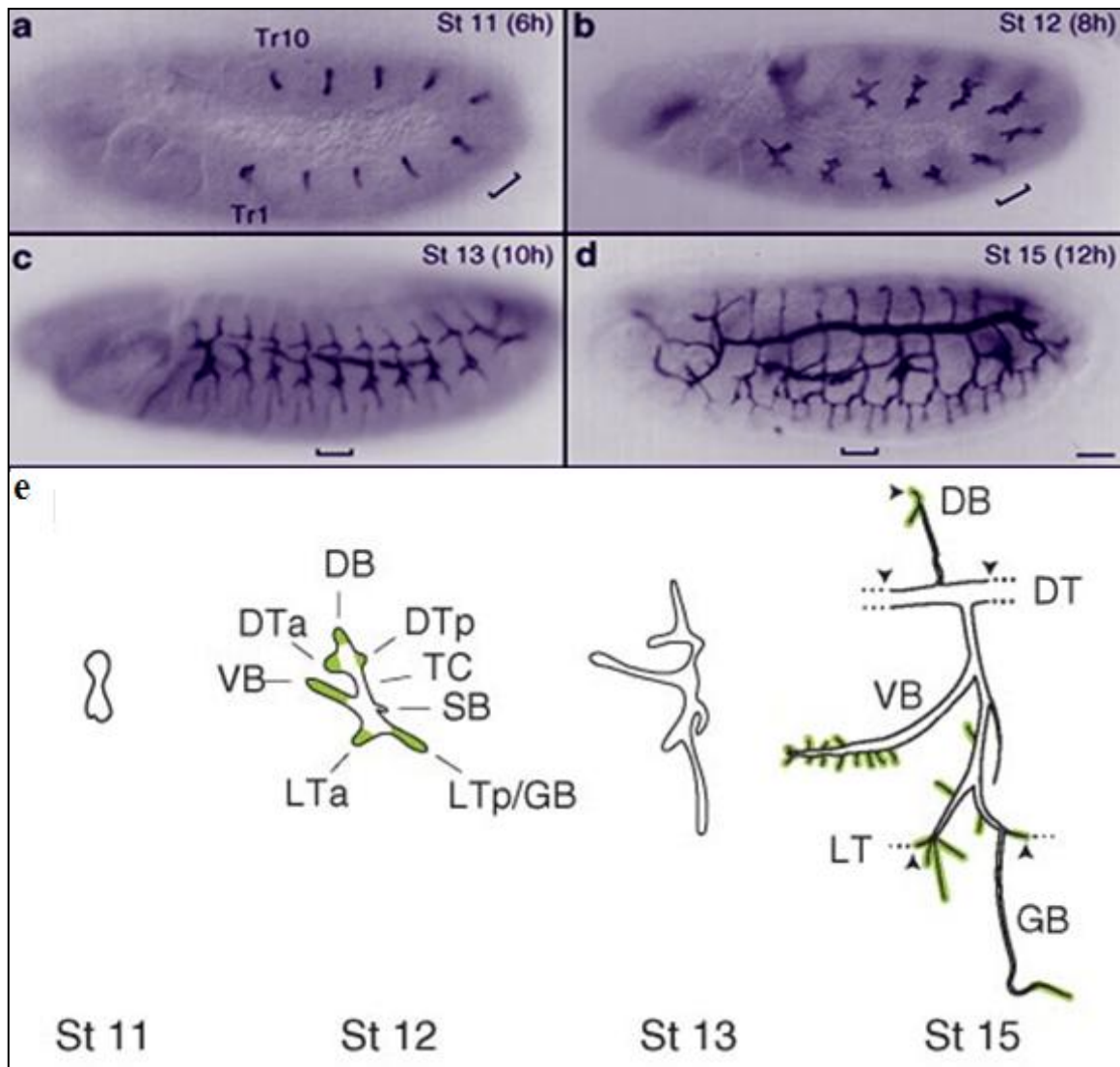
Figure 1: Stages of embryonic tracheal development in *Drosophila melanogaster*
The Drosophila tracheal system develops by sequential branching from a tracheal sac in each hemisegment. **(a–d)** Embryonic tracheal development visualised by immunostaining of the tracheal lumen. Embryo stage and age (in hours) are indicated. The first (Tr1) and the tenth (Tr10) tracheal hemisegments are indicated in (a). Brackets indicate position of fifth tracheal hemisegment (Tr5). Lateral views, anterior left, dorsal up. **(e)** Development of Tr5. The spiracular branch (SB), transverse connective (TC) and the six primary branches (DB, dorsal branch; DTa and DTp, anterior and posterior dorsal trunk; VB, visceral branch; LTa, anterior lateral trunk; LTp/GB, posterior lateral trunk/ganglionic branch) are indicated. Primary branches at stage 12 and secondary branches at stage 15 are highlighted green. Most secondary branches ramify to form terminal branches in the larval period (not shown). The branches that cease branching and fuse with branches in neighbouring hemisegments are indicated (arrowheads).Adapted from (GHABRIAL *et al.* 2003).

Branching morphogenesis of the trachea involves the Fibroblast Growth Factor (FGF) signalling pathway that is used repeatedly to control branch budding and outgrowth (GHABRIAL *et al.* 2003; METZGER 1999; SATO 2002; SKAER 1997). *branchless* (*bnl*) (SUTHERLAND *et al.* 1996), and *breathless* (*btl*) *(KLÄMBT et al. 1992)* encode the *Drosophila* homologues of the mammalian FGF and the FGF receptor and are critical for the induction

and maintenance of the tracheal system (Fig.2a). Although the Bnl/Btl signalling provides the cues for development, a different tubulogenesis mechanism is used at each level of branching concurrent with stages of development (Fig.2b).
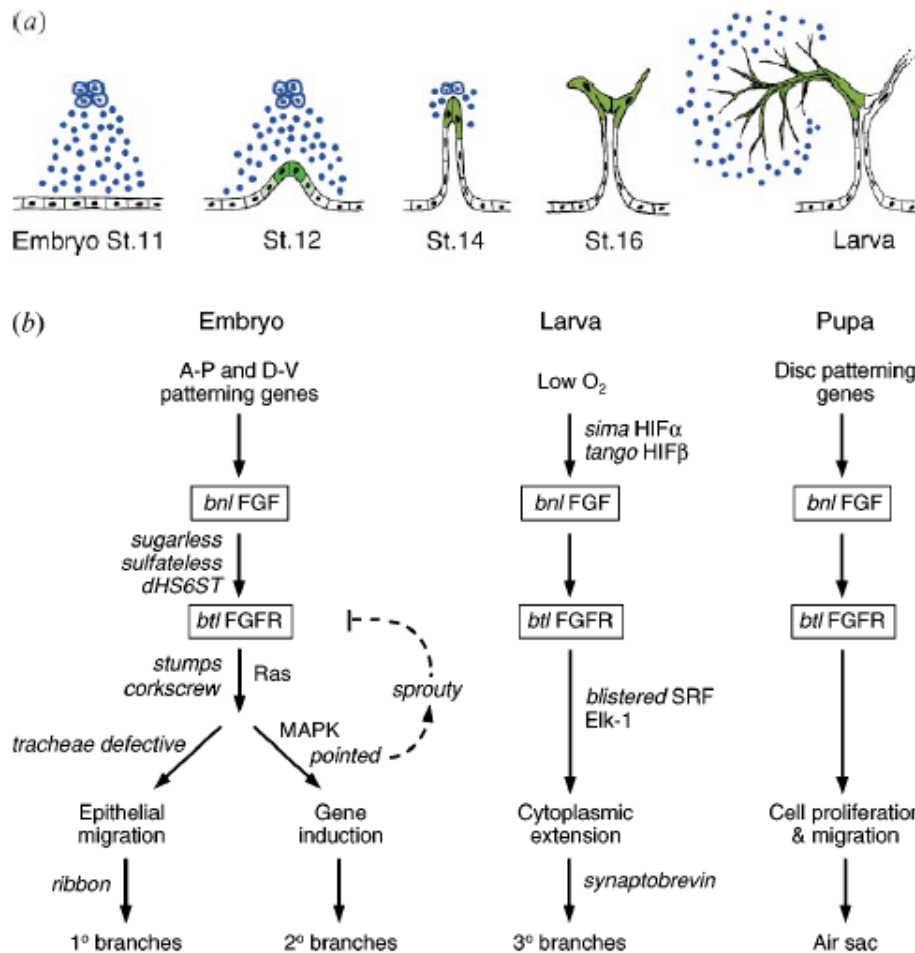
Figure 2: The Branchless FGF pathway controls each step of branching.
(a) *branchless/* FGF (*blue*) is expressed in clusters of cells surrounding the developing tracheal system, at each position where a primary branch will bud. The secreted growth factor activates the Breathless FGFR on nearby tracheal cells (*black*), and acts as a chemoattractant that guides outgrowth of primary branches. It also induces expression of secondary branch genes and triggers secondary branch sprouting at the ends of outgrowing primary branches (*green*; stages 12–16). *branchless* turns back on again, but in a completely different pattern, during larval life to control outgrowth of terminal branches. The gene is expressed yet again during pupal life where it controls budding of adult air sacs (not shown). **(b)** The genes that function upstream of Branchless and downstream of Breathless change during development, giving rise to different patterns and structures of branches at each step. Adapted from (GHABRIAL *et al.* 2003)

Further, different branches within each metamere have a fixed number of cells (SAMAKOVLIS *et al.* 1996) with each branch featuring characteristic tube dimensions (BEITEL and KRASNOW 2000). Primary branches are composed of multicellular tubes with two to five wedge-shaped

cells surrounding a lumen and interconnected by intracellular junctions (Fig.3a). In secondary branches, tubes are made up of interconnected cells lying in a single row that form a tube by folding over itself along the long axis and sealing via an autocellular junction (Fig.3b). However, unlike primary and secondary branches terminal cells form a junctionless and therefore "seamless" lumen (Fig.3c). Also present within the tracheal system are pairs of doughnut-shaped cells (fusion cells) that are derived from primary branches. Two fusion cells extending from the primary branches of each metamere connect to form a fusion anastomosis to give rise to a continuous network. The tube formed by fusion cells is as a result seamless and without intracellular junction (Fig.4). The developmental design of the primary and secondary branch formation is highly stereotyped and pre-programmed unlike branch formation in terminal cells, where branching is highly variable and regulated by oxygen demand.
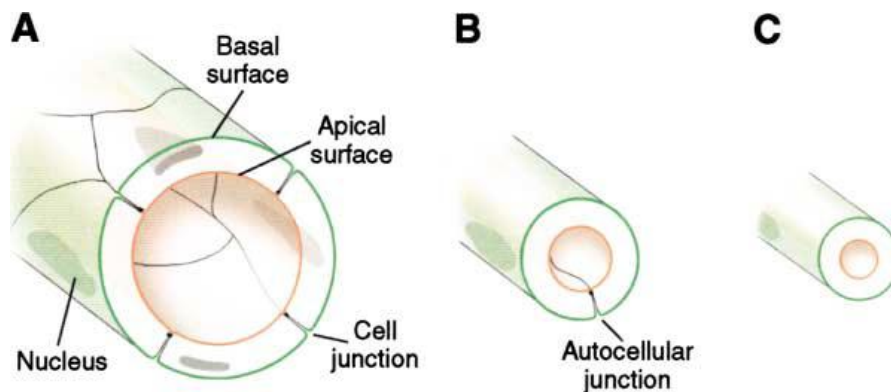
Figure 3: Types of simple epithelial tubes that constitute the *Drosophila* tracheal system
Tube walls are formed by polarised epithelial cells with their apical membrane surface (red) facing inward toward the lumen space and their basal surface (green) exposed to the extracellular matrix. **(a)** A multicellular tube with four curved cells in a cross-sectionof the tube; **(b)** A unicellular tube formed by a single cell, rolled up to enclose the lumen, and sealed with an autocellular junction; **(c)** A unicellular tube with the lumen in the cytoplasm of the cell. There is no autocellular junction; the tube is "seamless."Adapted from (LUBARSKY and KRASNOW 2003).
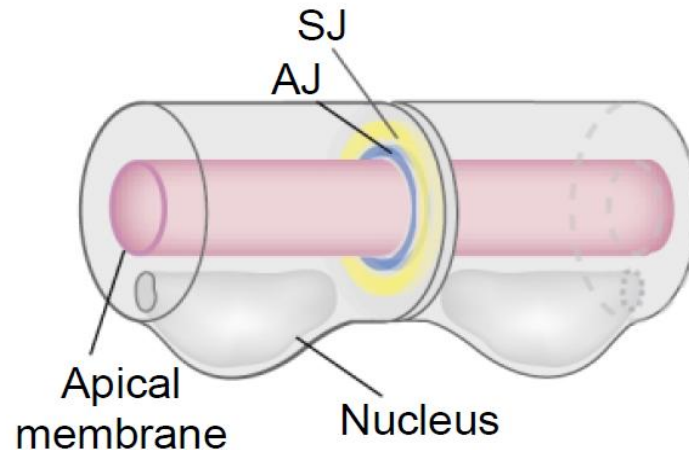
Figure 4: Schematic representation of fusion anastomosis
Fusion branches (anastomoses) connect the individual metameres and are made by two cells that, before fusion, are positioned at the tips of the two branches that will fuse. Each fusion cell is doughnut shaped with no autocellular junctions and forms intercellular junctions with its fusion partner and with the following cell in the primary branch Adapted from (Uv *et al.* 2003).

1.3 Terminal cell and branch development

Cells that do not participate in the formation of secondary branches are specified to become terminal cells. Though the specification to become terminal cells occurs in embryonic stages much of the development takes place during larval phases. Terminal cells are outposts of the tracheal system responsible for oxygen delivery to target tissues. Terminal branches originate as cytoplasmic protrusions that develop a lumen intracellularly (Fig.5). Branching morphogenesis in terminal cells is a reiterative process that occurs during the five days of larval development, involving rounds of cytoplasmic extension, followed by lumen formation to create a ramified network that contacts cells of the target tissue (KEISTER 1948). Oxygen carried through the terminal branches is made available at target tissues through diffusion that is facilitated by the close contact between the plasma membrane of the tissue and the blind-end of the terminal branch (MANNING 1993).

The terminal branches consist of a lumen whose diameter, decreases progressively along with the branch diameter with increasing distance from the nucleus. The average lumen diameter of a terminal is less than 1 μm (GUILLEMIN *et al.* 1996; LUBARSKY and KRASNOW 2003; WIGGLESWORTH 1954). Terminal cells also show apical-basal polarity, with the outer membrane being the basal membrane, and the membrane facing the lumen being apical which

shows enrichment of the apical polarity complex Par6/aPKC/Baz along with Crumbs (Jayan N. Nair, PhD thesis) (GERVAIS and CASANOVA 2010). Terminal cells on an average have 20 branches and the branching points are regularly spaced and do not cross over one another. The terminal cell arborisation may span distances over 100 μm. Unlike earlier stages of tracheal branching, terminal cell branching is not stereotyped but governed by oxygen physiology in tissues, resulting in terminal cells with varied branching patterns.
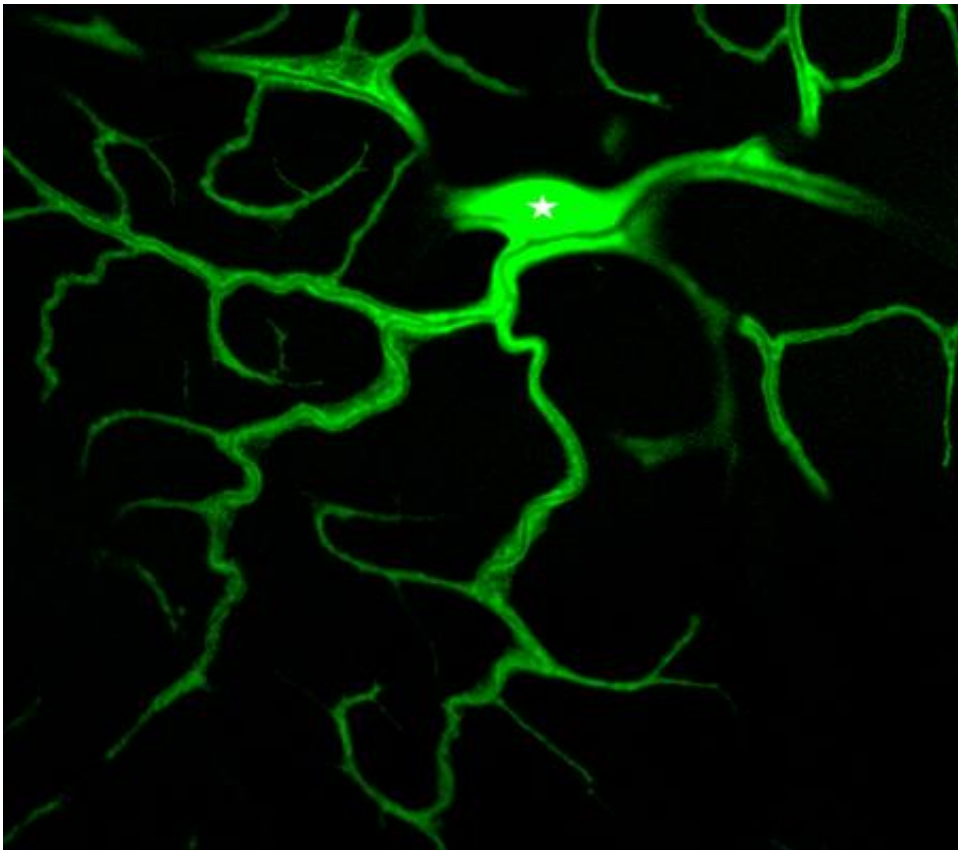
Figure 5: A terminal cells from a third instar larval trachea
The terminal cell is visualised by trachea specific expression of cytoplasmic GFP using *btl*Gal4. The terminal cell extends long processes toward target tissues, called the terminal branches. Each terminal branch bears a lumen within through which air is transported to be supplied to tissues. The terminal cell nucleus is marked with a star (Jayan N. Nair PhD thesis).

The process of lumen formation within the terminal branches is not quite well understood. Early work in *Drosophila* showed the presence of cytoplasmic vesicles in the terminal branches distal from the nucleus (Fig.6a) (SHAFIQ 1963). It is believed that these vesicles fuse to form a larger vesicular body that would coalesce with the already existing tracheal lumen. This is supported by the presence of Crumbs-positive vesicles at the distal regions of terminal branches that did not yet possess a lumen (Fig.6b) (Jayan N. Nair PhD thesis). Moreover,

these Crumbs-positive vesicles appear to line up parallel to each other as if forming a lumen. Further, work on angiogenesis using cell lines have shown that vacuoles are generated prior to lumen formation and a lumen is formed when these vesicles fuse together (FOLKMAN and HAUDENSCHILD 1980).
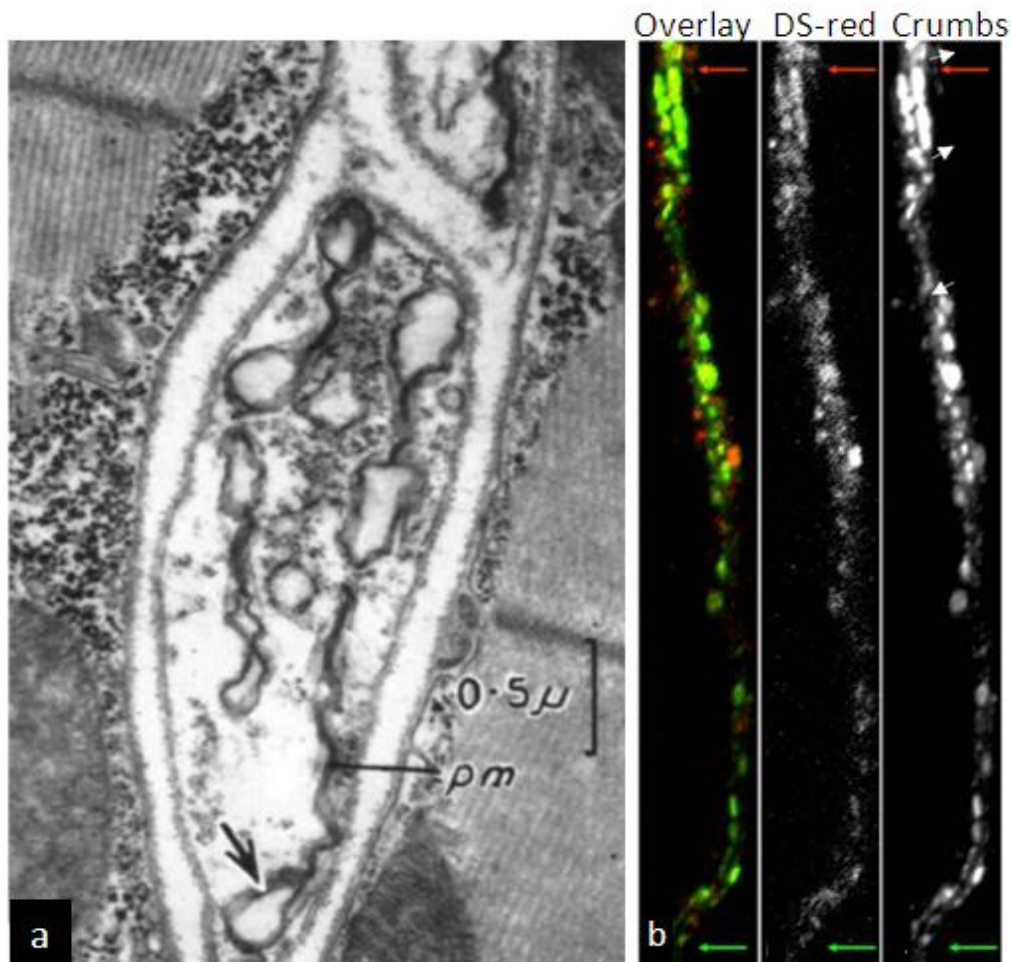
Figure 6: Growing ends of the tracheoles show multi-vesicular structures
(**a**) Electron micrograph of the tip of a developing tracheal branch. Arrows mark vesicular structures within the distil region of the tracheoles. (**b**) Crumbs-GFP localisation in vesicles at distal regions of a terminal branch where the lumen is beginning to develop. The branch is marked with DsRed expressed using *btl*Gal4. The red and green arrows mark the proximal (to the nucleus) and distal ends of the branch, respectively. Adapted from (a) (SHAFIQ 1963) and (b) Jayan N. Nair (PhD thesis).

However, contrary to the idea of *de novo* tube formation through vesicular fusion, lumen formation has also been described to occur in a proximal to distal manner. Work in embryonic tracheal system showed that lumen in terminal cells formed by the growth of a new membrane into the cell from the surface contacting the adjacent cell. The membrane formed was the apical membrane as seen from the accretion of apical polarity complexes, aPKC/Par6/Baz and Crb/DPatj complexes (GERVAIS and CASANOVA 2010). Perhaps lumen

formation is a combination of both mechanisms, where lumen formation in early stages of tracheal development is predominantly from extensions from previously existing membranes and then during later stages incorporating *de novo* tube formation in order to hasten the process of tube formation in response to local oxygen demand.

1.4 Factors influencing terminal branch development

Tracheation is modulated by oxygen availabilty in tissues. Both hypoxia and hyperoxia are known to influence tracheal branching (JARECKI *et al.* 1999; WIGGLESWORTH 1954). Under conditions of low oxygen, terminal branch formation is induced, whereas in hyperoxia terminal branch formation is supressed. The *Drosophila* counterparts of the mammalian hypoxia-inducible factor (HIF), Similar (*Sima*) and Tango (*Tgo*) which function as HIF-α and HIF-β homologues, activate the hypoxia induced signalling pathway (LAVISTA-LLANOS *et al.* 2002). Oxygen starved tissues produce a trachaetion signal which induces tracheal branching in regions depreived of oxygen (WIGGLESWORTH 1954). This tracheogenic signal was later identified as branchless (*bnl*). Bnl is a potent inducer and chemoattractant of terminal branches that results in proliferation of terminal branches (JARECKI *et al.* 1999). Btl signalling through FGFR induces terminal branching (REICHMAN-FRIED and SHILO 1995) and also the expression of the downstream targets important to terminal cell development, such as *srf/blistered/pruned/* (*srf/bs*). *srf* encodes the *Drosophila* homologue of the mammalian *serum response factor* and is specifically expressed in terminal cells. Mutants of *srf* fail to develop cytoplasmic outgrowths that later form terminal branches, thus severely affecting branching morphogenesis (AFFOLTER 1994; GUILLEMIN *et al.* 1996). Srf recruits the co-factor Elk-1(a Ternary Complex Factor, TCF) to the serum response elements (SRE) to form the ternary complex. FGF signalling activates MAPK pathway, activation of the MAPK pathway results in phosphorylation of TCFs which leads to activation of the SRE in response to growth factor signalling (MARAIS *et al.* 1993; TREISMAN 1994). Concordant with this observation, expression of the activated forms of Srf and Elk-1 resulted in overgrowth of cytoplasmic extensions and terminal branches.

Screens to identify genes that affect terminal branching have revealed a few genes involved in maintaining normal branching and terminal cell development. (BAER *et al.* 2007; LEVI *et*

al. 2006). Mutants of potential cytoskeletal regulators such as *Drosophila* talin (*rhea*), the β-integrin *myospheroid* (*βmys*) as well as double mutants of the α-integrins *inflated* (*if*) and multiple edematous wings *(mew)* have been shown to affect maintenance of tracheal tubes within terminal branches (Fig.7). Mutations in *ikkε* also affected tube formation within terminal cells (OSHIMA *et al.* 2006). The authors speculate that these genes contribute to tube stability by regulating the actin cytoskeleton. Further, work from our lab has shown the importance of *moesin* (*moe*) in terminal cell development (Jayan N. Nair PhD thesis). Much work remains to be done in order to understand the mechanisms behind tube formation and tube stability in terminal cells.
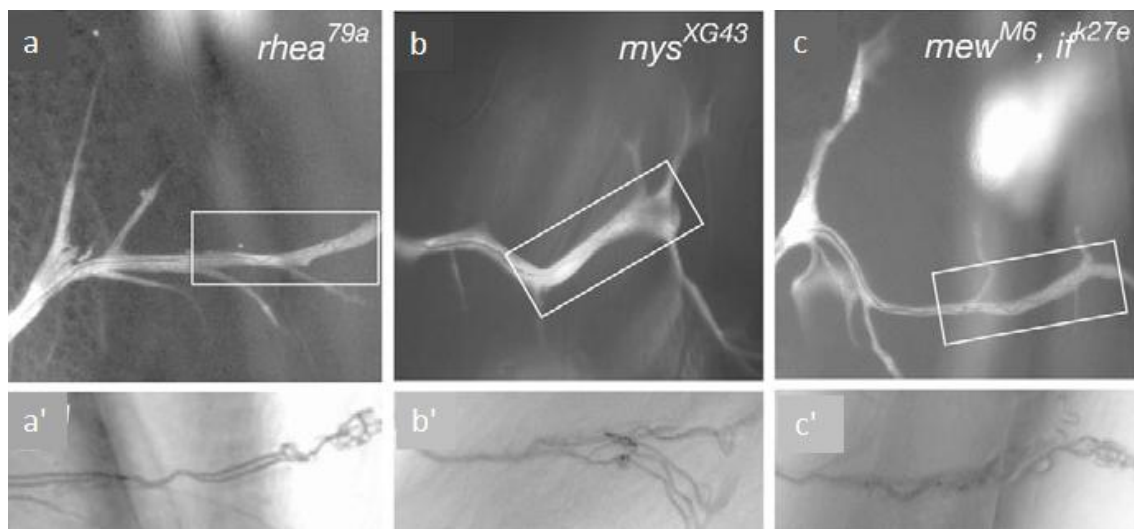
Figure 7: Multilumen phenotype in talin and integrin mutants
Bright field images of terminal cells showing multilumen phenotypes in mutant of **(a)** *talin* (*rhea*); **(b)** *β-intergrin* (*mys*); **(c)** and the two *α - integrins* (*mew* and *if* double mutants). a'-c' are enlargements of the boxed regions in a-c respectively. Adapted from (LEVI *et al.* 2006).

1.5 Moesin is essential for terminal cell development

Moesin (Moesin) is the only *Drosophila* homologue of the mammalian Ezrin-Radixin-Moesin (ERM) family of proteins. Activated Moesin (p-Moesin) acts as an anchor for F-actin at the apical membrane of polarised epithelia (BRETSCHER *et al.* 2002). Moesin is anchored to the membrane via various membrane anchors such as Phosphatidylinositol 4,5-bisphosphate (PtdIns(4,5)P$_2$), Crumbs and Bitesize (*btsz*) which are used in a cell specific context (MEDINA *et al.* 2002; NAKAMURA *et al.* 1999; PILOT *et al.* 2006).

The activation of ERM proteins is believed to occur upon recruitment to the apical membrane. In Drosophila embryos, *btsz* is involved in maintaining epithelial integrity and the stabilisation of adherens junctions through its interaction with Moesin (PILOT *et al.* 2006). Knockdown of *btsz* in the tracheal system leads to the loss of p-Moesin (Jayan N Nair, unpublished) in terminal cells, indicating that Btsz is an anchor for p-Moesin in the tracheal system. We also know that disruption of Moesin in the tracheal system through RNAi results in tube formation and branching defects within terminal cells (Jayan N Nair, PhD thesis). Recently, the kinase activating Moesin was identified as SLK and LOK like kinase (*slik*) (HIPFNER and COHEN 2003; HIPFNER *et al.* 2004). In order to better understand the relation between anchoring and activation of Moesin at the apical membrane and its importance in tracheal development, I explored the function of s*lik* in terminal cell development.

1.6 *slik*, a Sterile 20 like kinase involved in *Drosophila* growth control

SLK (sterile 20 like kinase) is a serine/threonine kinase and a member of the group II germinal centre kinases (GCKs) which includes MST1-3 (Macrophage Stimulating) and the LOK (Lymphocyte Oriented Kinase). SLK is cleaved by Caspase 3 in two domains with distinct activities: an activated N-terminal kinase domain that promotes apoptosis and cytoskeletal rearrangements and a C-terminal domain that disassembles actin stress fibres (SABOURIN *et al.* 2000). LOK was identified to be expressed in mammalian lymphocytes and to specifically phosphorylate ERM proteins.

slik (SLK- and LOK like kinase), a *Drosophila* member of the Ste20 kinase family, was identified in an overexpression screen as a gene causing increased growth of the posterior compartment of the wing imaginal disc (HIPFNER *et al.* 2002). *slik* was named on the basis of its similarity to the human SLK and LOK Ste20 kinases. *slik* shares high sequence similarity to the human *Slk* and *Lok* which is largely restricted to the N-terminal kinase domain and the conserved coiled-coil motif bearing C-terminus (Fig.8a). The sequence internal to the conserved domains of Slik is non-conserved and variable in length, a feature consistent within members of the same subfamily. The *slik* transcription unit covers approximately 11 kb and is predicted to have at least 12 exons. There are about 6 predicted transcripts based on cDNA clones and partial ESTs.

Two *slik* mutants, *slik^1* and *slik^{KG04837}*, have been described and used in various studies (HIPFNER and COHEN 2003; HIPFNER *et al.* 2004; HUGHES and FEHON 2006). *slik^1* represents a null allele which is a deletion of exons 2–8 and part of exon 9 of the *slik* transcript, including the translation start site and the entire kinase domain. *slik^{KG04837}* is a partial loss of function allele, an insertion of the P-element KG04837 in the first intron of *slik* (Fig.8b). *slik^1* mutant larvae display a striking phenotype through delay in overall growth and developmental timing. The mutant larvae grew at the maximum up to about one-third the size of wild type larvae and rarely progressed beyond third instar larval phase (Fig.9). Intriguingly, about 5% of the mutant larvae have exceptionally long life spans of 15 days which is three times the normal larval phase of development.
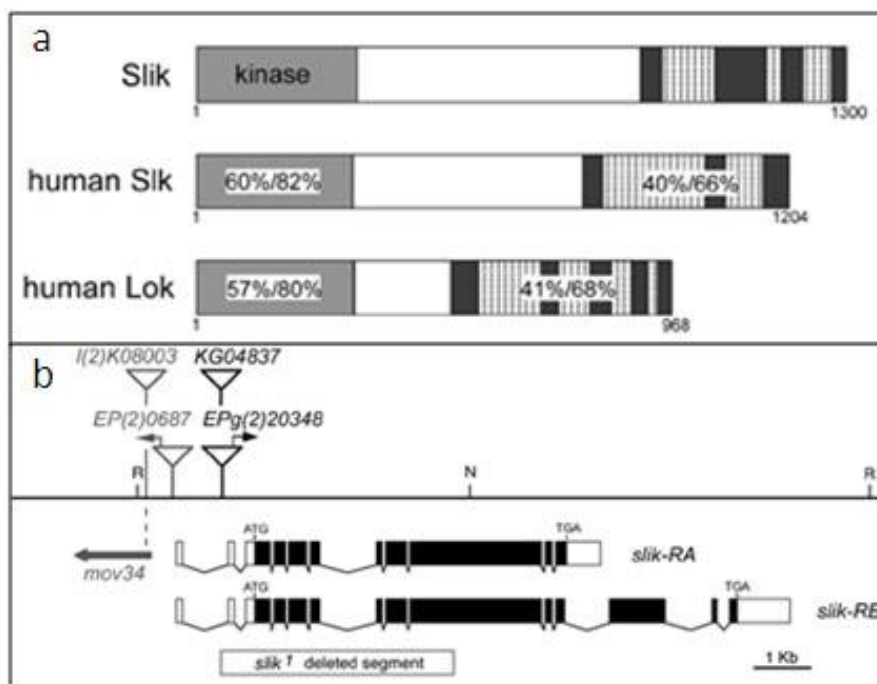
Figure 8: Schematic representation of Slik and the human homologues
(a) Comparison of Slik with human SLK and LOK proteins. Numbers show sequence identity/similarity within the indicated domains. Predicted coiled-coil regions in the C-terminal domain are indicated by hatching; **(b)** Detailed view of the slik region. The insertion sites of EPg(2)23048 and KG04837 in the first intron and the extent of the *slik^1* deletion are indicated. Adapted from (HIPFNER and COHEN 2003).
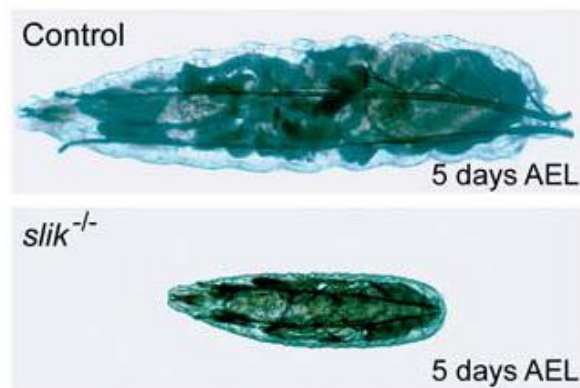
Figure 9: Growth defect in *slik* mutant larvae
Heterozygous slik[1]/+ control and homozygous slik[1] mutant larvae after 5d of growth under uncrowded conditions (HIPFNER and COHEN 2003).

1.7 Functional relevance of *slik* in *Drosophila* development

Hipfner et al. (HIPFNER *et al.* 2004), reported that Slik regulates cytoskeletal organisation during wing disc development by regulating the *Drosophila* ERM (ezrin/radixin/Moesin) protein Moesin. ERM proteins link cortical actin cytoskeleton to the cell membrane by the N-terminal FERM domain which binds to membrane proteins directly or through adaptor proteins, and the C-teminal actin binding domain which binds to F-actin. Slik was shown to be enriched at the apical membrane in cells of the wing imaginal disc. Also, Slik colocalised with activated Moesin (Phosphorylated Moesin/p-Moesin) and F-actin in these cells. *slik[1]* clones in wing discs showed a considerable reduction of p-Moesin levels in comparison to wild type cells. Further, expression of the kinase domain of Slik (Slik[kin]) in *slik* mutant wing discs restored p-Moesin to normal levels. These results suggest that Slik kinase activates Moesin through its phosphorylation.

Consistent with these results, in an RNAi screen in Drosophila Kc cells to identify kinases that activate Moesin during mitosis, *slik* was identified as a positive regulator of Moesin phosphorylation. During the onset of mitosis, cells retract their actin-based protrusion and change their morphology from a flattened to a rounded up form. Perturbing P-Moesin through *slik* RNAi mimicked the Moesin knockdown phenotype, i.e., failure to withdraw the actin rich protrusions, highlighting the importance of Slik in activating Moesin during cell division (KUNDA *et al.* 2008).

Recent work shows that Slik's localisation to the apical membrane is mediated by another protein, SRY interacting protein 1 (Sip1) (HUGHES *et al.* 2010). Sip1 is the *Drosophila* homologue of mammalian EBP50 (ERM binding protein 50) that acts as a scaffold linking ERM proteins to transmembrane proteins and other membrane associated cytoplasmic proteins. *Sip1* mutant follicle cells show a marked reduction of Slik levels and the subsequent loss of p-Moesin. On the other hand, *moesin* mutant cells show a drop in overall Sip1 levels, while s*lik* mutant clones showed an increase in Sip1 levels. In addition, Sip1 co-immunoprecipitates Moesin and Slik together, suggesting that both proteins form a complex with Sip1. Though the exact nature of the relationship between Sip1, Moesin and Slik is yet unknown, the authors suggest that Sip1 functions as a scaffold to bring Slik and Moesin in to proximity to phosphorylate Moesin (Fig.10).
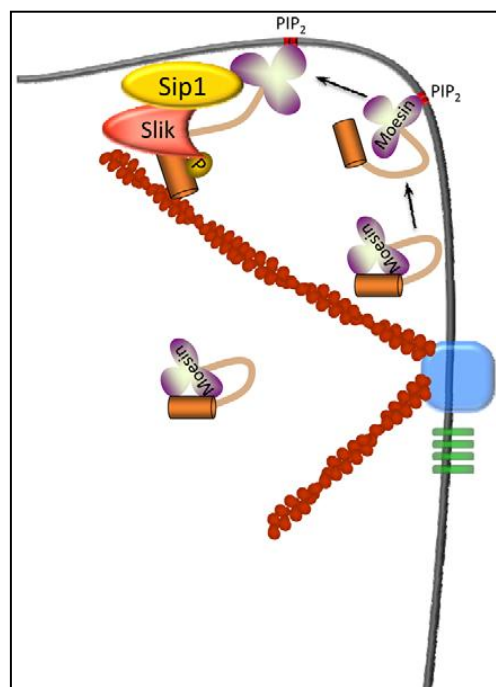
Figure 10: Possible model for Sip1 in Slik-dependent activation of Moesin.
Inactive, folded Moesin in the cell cortex might associate with PIP2 in the plasma membrane, inducing a conformational change which results in partial unfolding of Moesin. This event, or other modifications such as phosphorylation of residues in the FERM domain (Krieg and Hunter, 1992), allow Moesin, Sip1 and Slik to form a complex that results in phosphorylation of the C-terminal Threonine residue and full activation of Moesin. Adapted from (HUGHES *et al.* 2010).

In another study, Merlin (Mer), the *Drosophila* homologue of the human tumour suppressor Neurofibromatosis 2 (NF2) was shown to be under the control of Slik kinase (HUGHES and FEHON 2006). Merlin shares ~45% sequence similarity with ERM proteins and the similarity

is restricted to the N and C-terminal regions, which shares feature common to the ERM proteins and other family members. However, unlike ERM proteins that promote maintenance of epithelial integrity through the actin cytoskeleton (SPECK *et al.* 2003), Merlin has a distinct role in regulating cell proliferation (ROULEAU *et al.* 1993). Moreover, while ERM proteins are activated upon phosphorylation, phosphorylation of Merlin renders it inactive. *Merlin* mutant clones in eye and wings show overproliferation.

Merlin has a complex subcellular localisation that spans both the apical membrane and the endocytic compartments within the cytoplasm (HUGHES and FEHON 2006). In wild type wing disc epithelium Merlin is found to localise apically. However, loss of Slik results in an increase in Merlin levels in the mutant cells and bulk of Merlin is redistributed to the basolateral regions with an increased association with punctate structures. Western blotting analysis with extracts from Slik and Slik kinase dead (Slik^{kd}) overexpressing wing discs showed increased levels of phosphorylated Merlin upon Slik expression while remaining unchanged in Slik^{kd} expressing discs (HUGHES and FEHON 2006). Further, activated Merlin suppressed wing growth, which is suppressed by removal of a copy of *slik*, suggesting that Slik antagonises Merlin function. The authors also find that Moesin and Merlin are competitive substrates of Slik's kinase activity.

Additionally, experiments in S2 cells with wild type, phosphomimetic and non-phosphorylable forms of Merlin revealed a dynamic trafficking of Merlin depending on its phosphorylation status. In cells transfected with wild type Merlin, upon induction Merlin initially localised to the membrane but after 2-4 hours became enriched in endocytic compartments. When Merlin expression is induced in cells coexpressing Slik there is a drastic shift in the distribution of Merlin, with the majority localising to the membrane. In contrast, when Merlin expression is induced in Slik^{kd} transfected cells, Merlin localisation decreased at cell membranes but increased within endocytic compartments in the cytoplasm. Trafficking of activated/non-phosphorylated Merlin to the endocytic compartments may be of functional relevance in tumour suppression, by facilitating removal of receptors from cell surface that promote cell proliferation. *expanded* (*ex*), a Merlin-related tumour suppressor is partially redundant to Merlin in regulating proliferation and differentiation (MCCARTNEY *et al.* 2000). *Merlin:ex* double mutant cells in wing discs present abnormal accumulation of receptors such

as Notch and EGFR at the plasma membrane, possibly due to the lack of endocytosis of the receptor-bearing plasma membrane along with endocytosing Merlin fraction. Collectively, the activity of Slik kinase results in an orchestrated but opposite regulation of Moesin and Merlin to promote epithelial integrity and cell proliferation (Fig.11).
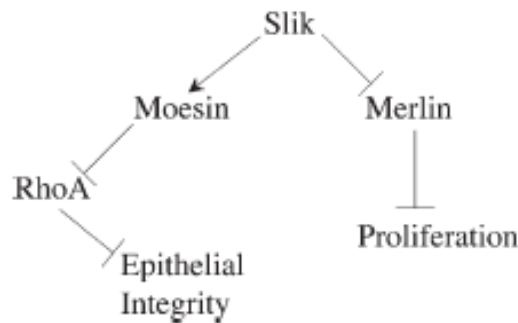
Figure 11: Schematic diagram of functional relationships between Slik, Merlin, Moesin, and the regulation of tissue integrity and proliferation in developing epithelia.
Slik activity simultaneously promotes Moesin function and inhibits Merlin. Previous results have shown that Moesin functions to negatively regulate Rho activity and promote epithelial integrity (Speck et al., 2003). Merlin functions to restrict proliferation in the same epithelia. Thus, the net result of Slik activity is to drive proliferation and simultaneously stabilise epithelial integrity (HUGHES and FEHON 2006)

Apart from its kinase activity, Silk also contributes to the growth of wing disc epithelium in a kinase independent manner. Overexpression of Slik in the *patched* (*ptc*) domain in wing disc caused wing overgrowth due to increased cell proliferation. However, the Slik driven wing overgrowth is counteracted by an increased number of apoptotic cells. Moreover, overexpression of Slik^{kd} recapitulated the Slik driven overgrowth of wings suggesting that the Slik derived cell proliferation is through a kinase-independent mechanism. Tissue overgrowth resulting from Slik overexpression is suppressed through removal of the *raf* and the wings are restored to normal proportions.

Apoptosis also occurs in *slik* mutant cells of the wing disc which is mediated by the c-Jun N-terminal kinase (JNK) and can be suppressed by removing *hemipterous* (*hep*/JNKK) which encodes the activating kinase. Additionally, reduction of Raf levels in *slik* mutant background further increased the numbers of apoptotic cells suggesting that Raf is an important downstream effector of Slik. Since Raf was found to coimmunoprecipitate both Slik and Slik^{kd}, the authors conclude that that activation of Raf is through its physical interaction with Slik, rather than phosphorylation by Slik. Finally, *slik* mutant cell's growth defect can be rescued by expression of activated Raf, but not by activated ERK (MAPK) suggesting a

signalling independent of the canonical ERK pathway. Briefly, Slik functions to maintain epithelial integrity and promote growth through proliferation in tissues. In conclusion Slik's activity is comparable to several oncogenes that promote proliferation and apoptosis in parallel.

1.8 Aim

This work aims to investigate the underlying role of Slik in tracheal development. It explores the contribution of Slik in terminal cell development through the phosphorylation of targets Moesin and Merlin. In addition, this work addresses the possible signalling input by Slik into the Btl/MAPK pathway, mediated through its interaction partner Raf.

2. MATERIALS AND METHODS

2.1 Materials

2.1.1 *Drosophila melanogaster* stocks

w[1118]; ; embryos were used for Slik antibody stainings

2.1.2 UAS Transgenes

From Bloomington stock centre

w[*]; P{w[+mC]=UAS-phl.gof}F179

w[1118]; P{w[+mC]=UAS-Ras85D.V12}TL1

From other sources

w[1118]; ;P{w[+mC]=UAS-Slik^{kin}/TM6B,Tb [1] (David Hipfner)

w[1118]; ;P{w[+mC]=UAS-Slik^{kd}/TM6B,Tb[1] (David Hipfner)

P{hsFLP}, w[1118]; P{neoFRT}42D P {w[+mC]=*tub*Gal80; P{w[+mC]=*btl*-Gal4, *btl-moesin-mRFP,* UAS-CD-GFP} T(2;3)CyO -TM6 (Mirka Uhlirova)

From VDRC stock centre

UAS-IR-*btl*	VDRC 27106
UAS-IR-*egfr*	VDRC 107130
UAS-IR *ex*	VDRC 109281
UAS-IR-*Merlin*	VDRC 7161
UAS-IR-*moesin*	VDRC 37917
UAS-IR-*raf*	VDRC 107766
UAS-IR-*slik*	VDRC 43783
UAS-IR-*srf*	VDRC 100609
UAS-IR-*cad 96Cb*	VDRC 103296

From NIG Japan

UAS-IR-*Ras*   NIG 9375-2

2.1.3 Gal4 driver lines

w[1118]; P{w[+mC]=*btl*-Gal4}; *+/+*

w[1118]; P{w[+mC]=UAS-dicer }; P{w[+mC]= *btl*-Gal4}, P{w[+mC]= UAS-GFP}

w[1118]; P{w[+mC]=*btl*-Gal4}, P{w[+mC]=UAS-2XEGFP}; MKRS/TM6B,Tb[1]

w[1118]; If/Cyo; {w[+mC]= *btl*-Gal4}, P{w[+mC]= UAS-GFP}

w[1118]; slik[1], {w[+mC]= *btl*-Gal4}, P{w[+mC]= UAS-GFP}/Cyo; MKRS/TM6B,Tb[1]

2.1.4 Mutants

y[1]; P{y[+mDint2] w[BR.E.BR]=SUPor-P}slik[KG04837]/CyO; ry[506]

w[1118]; slik[1]/Cyo, P{GAL4-kr}2, P{UAS- GFP};

w[1118]; P{neoFRT}42D slik[1]/CyO P{GAL4-kr}2, P{UAS- GFP};

2.1.5 Antibodies

The following primary antibodies were used: guinea pig anti-Slik (1:100, Hipfner et al 2004), mouse anti-SRF (1:200, DSHB), rat anti-E-Cadherin (1:200, DSHB), rabbit anti-Dof (1:200, Vincent *et al*., 1998), rabbit anti-P Moesin (1:200, S3149 Cell Signaling), rabbit anti-Moesin (1: 5000, François Payre), rabbit anti-GFP (1:500, Torrey Pines Biolabs Inc). Fluorophore conjugated secondary antibodies: Alexa468 and Alexa568 and Alexa647 (Molecular Probes) were used at a dilution of 1:2000.

2.1.6 Oligonucleotides

Btl RT_F	tccacacggaaacctcaaggacttc
Btl RT_R	acgtcgctctgtgagtcgtacttc
bs_RT_F	cgctgcccaacaagaagtctccgcctg
bs_RT_R	cagcttgcgcgtggcaaatgtgtaca
Ex_RT_F	acttctggggcagcagcagccgaa

Ex_RT_R	gtgggtgtgcgatgatcgccagc
Merlin _RT	tgtggctgggcgtcacctccgtg
Merlin _RT_R	gcaggtgctccatgctcttctccag
Moesin_F_500	cctggacaccgacgagcatatcaaggac
Moesin _R_SalI	acgcgtcgaccatgttctcaaactgatcgacgcg
Raf RT_F	actgctgtccgcttcaatatgagcag
Raf RT_R	ccagttttcctcggaacttttggcgt
RpL32 RT_F	tcctaccagcttcaagatgacc
RpL32 RT_R	cacgttgtgcaccaggaact
Slik RT_F	gatccgcaggtgaggcccacgacgga
Slik RT_R	gtttgtcaatgtcttggctctgcagc

2.1.7 Microscopes

Olympus FV1000, Leica TCS SP2, Zeiss Axioplan 2-imaging, Zeiss Apotome and Leica M2 16FA were used for microscopy.

2.1.8 Imaging and data analysis software

Image acquiring softwares FV10-ASW 2.0 Viewer, Leica Confocal Software LCS, Axiovision Rel 4.6 (Zeiss) and Axiovision 1 (Zeiss) were used. Images were edited using Adobe Photoshop (Adobe Systems) and ImageJ softwares. All images are maximum intensity projection unless otherwise mentioned. DNA sequence alignments, analysis and oligonucleotide designing were done using VectorNTI. Imaris (Bitplane) 3D/4D image processing software was used for 3D reconstruction of the tracheal system.

2.1.9 Reagents

TritonX 100, Tween20 and BSA were purchased from Sigma. Vectashield mounting media for fluorescent samples was from Vector Laboratories. Restriction enzymes used were from New England Biolabs. Expand High Fidelity PCR system was supplied by Roche

Diagnostics. Agarose electrophoresis grade was from Gibco BRL. Unless otherwise mentioned, all the other chemicals were purchased from Merck, Sigma or Roth.

2.2 Methods

2.2.1 Collection of embryos

The flies were maintained under standard conditions (Ashburner, 1989; Wieschaus and Nuesslein-Volhard, 1986).

To fix the embryos, an overnight egg lay (16 hr) was collected on an apple juice–agar plate, dechorionated using 50% bleach and washed in tap water. Embryos were fixed in 4% formaldehyde in PBS:heptane = 1:1 solution at 37°C for 20 minutes, with vigorous shaking, followed by devitellinilisation with methanol:heptane = 1:1 solution by vortexing for 30 seconds. Embryos were washed several times in methanol and stored in methanol at -20°C if not used immediately.

2.2.2 Immunostaining in embryos

The fixed embryos were rehydrated and washed with 0.3% PTX (1XPBS+ 0.3% TritonX 100) three times for 10 min each followed by 30 min incubation in blocking reagent (1X PBS+ 0.1% TritonX 100 + 1% BSA). After blocking, the liquid phase was taken off and the primary antibody was added to the embryos. The samples were left at 4°C overnight, on a rotating wheel. Embryos were washed with 0.3% PTX several times, at room temperature followed by incubation with Alexa coupled secondary antibody at room temperature for 90 minutes. The embryos were washed four times (15 minutes each) in 0.3% PTX at room temperature and mounted in Vectashield before imaging.

2.2.3 RNAi in the tracheal system

Crosses were set up using the UAS-RNAi transgenic line and the *btl*Gal4, UAS-GFP recombinant driver line, with UAS-dicer or excluding UAS-dicer in cases where

coexpression of UAS-dicer caused lethality or resulted in extremely small larvae. The crosses were maintained at 29°C unless otherwise mentioned. Wandering third instar larvae were collected and dissected to expose the tracheal system. Larvae were fixed using 4% paraformaldehyde in PBS for 20 minutes and washed with 0.3% PTX (1XPBS+ 0.3% TritonX 100) followed by mounting the larval fillets using Vectashield. In case where antibody staining was required the larvae were subjected to the antibody staining protocol described below.

2.2.4 Immunostaining in larvae

Post fixation fillets were washed with 0.3% PTX (1XPBS+ 0.3 % TritonX 100) three times for 10 min each followed by 30 min incubation in blocking reagent (1X PBS+ 0.1% TritonX 100 + 1% BSA). After blocking, the samples were incubated overnight in antibody solution at 4°C. Fillets were washed four times (15 minutes each) in 0.3% PTX after overnight incubation. Fillets were incubated in Alexa fluorophore conjugated secondary antibodies for 2 hours at room temperature. Next, the fillets were washed four times (15 minutes each) in 0.3% PTX at room temperature, mounted in Vectashield and taken for microscopy.

2.2.5 Generation of *slik^1* MARCM clones in the tracheal system

Crosses were set up using the appropriate stocks and maintained at 25°C. A 24-hr egg lay collection was taken and heat shocked for about 2 hours. After heat shock the tubes were placed at 29°C. Around day 5-6 post egg lay, wandering third instar larvae were collected, dissected and mounted on slides as described in the previous section.

2.2.6 Tracheal cDNA synthesis

Wild type third instar larvae were dissected, the tracheal system was isolated and the tissue macerated in Trizol (Invitrogen). RNA was isolated using the standard Trizol-based isolation protocol. RNA isolated was treated with DNase according to manufacturer's protocol (Invitrogen). 200 ng of RNA was used for cDNA synthesis using First strand synthesis

kit/SuperscriptIII according to manufacturer's instructions (Invitrogen) using a 1:1 mix of both random hexamers and oligo dT.

2.2.7 RT PCRs

1 μl of the tracheal cDNA was used as the template for PCR reactions. The reaction components were: 20 pmols of each primer, 1X Red Taq Readymix (Sigma) in a 20 μl PCR reaction mix. The PCR was carried out on a Thermoblock (Biometra). The PCR programme included a denaturation step of 2 minutes at 94°C followed by 30 cycles: 15 seconds at 94°C, 30 seconds annealing at 57°C, 30 seconds extension at 72°C. No final extensions were included in the programme. The PCR products were analysed on a 1.5% agarose gel.

3. RESULTS

3.1 Slik is required for tracheal development

Studies on tracheal development and more specifically on terminal cells have outlined the importance of Moesin in tube formation and maintenance of the tube within the branches. One of the factors that regulate Moesin in other tissues is the Moesin activating kinase Slik, implicated in wing imaginal disc development, mitotic events in S2 cells and normal development of follicle cells of oocytes (HIPFNER *et al.* 2004; HUGHES and FEHON 2006; HUGHES *et al.* 2010). This study explores the function of Slik in terminal cell development in conjunction with Moesin and another signalling molecule, Raf.

3.1.1 Slik is expressed in both the embryonic and the larval tracheal system

To analyse Slik distribution in the tracheal system, I used an antibody against Slik (HIPFNER and COHEN 2003). This antibody was previously used to examine Slik localisation in wing discs, oocytes and mitotic S2 cells (CARRENO *et al.* 2008; HIPFNER *et al.* 2004; HUGHES *et al.* 2010). Stainings from these studies showed that Slik was enriched at the apical membrane of cells in the wing imaginal disc and also in the follicular epithelium of oocytes. In mitotic S2 cells Slik is localised at the mitotic cortex of the dividing cells. To mark the tracheal cells antibodies against Dof was used. Dof is an adaptor protein specific to the two FGFRs, *breathless (btl)* and *heartless (htl)* which are active in the tracheal system and the migrating mesoderm, respectively (VINCENT *et al.* 1998). Dof is expressed through all stages of tracheal development. The distribution of Slik and Dof was visualised using secondary antibodies coupled to fluorescent (Alexa Fluor®) dyes (Fig.12).

At embryonic stage 10, tracheal development commences with the invagination of the tracheal placodes within each segment. In the invaginating tracheal placode, cells constrict their apical surface which is the concave side of the depression. Staining for Slik reveals that Slik is expressed in the invaginating placode with enrichment at the apical side of the cell (Fig.12a). In stage 12 embryos, cells within the migrating placode continue to have an apical enrichment of Slik (Fig.12b). At stage 14 of development, cells from each placode migrate

and are arranged side-by-side and interdigitate to form a continuous tube. At this stage of tracheal development Slik enrichment persists at the apical regions of cells forming the tube, i.e. the membrane facing the lumen of the developing tube (Fig.12c.) Also, previous studies in wing imaginal discs reported Slik to be enriched at the apical membrane of the cells (HIPFNER *et al.* 2004).
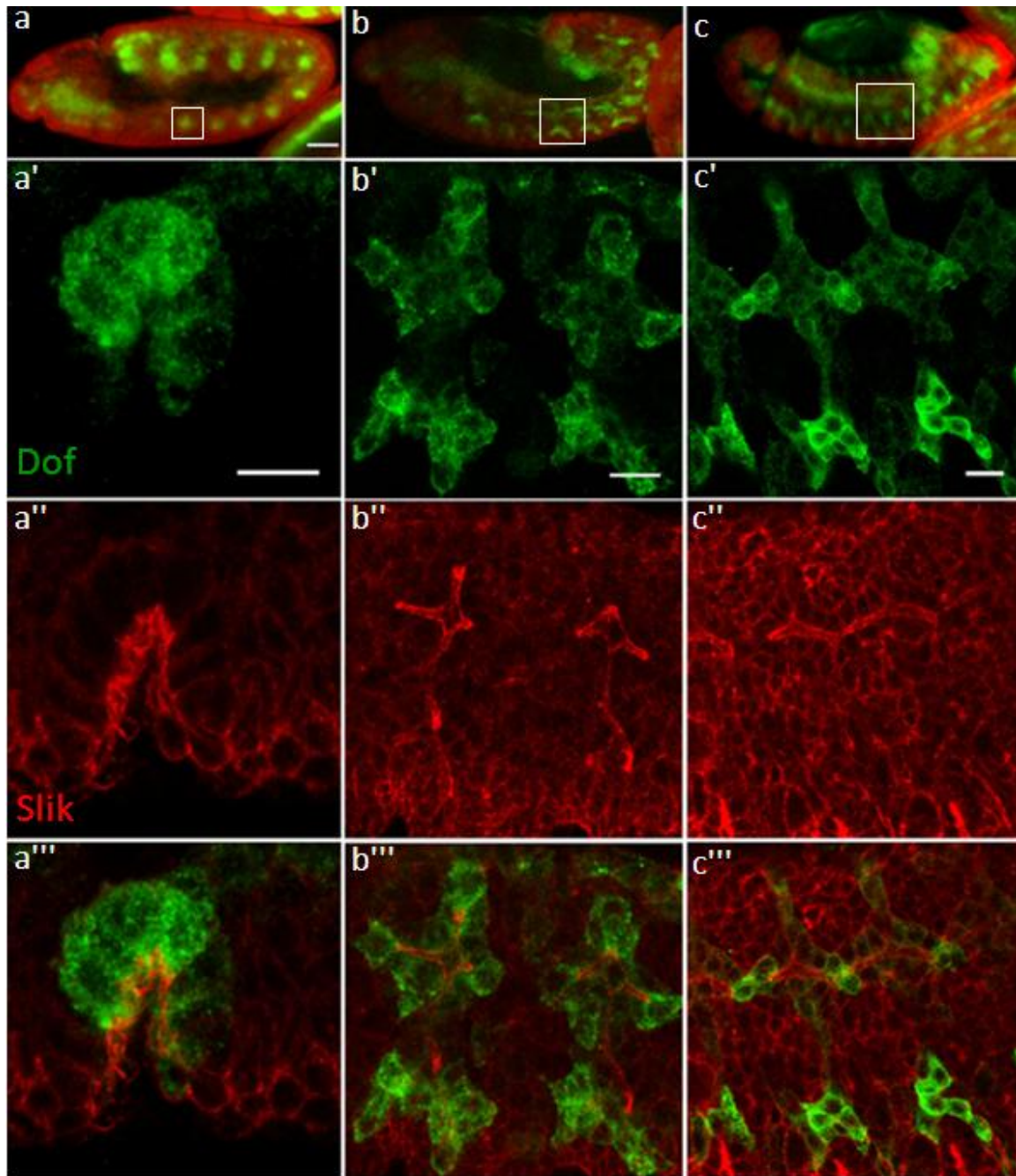
Figure 12: Slik expression during embryonic development of the tracheal system
Tracheal cells are visualised by anti-Dof staining **(a-c)**. **(a)** Slik expression during tracheal placode invagination at stage 10; **(b)** Outgrowth of primary branches at stage 12 and **(c)** Stage 14. Slik expression shows strong apical

enrichment within the trachea. a', b' and c' are enlargements of the corresponding stages in a, b and c. Scale a, b, c - 50 µm and a', b', c' - 10 µm.

At the end of embryonic development, patterning of the tracheal system is complete with the dorsal trunk, the dorsal branches, the lateral branches and the terminal cells in place. Terminal cells at this stage are morphologically distinct from those found in larvae as they possesses only a single branch extension with a tube within. Over the larval phases of development these cells generate multiple branches to form a functional terminal cell. Branching events in a terminal cell alter the morphology of the cell from a simple cell to a cell that is highly ramified and spanning over a large area (Fig.13). The tips of these branches establish direct contact with tissues requiring oxygen.
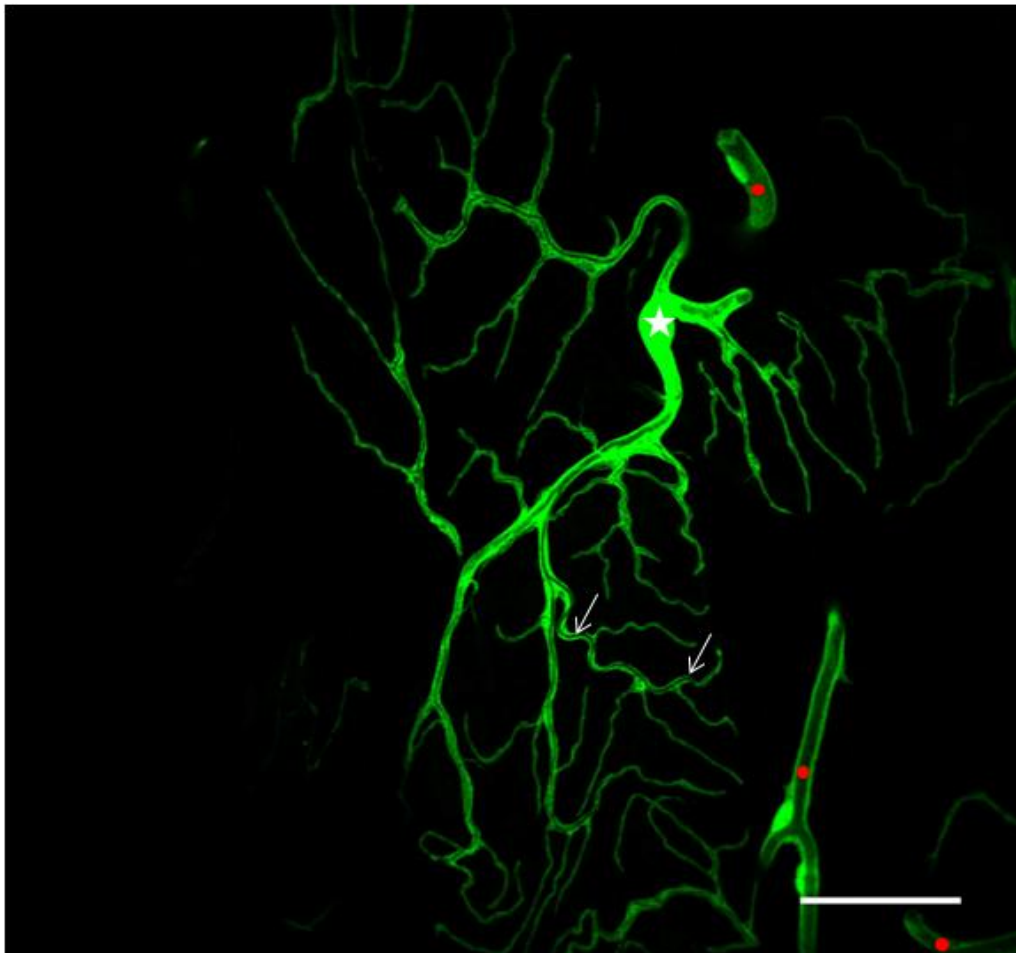
Figure 13: A terminal tracheal cell from a larva at third instar phase of development
Tracheal cells are visualised by tracheal specific cytoplasmic GFP expressed using *btl*Gal4. The terminal cell is highly branched and carries a tube within each branch (arrows). Oxygen is transported through these tubes to surrounding tissues and organs. Star denotes the cell nucleus. Also seen are parts of the secondary branches from adjacent areas (marked by dots). Scale - 50 µm.

To analyse the distribution of Slik in the terminal branches, Slik staining was performed in larvae expressing the UAS-GFP transgene in the tracheal cells using the tracheal specific *btl*-Gal4 line. The GFP is expressed in both the nucleus and the cytoplasm and hence is used to highlight the tracheal system. Staining for Slik in third instar larvae showed that Slik is expressed in the terminal cells (Fig.14a). Further, high resolution imaging showed that Slik is enriched at the apical membrane within the terminal branches, with occasional diffused staining at sub-apical regions (Fig.14b).
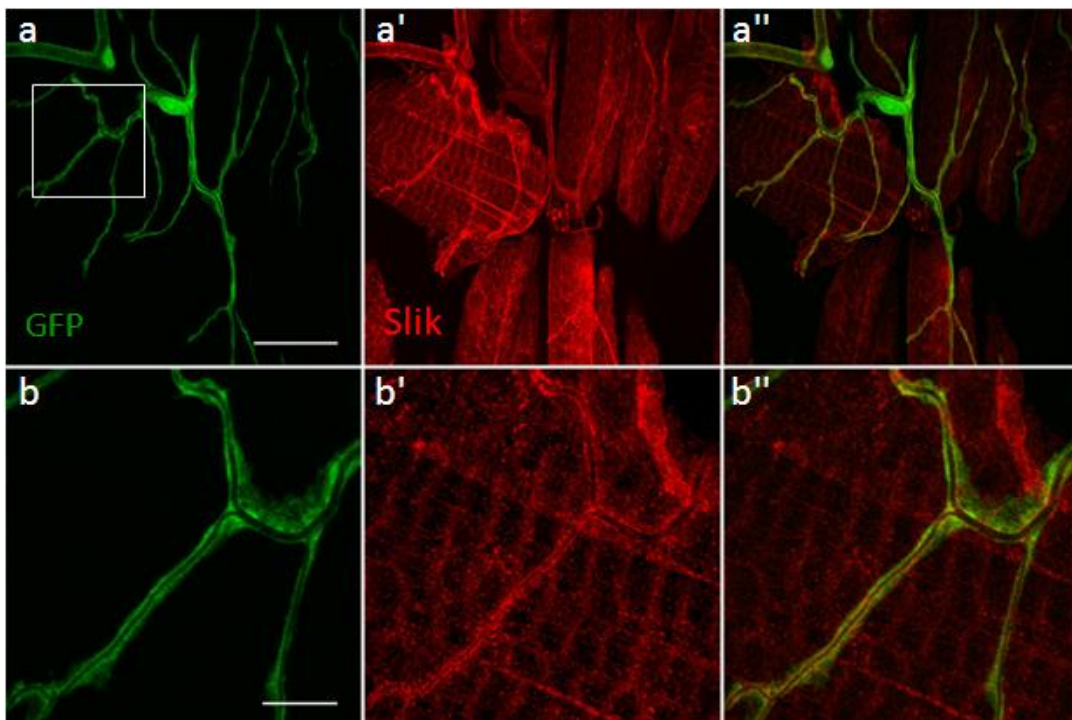
Figure 14: Slik expression in terminal cell of the tracheal system
Tracheal cells are visualised by tracheal specific cytoplasmic GFP expressed using *btl*Gal4 **(a, b)**. **(a)** Slik expression in a terminal cell; **(b)** Enlargement of the corresponding area in image a (boxed) showing Slik enrichment in the apical membrane of the branch. Scale a - 25 µm, b - 10 µm.

Next, I investigated the localisation of Slik within cellular junctions of the tracheal system. The tracheal terminal cells are junctionless cells except for a junction connecting terminal cells to the secondary branch. However, the dorsal trunk is a multicellular tube and therefore suited for studies on junctions within the tracheal system. Of particular ease in studying junctions within the tracheal system are the fusion cells, a pair of doughnut shaped cells that form the anastomoses of the dorsal trunk (Fig.4). In epithelial cells E-Cadherin (E-Cad) is localised to the apicolateral regions where it is a component of the adherens junction. In order to mark the junctions within the dorsal trunk I performed immunostaining for E-Cad. At the

point of fusion of the dorsal trunk E-Cad is expressed in 3 stripes, the central stripe which marks the adherens junction formed at the point of contact between fusion cells and the two other flanking stripes that delineate the junction between the fusion cell and the dorsal trunk at either side (Fig.15b). Analysis of the dorsal trunk for Slik protein expression shows that Slik is expressed in the fusion cells of the dorsal trunk (Fig.15a). A simple maximum intensity z-projection of images of the dorsal trunk was not sufficient to determine the localisation of Slik in relation to the junction. Therefore, I performed 2D reconstruction of the dorsal trunk using Imaris imaging software. 2D reconstruction of the dorsal trunk revealed that Slik expressed in the fusion cell localised to the apical membrane of the fusion cells. Optical sections across various planes of the dorsal trunk showed that the localisation of Slik was more apical to E-Cad at the lumen (Fig.15c). This result is consistent with the results from a previous study where the authors observed that Slik localised apical to the adherens junction in wing disc epithelium (HIPFNER *et al.* 2004)

3.1.2 Slik is required for normal branching, lumen formation and tube stability in terminal cell development

To investigate the function of *slik* in tracheal development, *slik[1]* mutant larvae were analysed. *slik[1]* is a null allele as it is a deletion that removes exons 2–8 and part of exon 9. This deletion removes the translation start site and the entire kinase domain. *slik* mutant clones of terminal cells were generated through the MARCM method. Also, I performed tracheal specific knockdown of *slik* through RNAi and analysed the outcome. Results from experiments using various approaches showed similar phenotypes and are discussed in the following sections.
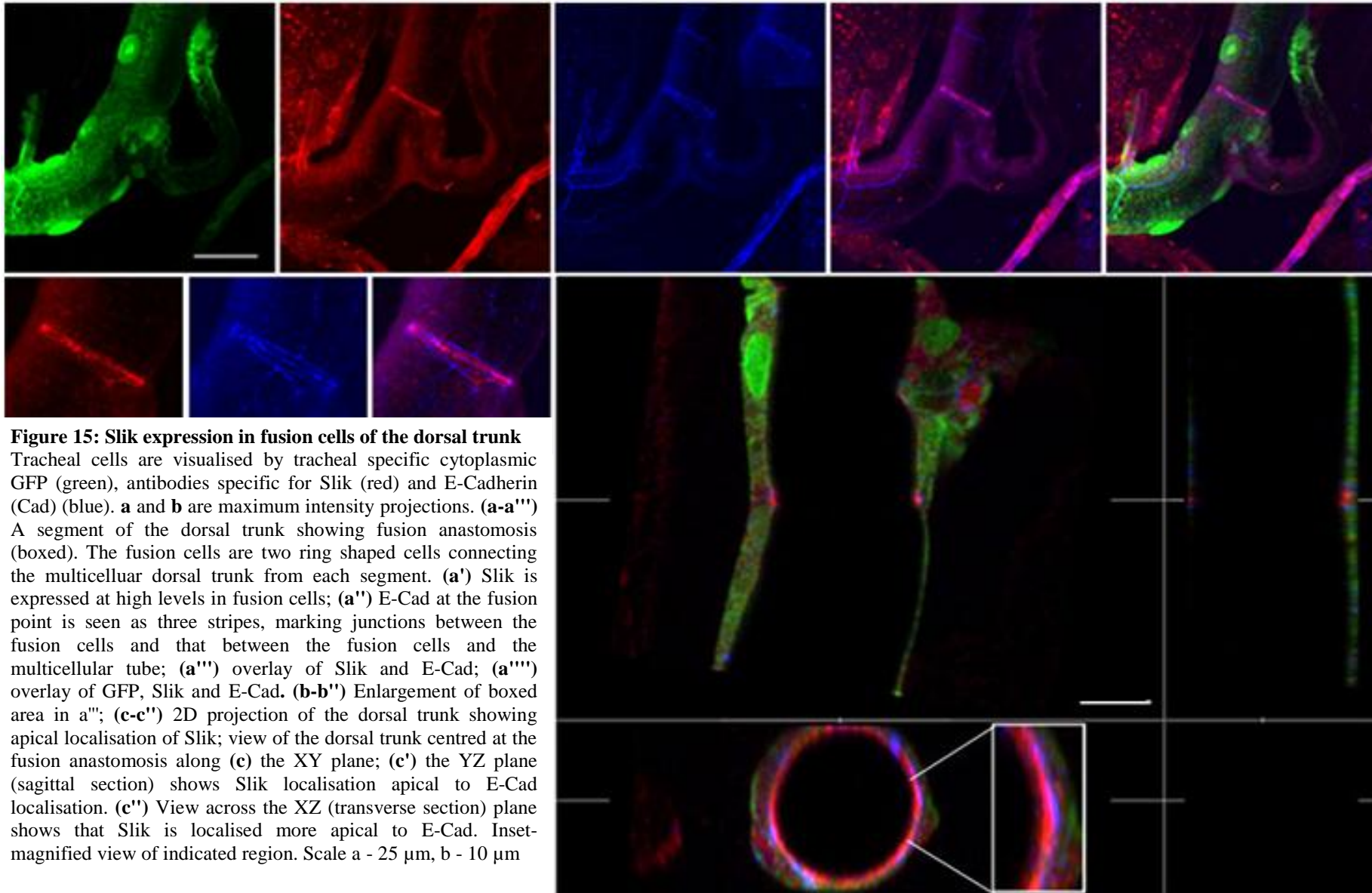
Figure 15: Slik expression in fusion cells of the dorsal trunk
Tracheal cells are visualised by tracheal specific cytoplasmic GFP (green), antibodies specific for Slik (red) and E-Cadherin (Cad) (blue). **a** and **b** are maximum intensity projections. **(a-a''')** A segment of the dorsal trunk showing fusion anastomosis (boxed). The fusion cells are two ring shaped cells connecting the multicelluar dorsal trunk from each segment. **(a')** Slik is expressed at high levels in fusion cells; **(a'')** E-Cad at the fusion point is seen as three stripes, marking junctions between the fusion cells and that between the fusion cells and the multicellular tube; **(a''')** overlay of Slik and E-Cad; **(a'''')** overlay of GFP, Slik and E-Cad. **(b-b'')** Enlargement of boxed area in a'''; **(c-c'')** 2D projection of the dorsal trunk showing apical localisation of Slik; view of the dorsal trunk centred at the fusion anastomosis along **(c)** the XY plane; **(c')** the YZ plane (sagittal section) shows Slik localisation apical to E-Cad localisation. **(c'')** View across the XZ (transverse section) plane shows that Slik is localised more apical to E-Cad. Inset- magnified view of indicated region. Scale a - 25 μm, b - 10 μm

3.1.2.1 Analysis of the tracheal system in *slik¹* mutant animals

slik¹ homozygous mutants are larval lethal and therefore very few escapers of the homozygous mutant larvae were obtained. The escaper *slik¹* mutant larvae had a smaller body size (Fig.16), which was consistent with previous observation (HIPFNER and COHEN 2003).

slik¹ homozygous third instar larvae were filleted and processed. The larvae showed gross abnormalities in the tracheal system. The dorsal branches showed lumen defects. In a wild type dorsal trunk the multicellular tube is composed of cells arranged with their apical surfaces facing the lumen. The apical surface of the tracheal cells expands permitting tube dilation and at the same time secretes chitin to reinforce the expanding tube. A bright field image of the wild type dorsal trunk showed that the lumen diameter spans almost the entire width of the dorsal trunk. By contrast, bright field images of the dorsal trunk from a *slik¹* mutant larva showed lumen defects. While the outer diameters of the dorsal trunk from both wild type and mutant larvae were comparable, the diameter of the lumen in the mutant was less than half as wide as in the wild type. The presence of a narrow lumen despite of the normal branch size indicated a failure in lumen expansion within the mutant dorsal trunk (Fig.17a', b').

To further analyse tracheal phenotypes in *slik¹* mutants, the terminal cells from these larvae were compared with the wild type cells. The mutant terminal cells showed defects in branching. Wild type terminal cells on an average had over 20 branches, whereas in *slik¹* mutant cells branching was restricted to fewer than 10 branches (Fig.13 and 18). In addition to reduction in number of branches the mutant terminal cells also exhibited luminal defects. Normally in terminal cells each branch bears a single lumen but in the mutant terminal cells multiple lumens were observed, either within a single branch or clustered near the nucleus. This phenotype is henceforth addressed as the mutilumen phenotype (Fig.18c').
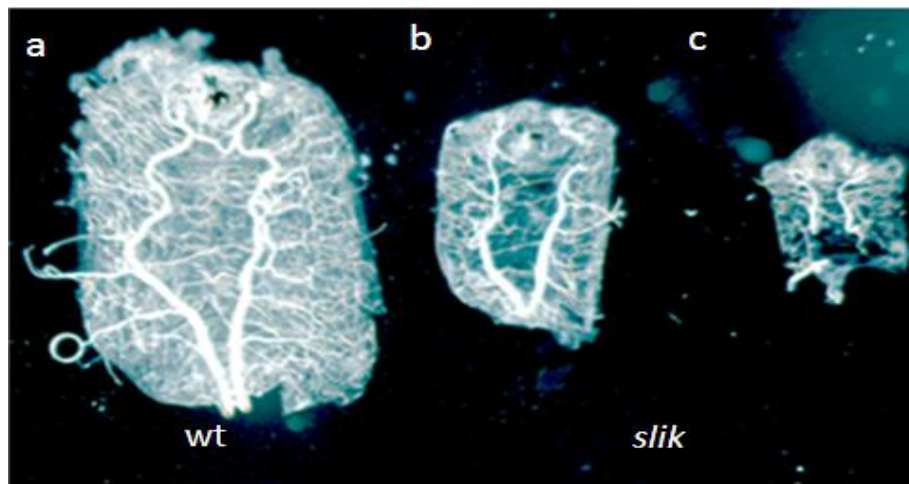
Figure 16: *slik¹* **mutant larvae show altered body size**
Larvae in the image above have been dissected on their ventral side to expose the tracheal system. **(a)** wild type third instar larva; **(b)** and **(c)** are *slik¹* mutant larvae also at third instar larval stage as judged by the presence of completely extruded anterior spiracles with spiracular papillae, but exhibiting smaller body sizes.
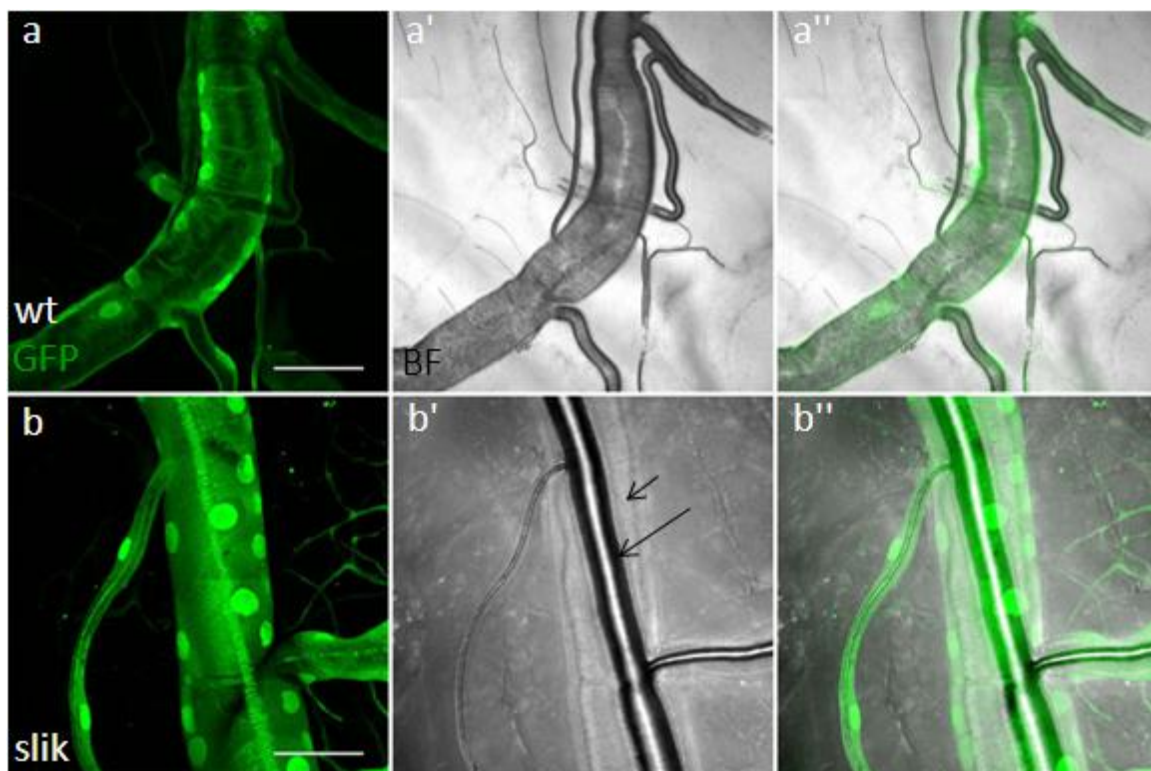
Figure 17: *slik¹* **mutant larvae show tube defects within the dorsal trunk**
slik¹ mutant tracheal system is visualised by tracheal specific cytoplasmic GFP (green) expressed using *btl*Gal4 and tubes within the trachea are visible in bright field (BF) **(a, b)**. **(a-a'')** Dorsal trunk from a wild type larva; **(b-b'')** dorsal trunk from a *slik* mutant larva. **(a')** Bright field image of the wild type trachea shows that the dorsal trunk and the tube within are almost of the same diameter and therefore not clearly visible as two distinct components. **(b')** Dorsal trunk from a *slik* mutant larva shows that the dorsal trunk and the tube (marked by short and long arrow respectively) are easily identified. The tube within the dorsal trunk is not centrally positioned and has not expanded sufficiently to line the inner wall of the dorsal trunk. Scale - 50 μm.

.
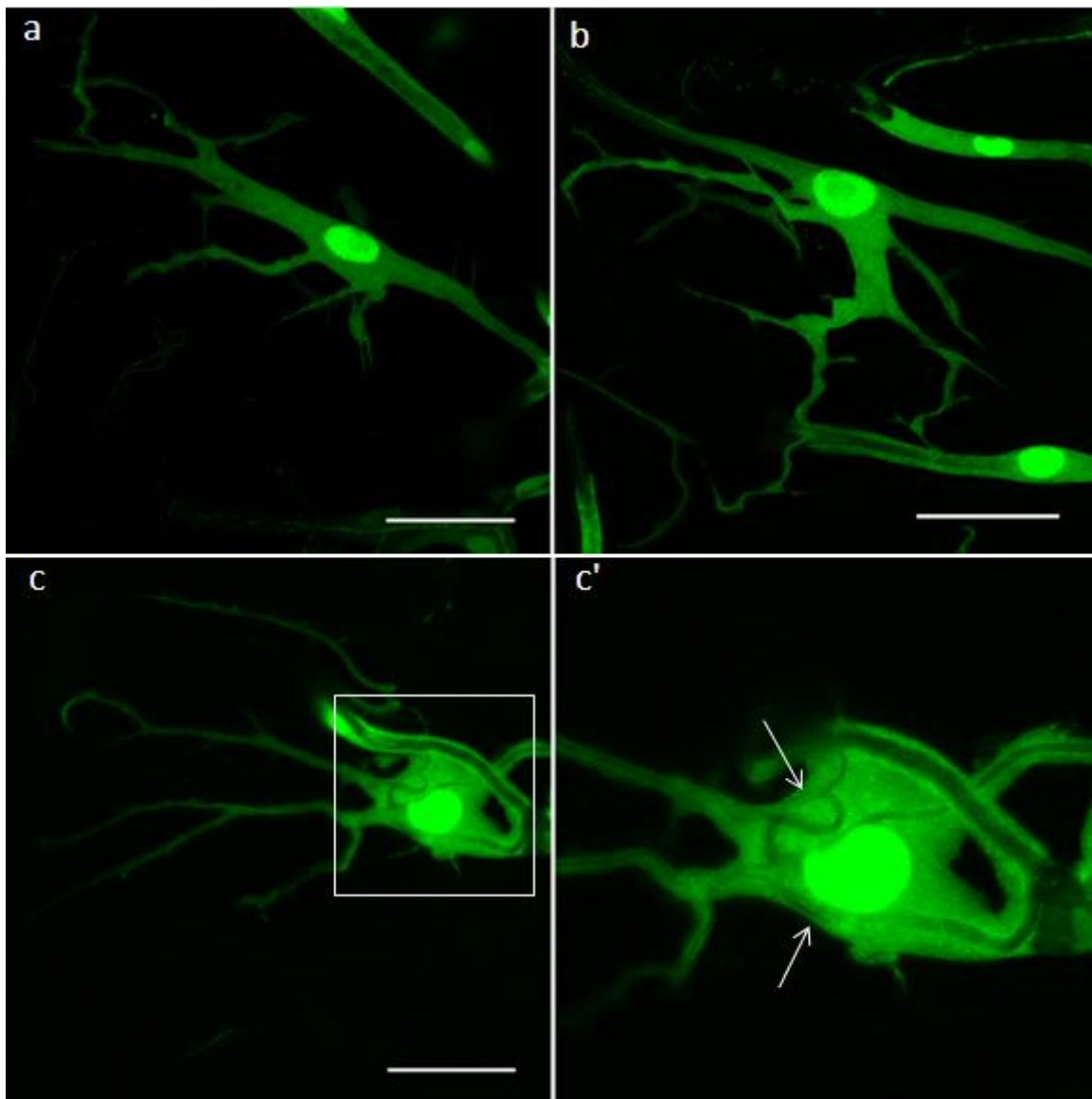
Figure 18: Terminal cells from *slik¹* mutant third instar larvae show branching and lumen defects
Tracheal system is visualised by tracheal specific cytoplasmic GFP (green) expressed using *btl*Gal4. **(a-c)** Terminal cells from *slik¹* mutant larvae show reduced branching. **(c')** Enlargement of the corresponding area in image c (boxed), showing multilumen (multiple tubes within a branch) phenotype. Scale - 25 μm.

3.1.2.2 Analysis of *slik¹* MARCM clones in the tracheal system

In addition to analysis of the *slik¹* mutant tracheal system, *slik¹* mutant clones were generated in the tracheal system using the MARCM (Mosaic Analysis with a Repressible Cell Marker) technique. I chose this approach due to the unavailability of sufficient numbers of homozygous mutant third instar escapers, coupled with the difficulty of dissecting small sized larvae. The mutant terminal cells express GFP which distinguishes these cells from the

neighbouring wild type cells. Very few terminal cells (MARCM clone) of the mutant genotype were obtained indicating that *slik* is required for cell survival. The few MARCM clones that survived showed abnormal terminal cell development. Like terminal cells from *slik^1* homozygous mutant larvae, mutant terminal cells from the MARCM clones displayed tube and branching growth defects. The mutant terminal cell had fewer branches (Fig.19a,b). Clonal *slik^1* terminal cells also showed the multilumen phenotype (Fig.19a) as observed with *slik^1* homozygous mutant larvae. These results indicated that *slik* definitely has a role in branching morphogenesis of terminal cells.
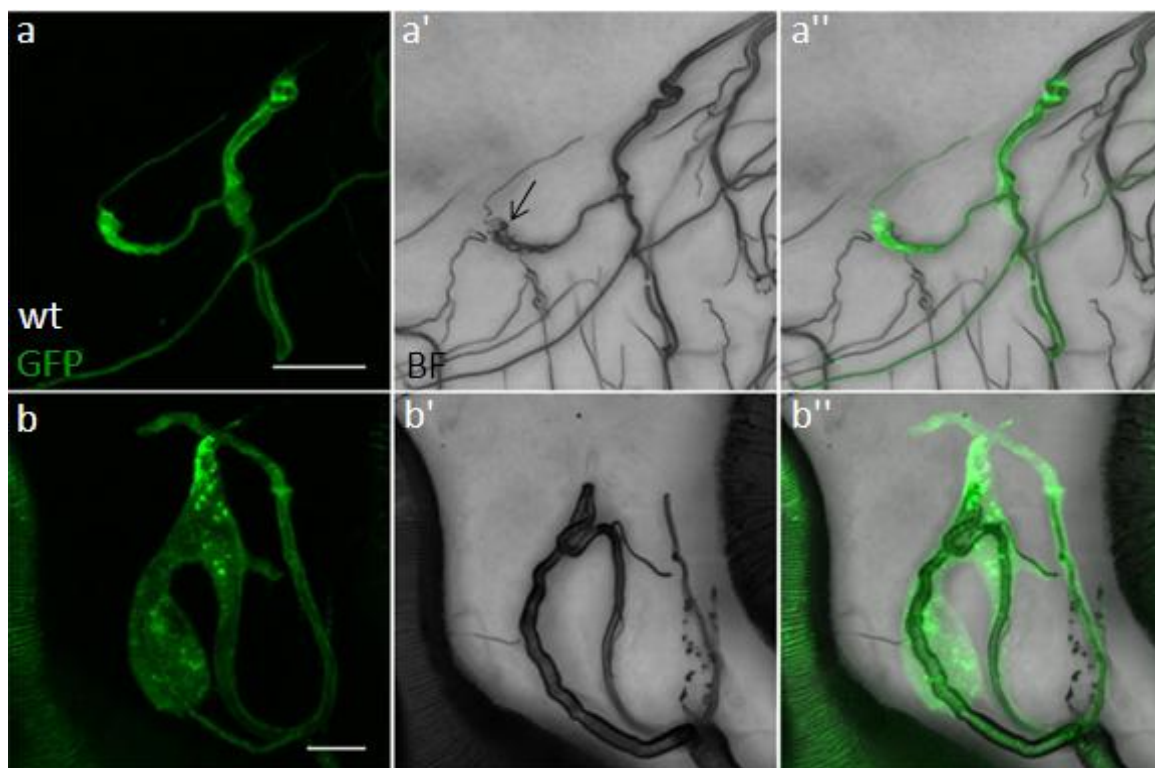
Figure 19: *slik^1* MARCM clones in the tracheal system from third instar larvae
slik^1 mutant clonal terminal cells generated by MARCM technique express cytoplasmic GFP. **(a-a'')** A terminal cell showing multilumen phenotype (marked by an arrow); **(b-b'')** mutant terminal cell showing reduced branching phenotype, Scale a -25 µm and b - 10 µm

Given the low frequency of occurrence of the MARCM clones and the difficulty in working with *slik^1* mutant larvae that barely grew in size, RNAi mediated knockdown of *slik* was employed to study the *slik* mediated terminal cell development.

3.1.2.3 Analysis of *slik* mutant tracheal system using RNAi

An alternate *in vivo* strategy to study the function of genes is to deplete the protein by knocking down the gene products within tissues. Slik levels in the tracheal system were depleted using *slik* RNAi constructs expressed specifically in the tracheal system using *btl*Gal4. Two *slik* RNAi lines were tested in the tracheal system, VDRC 43783 and VDRC 43784. Since both these lines had a potential off-target, pKC98E, RNAi for this gene in the tracheal system was performed as control. Knockdown for pKC98E did not result in any observable phenotypes; therefore I concluded that knockdown of *slik* using these lines gives only Slik specific phenotypes. Knockdown of *slik* using both lines resulted in similar phenotypes; therefore all further experiments were performed using line VDRC 43783.

The knockdown of *slik* resulted in a similar phenotype as seen in *slik^1* mutants. The most obvious effect of *slik* knockdown in the tracheal system was the reduction of the larval body size (Fig.20), but still larger than *slik^1* mutant larvae. Moreover, the larvae had substantially smaller fat bodies than a wild type animal which gave the larvae a more transparent appearance. Reduction in body size could be an effect of reduced metabolism resulting from a deficit in oxygen supply due a physiologically inefficient tracheal system as a result of defective terminal branching. Next, I investigated if *slik* knockdown affected terminal cell differentiation.

To address this, immunostainings with antibodies against *Drosophila* Serum response factor (Srf) was performed. Srf is a transcription factor expressed only in terminal cells among all tracheal cells. *srf* is also expressed in muscle nuclei, but since the tracheal system is marked by GFP the terminal cells nuclei can be identified by the overlay (Fig.21). Terminal cells identified by Srf expression were counted in five animals from both wild type and *slik* RNAi animals. Terminal cells from the tracheal segments tr3-5 were counted which were located by the presence of tracheoblast at the dorsal trunk (Fig.21). The results from these cell counting experiments showed that the number of terminal cells, both in wild type and *slik* RNAi, were comparable. (Fig.22, Appendix Fig.50). The average terminal cells count in both genotypes were as follows, wild type = 29.2 ± 2.68, *slik* RNAi = 31± 3.08. The p value from a Student's t-test was p = 0.35. Thus branch counting showed that *slik* knockdown in the tracheal system

does not interfere with the specification of terminal cells but rather with the development of terminal cells and branches.
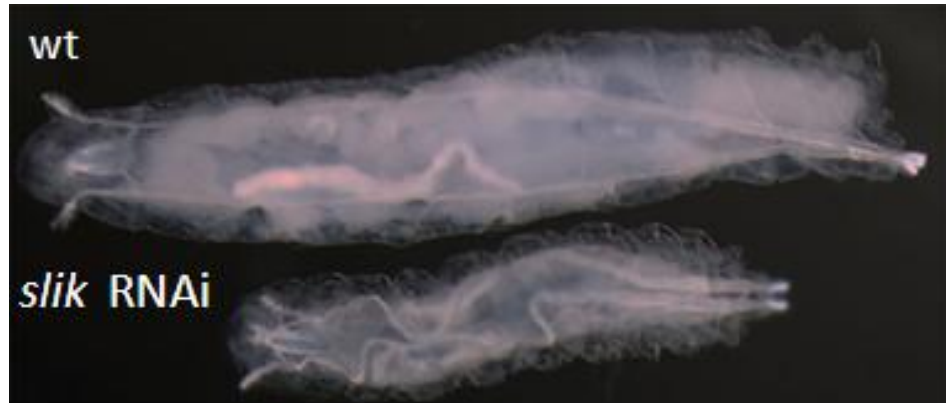
Figure 20: Knockdown of *slik* in the tracheal system affects larval body size
Comparison of third instar *slik* knockdown larva with a wild type larva of the same stage. The larvae were raised at 29°C. Third instar larva were identified by the presence of the characteristically exposed spiracular papillae of the anterior spiracles. Tracheal specific knockdown of Slik reduced body size in larvae.
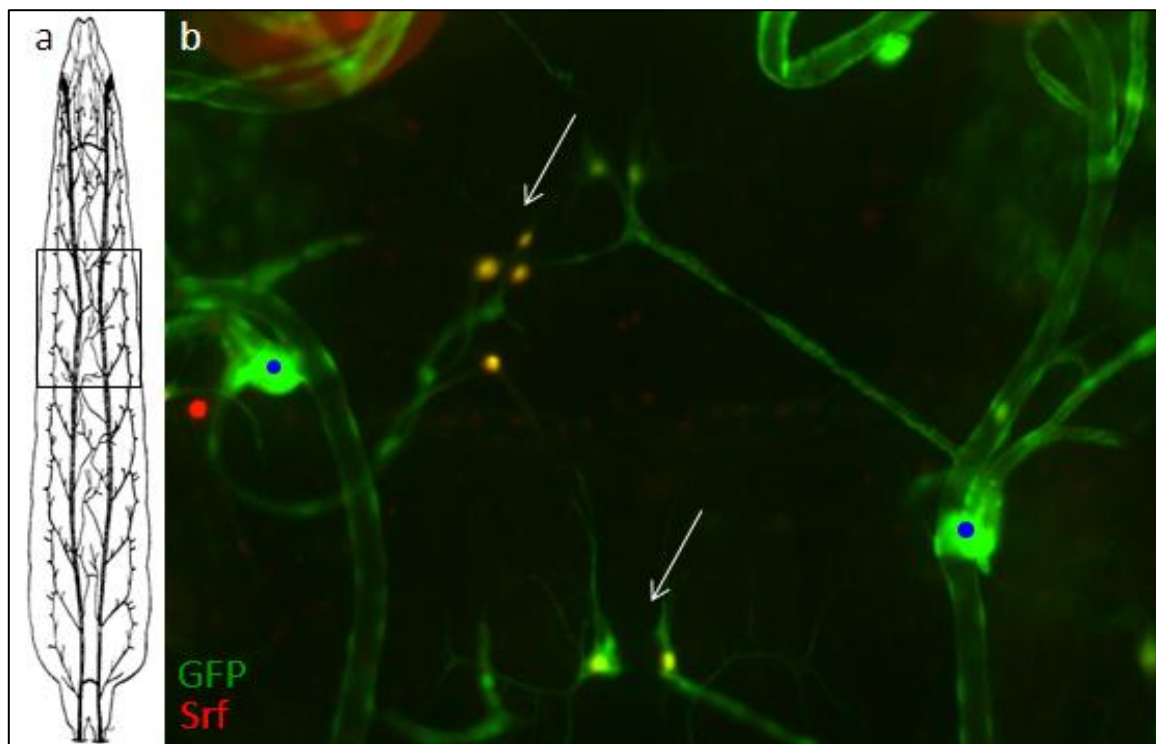
Figure 21: Dorsal terminal cells of the tracheal segments tr3-tr5 from third instar larvae
Tracheal system is visualised by tracheal specific cytoplasmic GFP (green) expressed using *btl*Gal4 and the terminal cells are identified by Srf staining (red). **(a)** Schematic representation of the tracheal system in a third instar larva, marking tracheal segments tr3, tr 4 and tr5. **(b)** An assembly of a series of snapshots that cover tr3, the specific tracheal segment is identified by the presence of tracheoblasts (blue dots) while the preceding tracheal segment lacks the tracheoblast. Terminal cells express Srf (marked by arrows) and therefore in this overlay are seen as yellow.
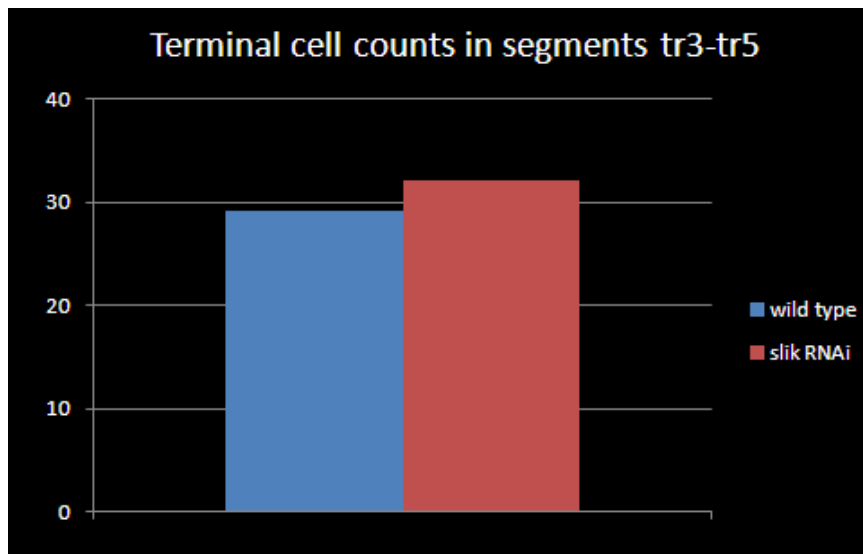
Figure 22: Average terminal cell counts in wild type and *slik* RNAi trachea
Third instar wild type and *slik* RNAi larvae were dissected and the terminal cells from tracheal segments tr3-5 were counted. Terminal cells from five animals were counted for each genotype and the bars represent the average of terminal cells counted. The average values were as follows wild type = 29.1 and *slik* RNAi = 31. A Student's t-test gave the value p = 0.35.
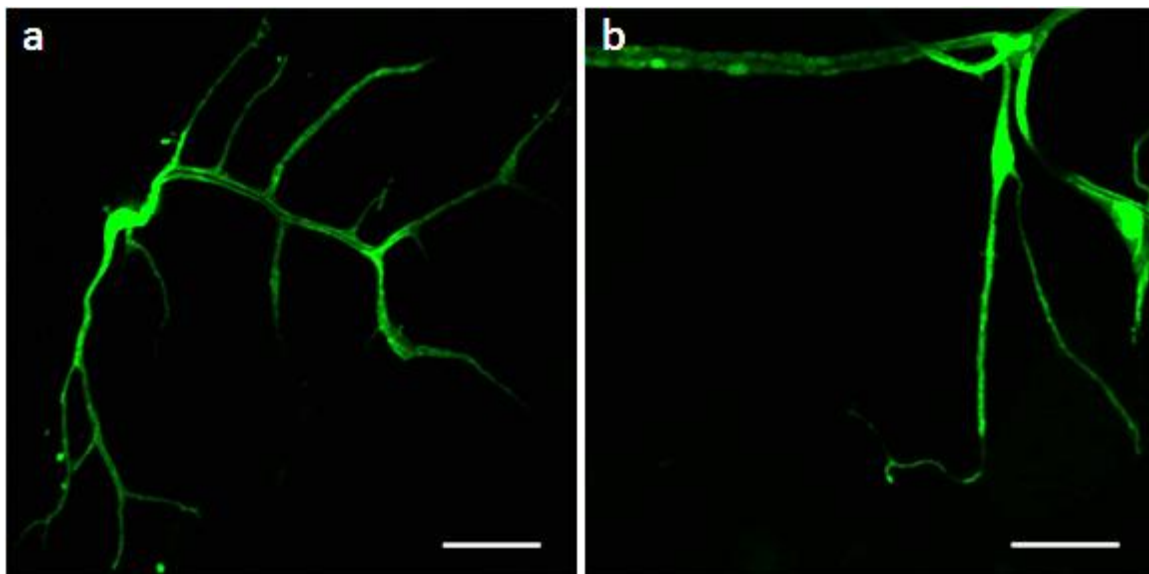
Figure 23: Knockdown of *slik* in the tracheal system affects branching in terminal cells
(a, b) Terminal cells from a *slik* knockdown larva show reduced branching with branch points varying between **(a)** 6 and in an extreme case **(b)** 2 branches. Branching points were counted by scoring branches that possessed a lumen that was connected to the parent/previous branch's lumen. Scale - 50 μm.

Analysis of terminal cells in *slik* knockdown larvae revealed multiple defects. First, terminal cells in knockdown larvae showed an overall reduction in branching. Consistent with *slik*[1] mutants and MARCM clones, on average fewer than 10 branches per terminal cell were observed compared to about 20 branches per cell in the wild type (Fig.23a). In some terminal

cells the knockdown resulted in severe branching defects such that the terminal cells were restricted to just two branches (Fig.23b). In addition to the branching phenotype, the terminal cells also showed tube abnormalities. Knockdown of *slik* in terminal branches lead to the formation of multiple lumens (multilumen phenotype) within the branches (Fig.24), as also observed in *slik^1* mutants.

Figure 24: Knockdown of *slik* in the tracheal system affects lumen formation in terminal cells
Tracheal system is visualised by tracheal specific cytoplasmic GFP (green) expressed using *btl*Gal4. Terminal cell branches show multiple lumens upon *slik* RNAi in the tracheal system. The multiple tubes/lumens are marked by arrows. Scale - 25 μm.

3.2. Slik, Moesin and Merlin in tracheal development

We know that Slik is expressed in the tracheal system and enriched at the apical membrane within branches of the terminal cell. Further, Slik is essential for terminal cell development as mutants for *slik* do not have normal branch and lumen formation. Earlier reports have described Moesin and Merlin as two known targets of Slik (HIPFNER and COHEN 2003; HIPFNER *et al.* 2004; HUGHES and FEHON 2006). Slik phosphorylates both these proteins and regulates their activity in various cellular processes. *slik* RNAi phenotypes could arise as a result of loss of Slik's function over Moesin and Merlin. To address this possibility I looked at moesin and Merlin expression in the tracheal system.

3.2.1 Moesin and its activated form (p-Moesin) are expressed in the tracheal system

Slik is known to activate Moesin through phosphorylation and activated Moesin (p-Moesin) stabilises filamentous actin by anchoring it to the plasma membrane (POLESELLO *et al.* 2002). Phosphorylation of Moesin induces conformational changes in the protein, from closed to open state, thereby activating and facilitating its interaction with the actin cytoskeleton. Multiple lumens can be associated with loss of stabilisation of actin cytoskeleton as a result of depletion of the crosslinker proteins (LEVI *et al.* 2006). Thus disruption of Moesin function by knockdown of its activating kinase could lead to tube destabilisation within branches resulting in the multilumen phenotype. This is supported by evidence from previous work which that showed knockdown of Moesin in the tracheal system resulted in reduced branching and multiple lumen phenotypes in terminal cells (Jayan N.Nair, PhD Thesis). Since Slik is critical in terminal cell development, I examined the subcellular localisation of Moesin.

Figure 25: Moesin is expressed in terminal cell of the tracheal system
Tracheal cells are visualised by tracheal specific cytoplasmic GFP (green) expressed using *btl*Gal4 **(a, b)** and antibodies specific for Moesin (in red) **(a', b')**. **(a-a')** Overview of a terminal cell; **(b-b')** enlargement of the corresponding area in image **a** (boxed) showing Moesin enrichment in the apical membrane of the branch. Scale a - 50 μm, b - 10 μm.

Immunostaining using antibodies against Moesin was performed on third instar larval fillets expressing UAS-GFP in the tracheal system. The stainings showed that Moesin was expressed in the tracheal system. Moesin was found enriched at the apical membrane within terminal cell branches (Fig.25). As Moesin is also expressed in all other tissues, Moesin from the underlying muscle tissue was also detected.

Fly Moesin is phosphorylated at amino acid residue Threonine[556] and so far Slik is the only kinase known to regulate this phosphorylation. To visualise activated p-Moesin in terminal branches, an antibody that specifically recognised phosphorylation at T^{556} of Moesin was used. Immunostainings showed that p-Moesin was enriched at the apical membrane of terminal cells. The results were consistent with the earlier published data where immunostainings in wing discs showed p-Moesin enriched at the apical membrane (HIPFNER *et al.* 2004)
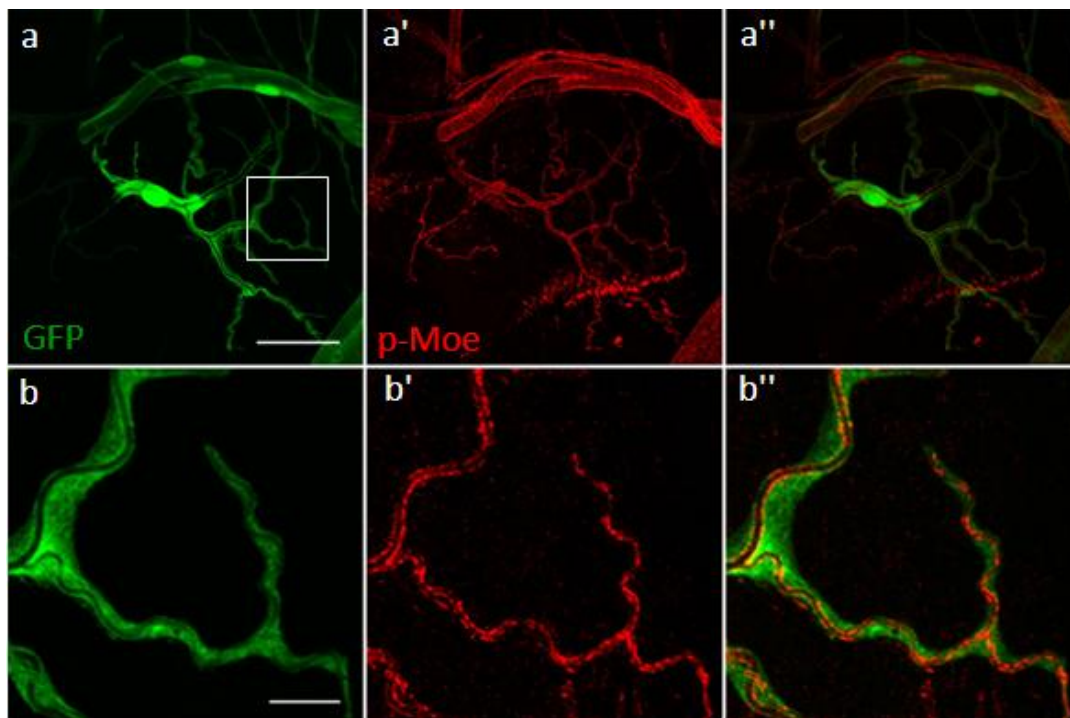
Figure 26: Phosphorylated-Moesin expression in terminal cell of the tracheal system
Tracheal cells are visualised by tracheal specific cytoplasmic GFP (green) expressed using *btl*Gal4 **(a, b)** and antibodies specific for the phosphorylated form of Moesin (red) **(a', b')**. **(a-a')** Overview of a terminal cell; **(b-b')** enlargement of the corresponding area in image **a** (boxed) showing p-Moesin enrichment in the apical membrane of the terminal branch. Scale a - 50 µm, b - 10 µm

A previous study on p-Moesin in the tracheal system (Jayan N. Nair 2008, PhD thesis) has shown that p-Moesin is localised at the apical membrane, which was confirmed here for the terminal cells (Fig.26). p-Moesin expression was also analysed in the dorsal trunk. The dorsal trunk showed a clear enrichment of p-Moesin at the junctions between fusion cells and those between the dorsal trunk and the fusion cells, visible as diffuse stripes (Fig.27). These experiments confirm that activated Moesin is expressed in the tracheal system and shows a clear apical membrane localisation in terminal cells and junctions of the fusion cells in the dorsal trunk.

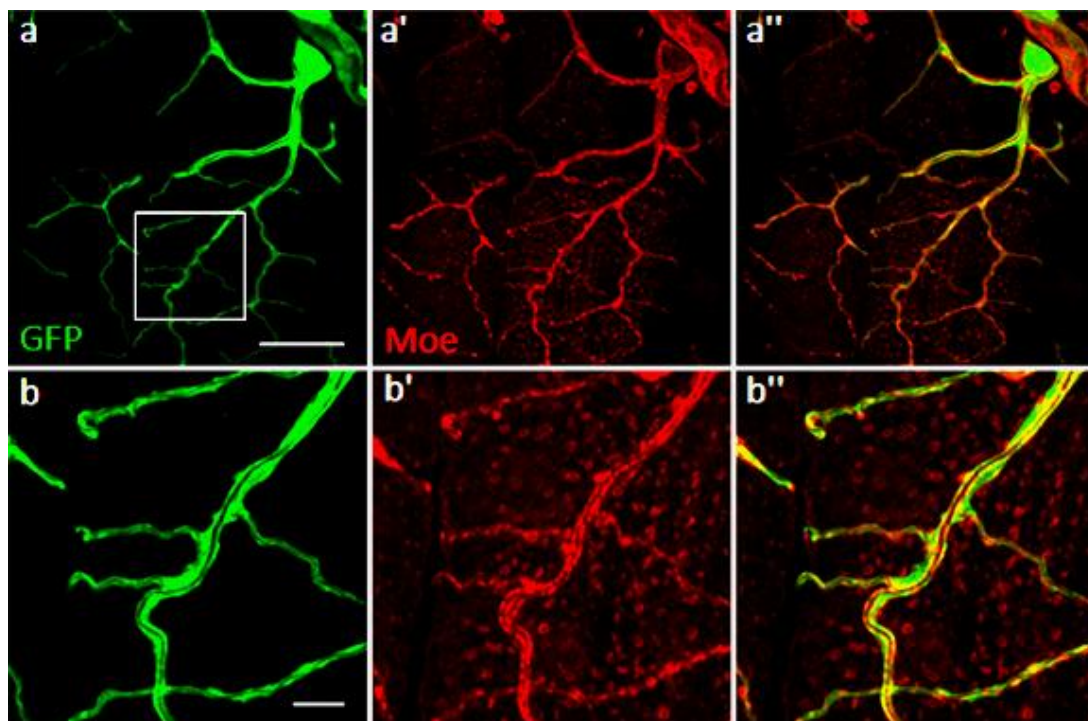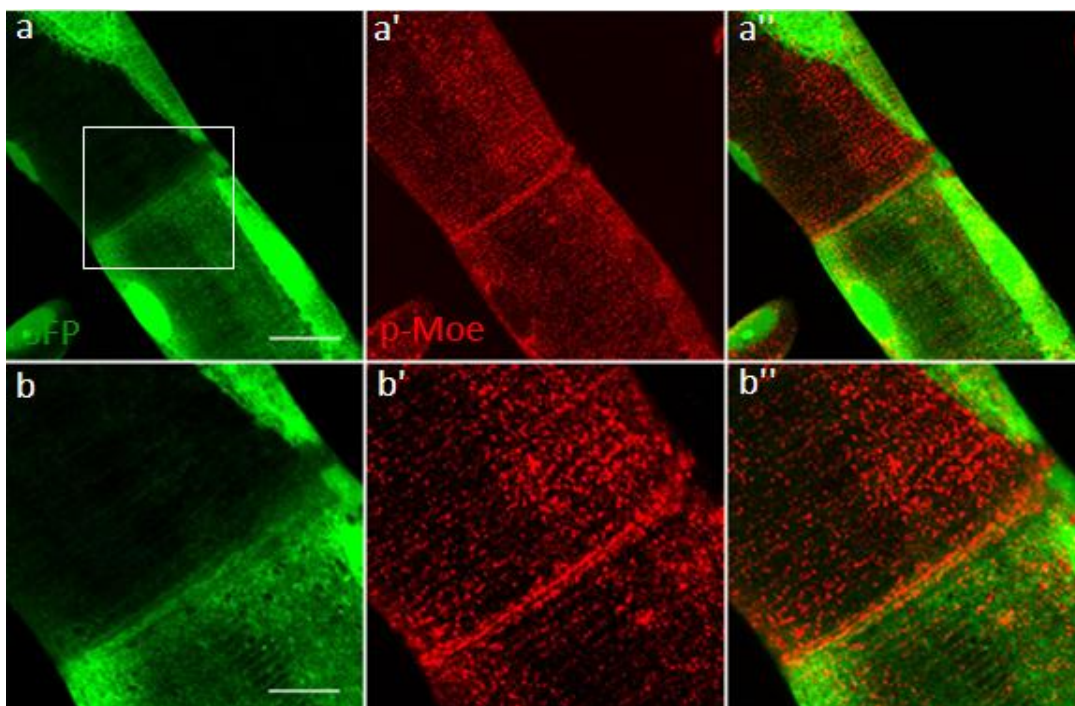**Figure 27: Phosphorylated Moesin is expressed in fusion cells of the dorsal trunk**
Tracheal cells are visualised by tracheal specific cytoplasmic GFP (green) expressed using *btl*Gal4 and antibodies specific for the phosphorylated form of Moesin (red) (**a, b**). (**a-a'**) p-Moesin expression in dorsal trunk; (**b-b'**) enlargement of the corresponding area of the dorsal trunk (boxed) showing p-Moesin enriched within the fusion cells. Scale a - 20 µm, b - 10 µm.

3.2.2 Merlin is expressed in the tracheal system

Merlin the *Drosophila* homologue of the human Neurofibromatosis 2 (NF2) tumour suppressor is also a target of Slik's kinase activity. In the *Drosophila* embryonic epithelium Merlin is expressed as punctae both at the apical membrane and the cytoplasm (MCCARTNEY and FEHON 1996). *expanded* (*ex)* is a tumour suppressor closely related to *Merlin.* Ex and

Merlin has been shown to function in a redundant manner participating in receptor endocytosis and trafficking (MAITRA *et al.* 2006). The subcellular distribution of Merlin in the tracheal system could not be analysed by immunostaining due to unavailability of the antibody. Therefore, I tested for the presence of Merlin in trachea by reverse transcription PCR (RT-PCR). Tracheae from wild type larvae were dissected and total RNA was isolated from the dissected samples. cDNAs were synthesised by reverse transcription reaction followed by detection with PCR with oligonucleotides specific for *slik, moesin, Merlin* and *ex*.

Oligonucleotides used spanned over two exons so that amplicons from both genomic DNA and transcripts were identifiable as genomic products were larger than the products amplified from transcripts. As control, ribosomal protein L32 (RpL32), a component of the 60S subunit of the ribosome was used. The results showed that in addition to *slik* and *moesin*, as observed with immunostaining, both *Merlin* and its interaction partner *ex* were indeed expressed in the tracheal system (Fig.28).
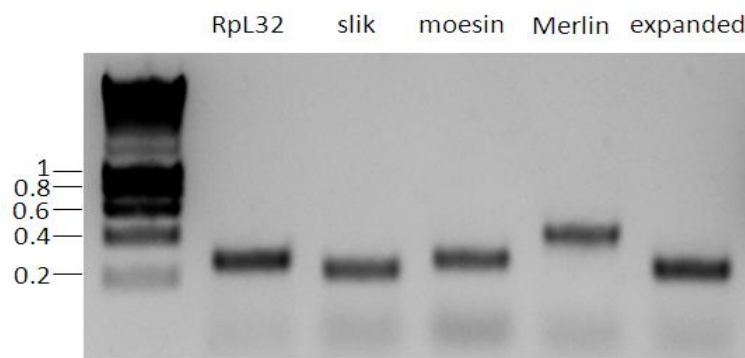
Figure 28: *slik*, *moesin* and *Merlin* are expressed in the *Drosophila* tracheal system
RT-PCR using tracheal cDNA shows that *slik*, *moesin* and *Merlin* are expressed in the tracheal system. The products here are amplicons from cDNA as they are of expected sizes. The control, RpL32 encodes for the ribosomal protein L32. The RT-PCR shows that Expanded, a protein distantly related to Merlin and also an interaction partner of Merlin is expressed in the tracheal system.
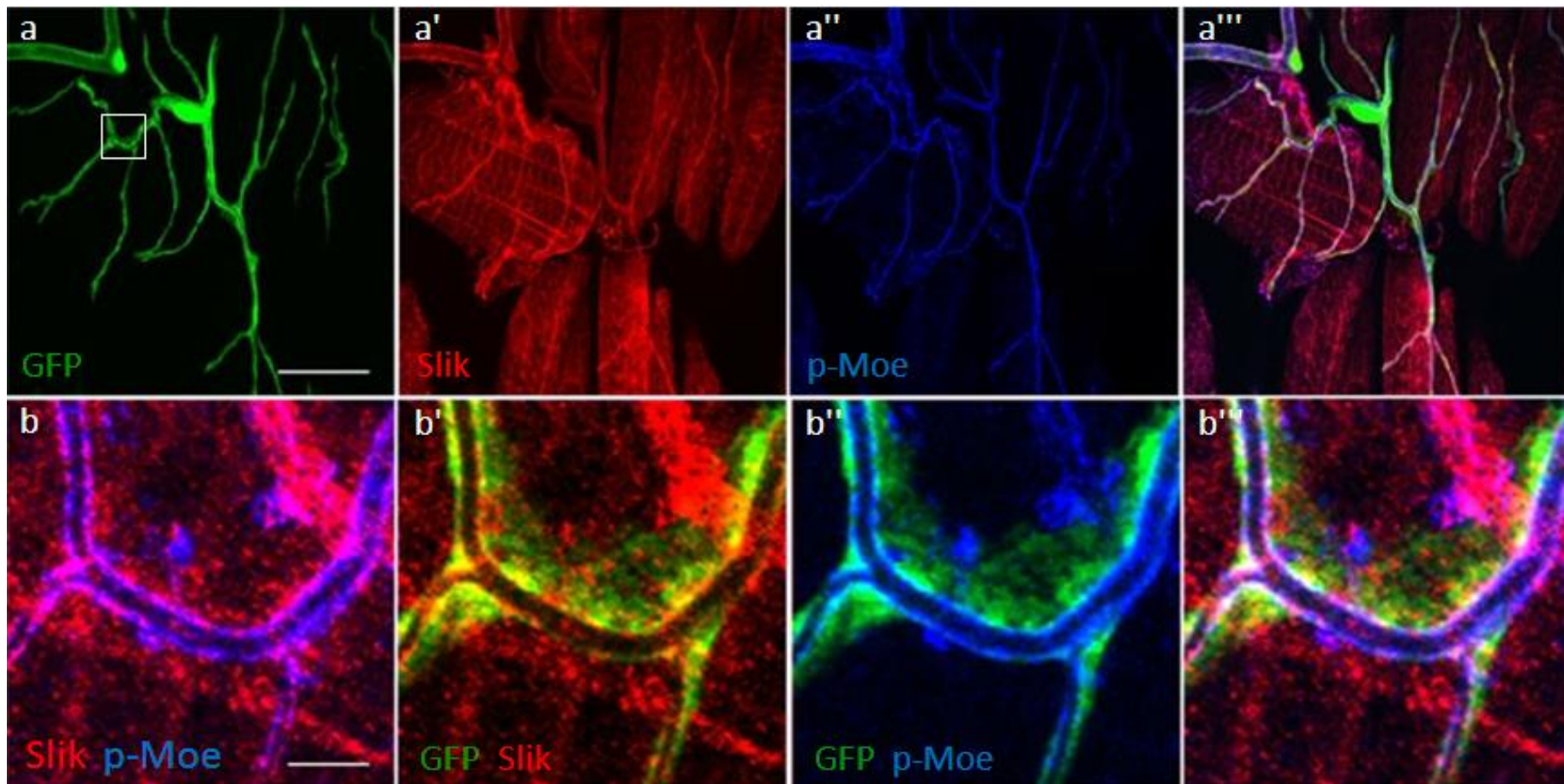
Figure 29: Slik and phosphorylated Moesin colocalise at the apical membrane within terminal cell branches
(a-a''') Tracheal cells are visualised by tracheal specific cytoplasmic GFP (green), antibodies specific for Slik (red) and the phosphorylated form of Moesin (p-Moesin) (blue). **(b -b''')** enlargement of the corresponding area in image **a** (boxed) showing; **(b)** Slik - Moesin colocalisation at the apical membrane; **(b')** Slik and **(b'')** p-Moesin enrichment at apical membrane; **(b''')** overlay of GFP, Slik and p-Moesin. Positions at which all three proteins are present are seen as white in the overlay, and are restricted to the apical membrane of the cell. Scale a - 50 µm, b - 5 µm.

3.3 Slik and Moesin colocalise at the apical membrane in terminal cells

The above observations from immunostainings and RT-PCRs have confirmed the expression of Slik and its phosphorylation targets Moesin and Merlin in the tracheal system. To investigate if Moesin was indeed a target of Slik in the tracheal system like in other tissues, I first investigated the localisation of these two proteins by double labelling with both anti-Slik and anti-p-Moesin antibodies. The stainings were performed in larvae expressing cytosolic GFP in the tracheal system under the *btl*Gal4 driver (Fig.29). The immunostainings were visualised by detection with secondary antibodies coupled to fluorophore (Alexa Fluor®) dyes. Analysis of the immunostainings revealed that Slik and Moesin colocalised at the apical membrane of terminal branches (Fig.29b), which was consistent with earlier reports on wild type wing imaginal discs (HIPFNER *et al.* 2004).

3.4 Knockdown of *moesin* in the tracheal system results in phenotypes similar to slik RNAi

Moesin plays multiple roles in *Drosophila* development and is involved in processes such as oocyte anterior/posterior axis specification (JANKOVICS *et al.* 2002), actin cytoskeleton organization (KUNDA *et al.* 2008), establishment or maintenance of epithelial cell apical/basal polarity of larval imaginal disc epithelium (SPECK *et al.* 2003) and rhabdomere development (KARAGIOSIS and READY 2004). In addition, Moesin is regulated by Slik kinase activity. As *moesin* mutant animals are not viable, I used *moesin* RNAi constructs to study the effect of Moesin depletion in the tracheal system. The *moesin* RNAi construct VDRC 37917 was used along with UAS-dicer and UAS-GFP driven by *btl*Gal4 to have a tracheal specific expression. However, only very few progeny grew up to third instar larval stages and these were comparable in size to a wild type first instar larva. To reduce the severity of the knockdown phenotype I performed the knockdown without expressing dicer. The larvae thus obtained were of moderate size and suitable for dissection.

moesin mutant terminal cells exhibited abnormal branching and lumen phenotypes as observed in case of *slik* knockdown. The number of branches in terminal cells of *moesin* mutant larvae was significantly reduced compared to wild type larvae (Fig.30). Moreover, the

mutant terminal cells also showed the multilumen phenotype (Fig.30b) though the phenotype was not completely penetrant. Apart from *slik* mutants, multilumen phenotype has also been reported with mutants for *bitesize* (*btsz*). A previous study showed that Btsz protein localised apically in epithelial cells and was required for recruiting Moesin to the adherens junctions (PILOT *et al.* 2006). Work from our lab showed that *btsz* RNAi in tracheal cells lead to destabilised tubes and similar branching defects (unpublished data Jayan N. Nair Appendix Fig.49).
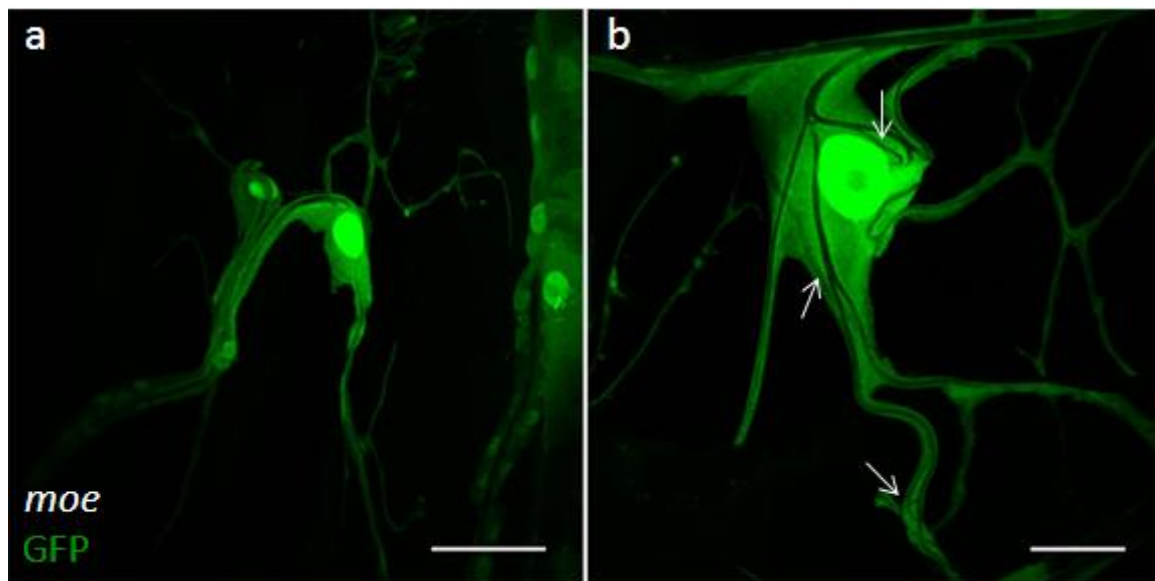
Figure 30: Effect of *moesin* RNAi on terminal cells
moesin RNAi transgene was expressed in trachea marked with cytosolic GFP. Terminal cells from a third instar *moesin* knockdown shows **(a)** a terminal cell with few branches; **(b)** a terminal cell displaying the multilumen phenotype, multiple lumens are marked by arrows. Scale a - 50 µm, b - 25 µm

3.5 Knockdown of *Merlin* and *expanded* in the larval tracheal system

Previous studies showed that Slik negatively regulated Merlin through phosphorylation. Since RT analysis of the tracheal system confirmed the expression of *Merlin*, I investigated whether *Merlin* has any role in larval tracheal development. For this purpose, *Merlin* RNAi construct VDRC 7161 was used along with the UAS-dicer and UAS-GFP driven by *btl*Gal4 to achieve tracheal specific expression. Knockdown of *Merlin* in the tracheal system did not affect the larval growth unlike the *slik* and *moesin* knockdowns, more importantly the knockdown did not result in branching defects as seen with *slik* and *moesin* RNAi.

However, *Merlin* knockdown resulted in terminal cells with abnormal morphology. To exclude the possibility that the phenotype was an off-target effect, I tested the predicted off-target *Cad96Cb* as control. RNAi for *Cad96Cb* did not result in any tracheal phenotypes. Terminal cells from *Merlin* knockdown larvae showed a phenotype different from those observed previously for *slik* or *moesin*. Terminal branches were larger in comparison to the wild type branches. Though the terminal cell nuclei were of comparable sizes, the branches from *Merlin* depleted cells appeared to have large amounts of cytoplasmic material (Fig.31). This phenotype was unexpected, but fits with the known function of *Merlin*, a tumour suppressor. *Merlin* mutants tissues and organs are known to grow to enormous sizes (Yi and Kissil 2010).
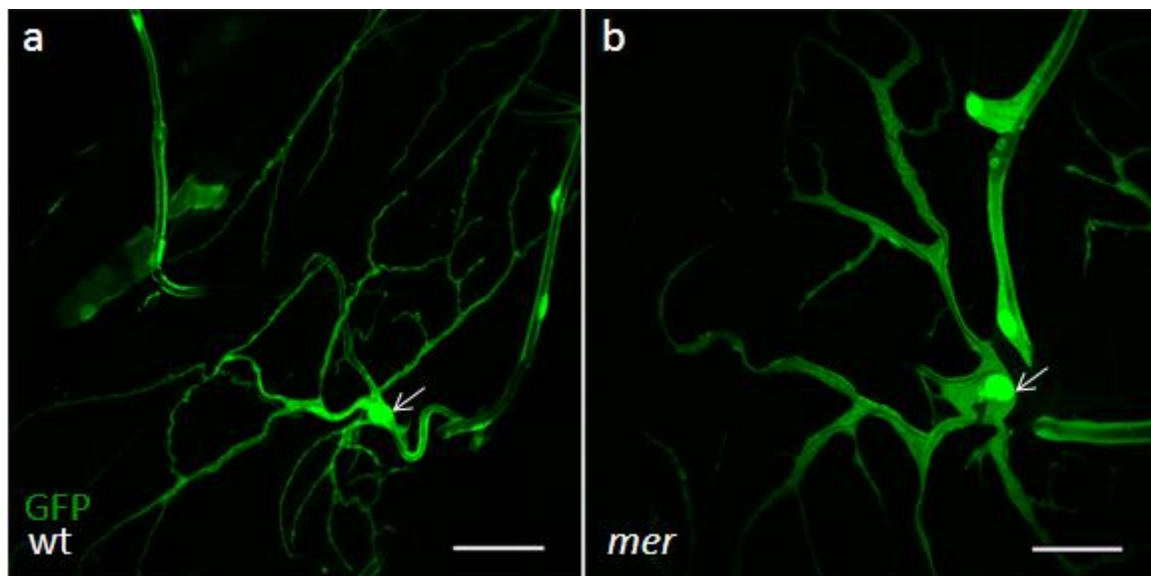
Figure 31: Effect of *Merlin* RNAi in larval terminal cells
Tracheal system is visualised by tracheal specific cytoplasmic GFP (green) expressed using *btl*Gal4. **(a)** Wild type terminal cell; **(b)** terminal cells from a *Merlin* knockdown larvae showing increased cytoplasm in the branches. Note nuclei (marked by arrows) are of comparable sizes. Scale - 50 µm.

Since *Merlin* RNAi did not result in any phenotypes similar to either *slik* and/or *moesin* knockdowns, I investigated if the difference was due to the presence of Ex the interaction partner and a protein functionally redundant to Merlin. To determine if Ex had any role in terminal cell development, *ex* specific RNAi construct was expressed in the tracheal system. The line used in the experiment was VDRC 109281, which had no predicted off-targets. However, the knockdown of *ex* in trachea did not result in any observable phenotype whatsoever. This suggests that Ex has no function in terminal cell development.

Alternatively, since *ex* RNAi knockdown was performed alone, the possible compensation by Merlin for the loss of Ex in trachea cannot be ruled out.

3.6 Knockdown of *slik* leads to loss of activated Moesin in terminal cells

Moesin is activated by phosphorylation on the conserved threonine residue (T^{556}) in the C-terminal domain of the protein. It is known that Slik can phosphorylate Moesin and that activated Moesin (p-Moesin) is lost in $slik^{1}$ clones and on *slik* RNAi in S2 cells. To study the phosphorylation of Moesin in *slik* mutant terminal cells, I performed immunostainings with the p-Moesin antibody in third instar larvae. Third instar larvae expressing UAS-*slik* RNAi (VDRC 43783), UAS-GFP and UAS-dicer under the *btl*Gal4 were dissected to analyse the tracheal system. p-Moesin staining was performed on *slik* depleted and as well as wild type larvae.
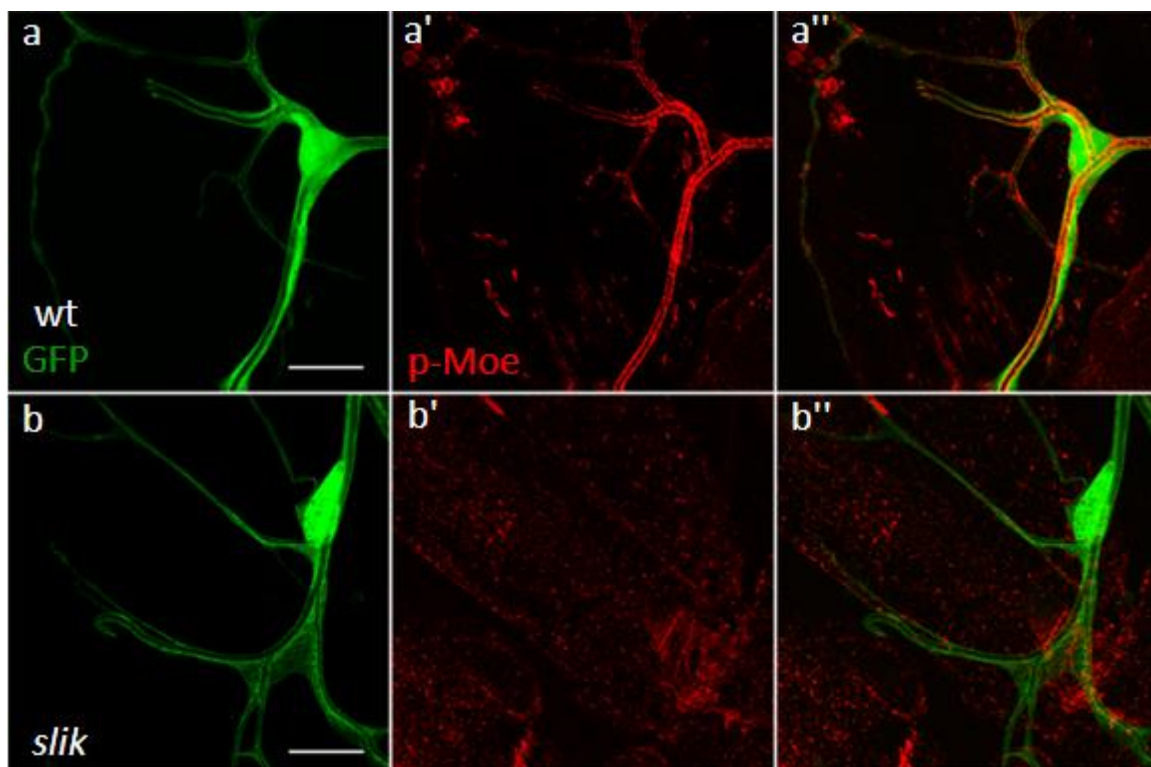
Figure 32: Effect of *slik* RNAi on p-Moesin levels in larval terminal cells
Terminal cells from larvae of the genotypes (**a-a''**) wild type; (**b-b''**) *slik* RNAi, visualised by tracheal specific cytoplasmic GFP (green) and p-Moesin (red). p-Moesin expression is lost in terminal cells of a *slik* knockdown larva (**a'** and **b'**). p-Moesin is expressed in all tissues therefore Moesin from surrounding tissues is also detected. Scale - 25 µm.

In wild type terminal cells, p-Moesin was localised at the apical membrane of the terminal cell branches (Fig.32a). However, in *slik* mutant terminal cells, the apical localisation of p-Moesin was completely lost (Fig.32b), consistent with loss of p-Moesin in the *slik[1]* clones in wing disc. Even with increased exposure parameters while imaging no p-Moesin was detected in the terminal branches in case of mutants, which is substantiated by the effect of increased signal from underlying muscle tissue exceeding levels seen in wild type (compare Fig.32a' and b'). As all tissues express p-Moesin, p-Moesin is detected from underlying muscle tissues. These results confirm that Slik regulates p-Moesin expression/localisation at the apical membrane in the terminal cells and that loss of Slik leads to the subsequent loss of p-Moesin from terminal branches. The results are consistent with previously published data from wing disc (HIPFNER and COHEN 2003; HIPFNER *et al.* 2004).

3.7 Slik's kinase function is critical in terminal cell lumen formation

Loss of Slik from the tracheal system lead to the loss of phosphorylated Moesin and also resulted in similar tracheal phenotypes, i.e. multilumen defects. The multilumen phenotype probably results from the destabilisation of tubes resulting from depletion of the activated crosslinker p-Moesin, the function of which is regulated by Slik. To test this, I expressed the following functional variants of Slik in the tracheal system - Slik kinase dead (Slik^{kd}) and Slik kinase domain (Slik^{kin}) (Fig.33). Slik^{kd} is a slik mutant construct that lacks the kinase function as a consequence of a missense mutation in Asp^{176} residue within the kinase subdomain VII of the protein (HIPFNER and COHEN 2003). The Slik^{kd} mutation does not interfere with the protein's ability to carry out its kinase independent function through the interaction with Raf (HIPFNER and COHEN 2003). On the other hand the Slik^{kin} construct retains only the kinase domain and lacks all other regions of the protein. Expression of the Slik^{kin} construct in wing disc has shown to increase levels of p-Moesin in cells (HIPFNER *et al.* 2004).

Slik^{kd} overexpression in the larval tracheal system resulted in lethality during early larval stages and therfore only very few third instar larvae expressing the construct were obtained. Larvae from the overexpression experiment were dissected to examine the terminal cells. Overexpression of the Slik^{kd} construct resulted in terminal cells displaying the multilumen phenotype, similar to Slik/Moesin depletion (Fig.34a), suggesting that Slik's kinase function

is responsible for the Slik depletion phenotype. A similar effect was observed with Slik[kin] overexpression, resulting in lethality with very few escapers. Examination of the terminal cells from Slik[kin] overexpressing larvae revealed the occurrence of the multilumen phenotype (Fig.34b). On the other hand, expression of UAS-*slik* constructs did not result in any observable phenotypes in the tracheal system.
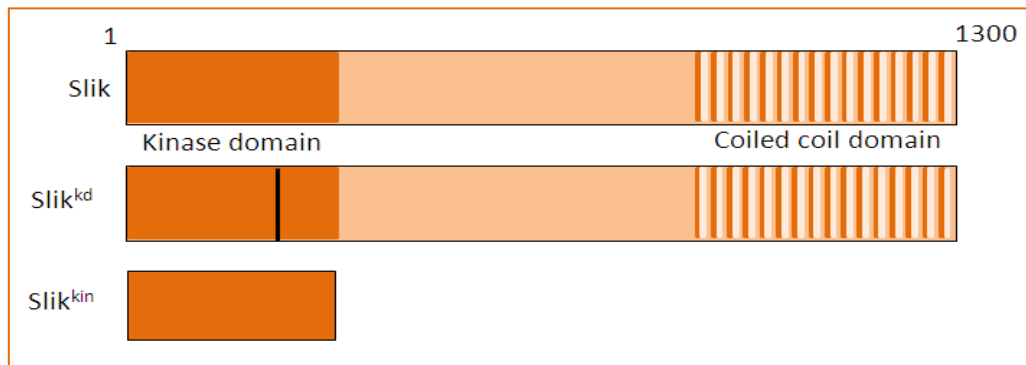
Figure 33: Schematic representation of Slik variants used in the tracheal system
Two variants constructs of Slik were used to study the effect of interfering with Slik kinase function. Wild type Slik protein is about 1300aa. The Slik kinase dead (Slik[kd]) construct is mutated in the kinase domain via substitution of the aspartate[176] to asparagine and therefore is not capable of performing the phosphorylation function. The Slik kinase domain (Slik[kin]) construct lacks the entire C-terminus retaining only the kinase domain of the protein.
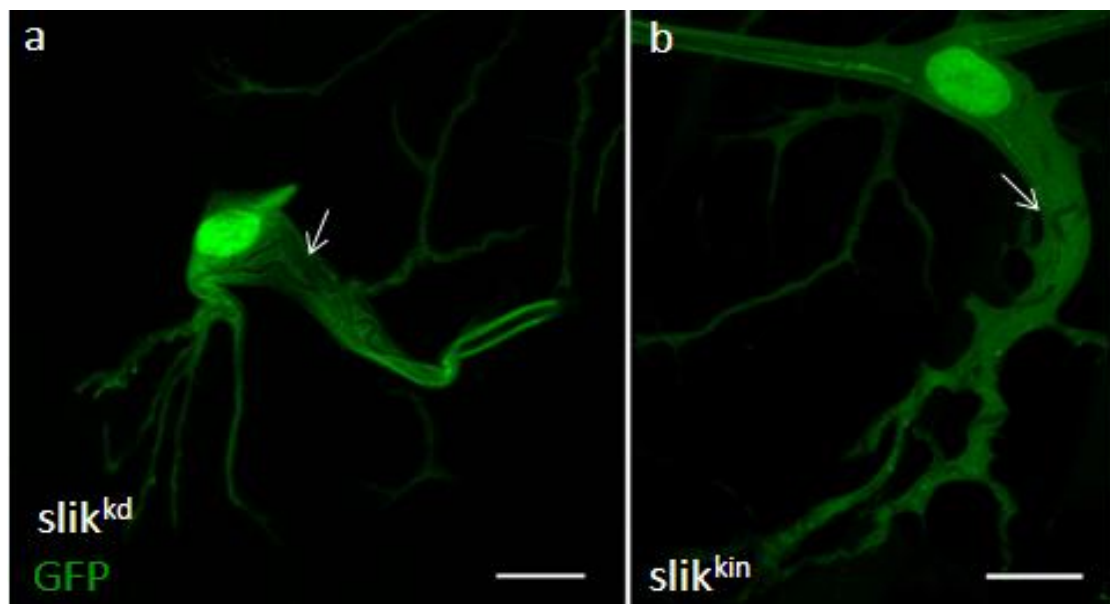
Figure 34: Effect of overexpression of the kinase variants of Slik
Terminal cells from third instar larvae visualised by tracheal specific cytoplasmic GFP (green) in (a) Slik[kd] overexpressing cell and; (b) Slik[kin] overexpressing cell. Over expression of both the Slik variant constructs result in the same multilumen phenotype. Scale - 25 µm.

3.8 Breathless regulates expression of p-Moesin in the tracheal system

To determine if the loss of p-Moesin seen in terminal cells was specific to *slik* RNAi, control knockdowns were also performed. I tested the expression of p-Moesin in knockdowns of other kinases expressed in the tracheal system. *btl, raf and egfr* were the kinases analysed by knockdowns. FGF signalling involving the ligand *branchless (bnl)* and the Receptor Tyrosine Kinase (RTK) *breathless (btl)* is indispensible for normal tracheal morphogenesis (GLAZER and SHILO 1991). Loss of *btl* expression or of any downstream signalling components such as *Ras* or *raf* perturbs tracheal development (LEE *et al.* 1996; REICHMAN-FRIED *et al.* 1994). Further, *egfr* is also involved in tracheal placode invagination and tracheal cell migration (CELA and LLIMARGAS 2006; LLIMARGAS and CASANOVA 1999). The results from the experiments are discussed below.

3.8.1 p-Moesin levels are affected by *breathless* knockdown

btl RNAi in the tracheal system was performed using the transgenic line VDRC 27106, a line with no potential off-target effect. The RNAi construct was expressed in the tracheal system using *btl*Gal4 along with the expression of UAS-GFP and UAS-dicer. Knockdown of *btl* was performed at 25°C unlike other knockdowns performed at 29°C as larvae at higher temperatures were small in size and difficult to dissect. The larvae were filleted to reveal the tracheal system and stained using anti-Slik antibody. The phenotypes associated with the knockdown are described in section 3.9.1.

Immunostaining for p-Moesin was done in *btl* RNAi larvae along with control larvae to check p-Moesin levels in terminal cells. Wild type larvae showed p-Moesin enriched at the apical membrane of terminal branches (Fig.35a). Surprisingly, the *btl* mutant larvae showed a complete loss of p-Moesin from the terminal cell branches (Fig.35c), similar to that observed in the case of *slik* knockdown (Fig.35b). To check if this phenotype was a result of the loss of signalling through the RTK-MAPK pathway, knockdown for *raf* was performed and analysed through immunostainings for p-Moesin.
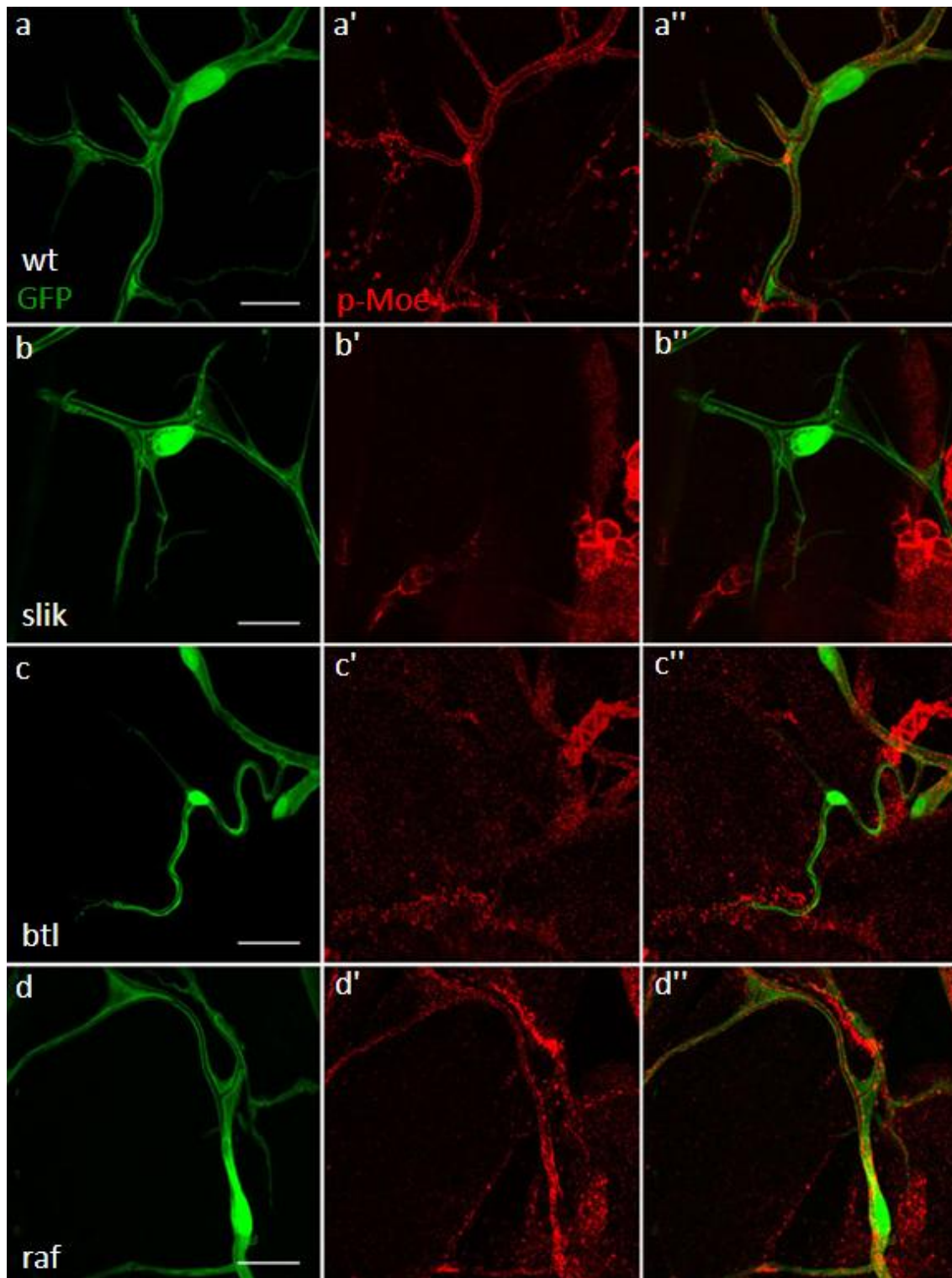
Figure 35: Effect of knockdown of *slik*, *btl* and *raf* on p-Moesin in larval terminal cells
Terminal cells from larvae of the genotypes **(a-a'')** wild type; **(b-b'')** *slik* RNAi; **(c-c'')** *btl* RNAi and **(d-d'')** *raf* RNAi, are visualised by tracheal specific cytoplasmic GFP (green) and antibodies specific for the phosphorylated form of Moesin (p-Moesin) (red). While the p-Moesin is clearly seen in surrounding tissues, levels of p-Moesin are reduced within the terminal cells upon *slik* **(b')** and *btl* **(c')** knockdown in comparison to wild type **(a')** and levels that remain unchanged in *raf* knockdown **(d')**. As p-Moesin is ubiquitously expressed, p-Moesin from underlying muscle tissue is also detected. Scale - 25 µm.

raf knockdown was performed using the RNAi transgenic line VDRC 107766 which has no predicted off-targets. Crosses set at a higher temperature (29°C) resulted in larvae of small size and therefore difficult to dissect. RNAi was performed at 25°C as in the case of *btl* knockdown. Immunostaining for p-Moesin in the *raf* knockdown larvae did not show any changes in levels of p-Moesin (Fig.35d) suggesting that *raf* or the signalling pathway downstream of Btl is not involved in maintaining p-Moesin levels in terminal cells. Together, these results indicate that both *slik* and *btl* are critical for the p-Moesin levels in the terminal cell. There are no precedents implicating *btl* as an upstream activating kinase of Moesin. In order to determine if the loss of p-Moesin was as result of transcriptional regulation of *slik* by *btl*, I performed immunostainings for Slik in *btl* knockdown larvae.

3.8.2 *breathless* RNAi does not affect slik expression in terminal cells

Staining for Slik in the tracheal system showed that Slik expression in terminal cells was not affected by *btl* knockdown (Fig.36). This result implied that Slik expression was not controlled by Btl and it was unlikely to be a transcriptional target of Btl signalling. However this does not exclude the possibility that Slik is post-translationally activated by Btl. Therefore I investigated if Moesin is a transcriptional or a post-translational target of the Btl signalling.
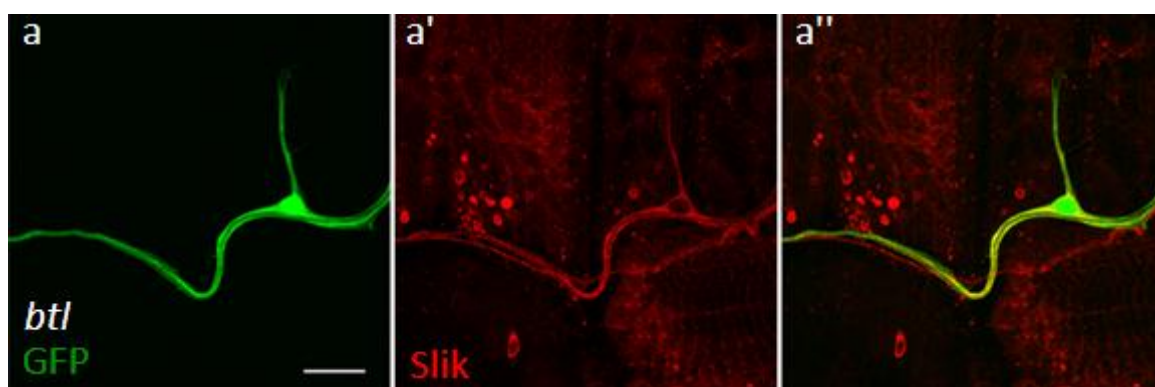
Figure 36: Effect of *btl* RNAi on Slik levels in larval terminal cells
Terminal cell from a *btl* knockdown third instar larva **(a-a'')**. **(a)** Terminal cell is visualised by tracheal specific cytoplasmic GFP (green) and **(a')** anti-Slik antibody staining (red). Slik expression is undisturbed upon *btl* knockdown. Slik expressed in surrounding tissues is also detected. Scale - 25 μm.

3.8.3 Moesin is a phosphorylation target specific to Breathless

In order to ascertain whether the observed down regulation of p-Moesin in the *btl* RNAi terminal cells was a result of transcriptional or post-translational regulation, I carried out immunostainings for Moesin using a pan-Moesin antibody (F. Payre) in wild type and *btl* RNAi larvae. Staining for Moesin in wild type terminal cells showed that Moesin was distributed within the cytoplasm, with enrichment at the apical membrane (Fig.37a). In *btl* mutant terminal branches, Moesin distribution remained unchanged. This result indicated that Moesin expression was not under the transcriptional control of Btl. Together with the observation from p-Moesin immunostainings in *btl* mutants, these results support the idea that Moesin directly or indirectly (perhaps through Slik), is a post-translational target of Btl's activity. This implies a novel role for *btl* in regulating the activity of Moesin through phosphorylation.
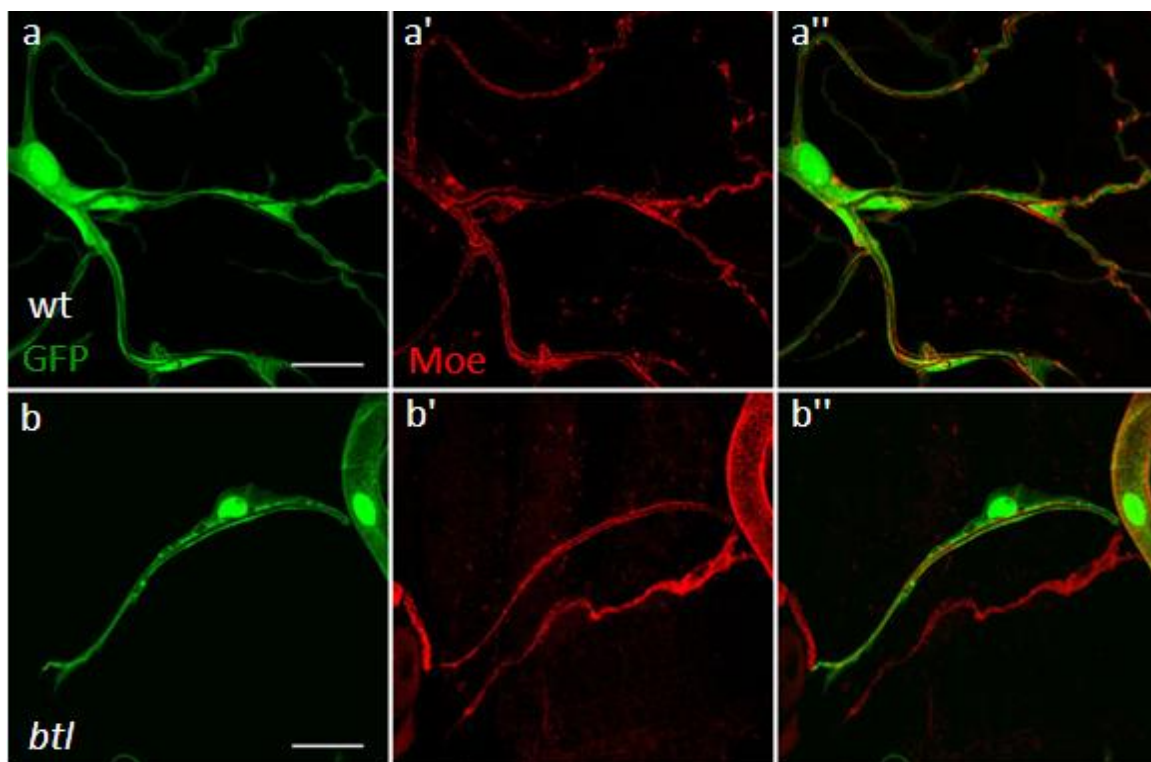
Figure 37: Effect of *btl* RNAi on Moesin levels in larval terminal cells
Terminal cells from larvae of the genotypes **(a-a'')** wild type; **(b-b'')** *btl* RNAi, visualised by tracheal specific cytoplasmic GFP (green) and antibodies specific for Moesin (red). Levels of Moesin remain unaltered in a *btl* knockdown terminal cell (a' and b'), unlike levels of p-Moesin that is reduced upon *btl* knockdown. Moesin is expressed in all tissues therefore Moesin from surrounding tissues is also detected. Scale - 25 µm.

3.9 Knockdown of RTK/MAPK pathway components affect terminal cell branching

The Bnl/Btl RTK pathway is essential for tracheal development in both embryonic and larval phases of development. The signalling from the RTK pathway is modulated through downstream effector molecules such as Ras/Raf and the MAPK. An important target of this Bnl/Btl MAPK signalling is the expression of the target gene *srf*. Srf is a transcription factor specifically expressed in the terminal cells. Loss of Srf results in loss of cytoplasmic outgrowth during terminal branching (AFFOLTER 1994; GUILLEMIN *et al.* 1996). It is also known that Slik apart from its kinase dependent function genetically and physically interacts with Raf and is consequently involved in the signalling mediated by Raf to promote cell growth and proliferation. However the growth and proliferative effect of Raf signalling has been shown to be independent of the MAPK pathway in wing imaginal discs (HIPFNER and COHEN 2003). In the tracheal system the RTK-MAPK signalling is active and we know that Slik is expressed and has a crucial role in normal tracheal development. The multilumen phenotype in *slik* RNAi can be attributed to the loss of activated Moesin, however these terminal cells also showed reduced branch growth. As *raf* functions to promote cell growth it would be interesting to know if the branching phenotype was a result of impaired Slik-Raf signalling in *slik* mutants. To study the possibility that in s*lik* mutants the branching defects could be due to perturbed signalling via Raf*,* or as a consequence of disruption of the MAPK signalling pathway and the subsequent loss of Srf expression, I performed RNAi on the components of the pathway. RNAi was performed for the following genes, the two RTKs *btl* and *egfr*, the transducers *Ras* and *raf* and finally the terminal specific target, *srf*. I analysed the outcomes from various knockdowns and scored for branching phenotypes.

3.9.1 Effect of *breathless* RNAi in the larval tracheal system

btl RNAi knockdown was performed in terminal cells as previously described in chapter 3.8.1
.

3.9.1.1 Knockdown of *breathless* disrupts branching in terminal cells

Apart from the regulation of p-Moesin described earlier, knockdown of *btl* produces tracheal defects. In *btl* RNAi terminal cells branching was severely compromised with no more than two branches per terminal cell (Fig.38). This is consistent with the branching phenotype seen in *slik* RNAi. The phenotype was observed in all terminal cells from the *btl* knockdown animals.

Figure 38: Effect of *btl* RNAi on branching in terminal cells
A terminal cell from a *btl* RNAi larva. Terminal cell were visualised by the tracheal specific expression of cytoplasmic GFP using *btl*Gal4. Depletion of *btl* severely affects growth of terminal branches and the phenotype was 100% penetrant with no terminal cells having more two branches. Scale - 25 µm.

3.9.1.2 *breathless* RNAi results in abnormal morphology of the cells of the dorsal trunk

In addition, I also examined the dorsal trunk in the mutant larvae. To visualise the cells of the dorsal trunk E-Cadherin (E-Cad) staining was performed. E-Cad localises to the membrane marking cell-cell junctions. In wild type, the dorsal trunk is composed of regular shaped cells that are intercalated, with the junctions between these cells having a smooth appearing (Fig.39a). In *btl* RNAi animals the staining showed distinct morphological changes in the cells of the dorsal trunk. The cells appeared to have lost their regular shape as visualised by the presence of irregular cell boundaries, as outlined by E-cad staining (Fig.39b).
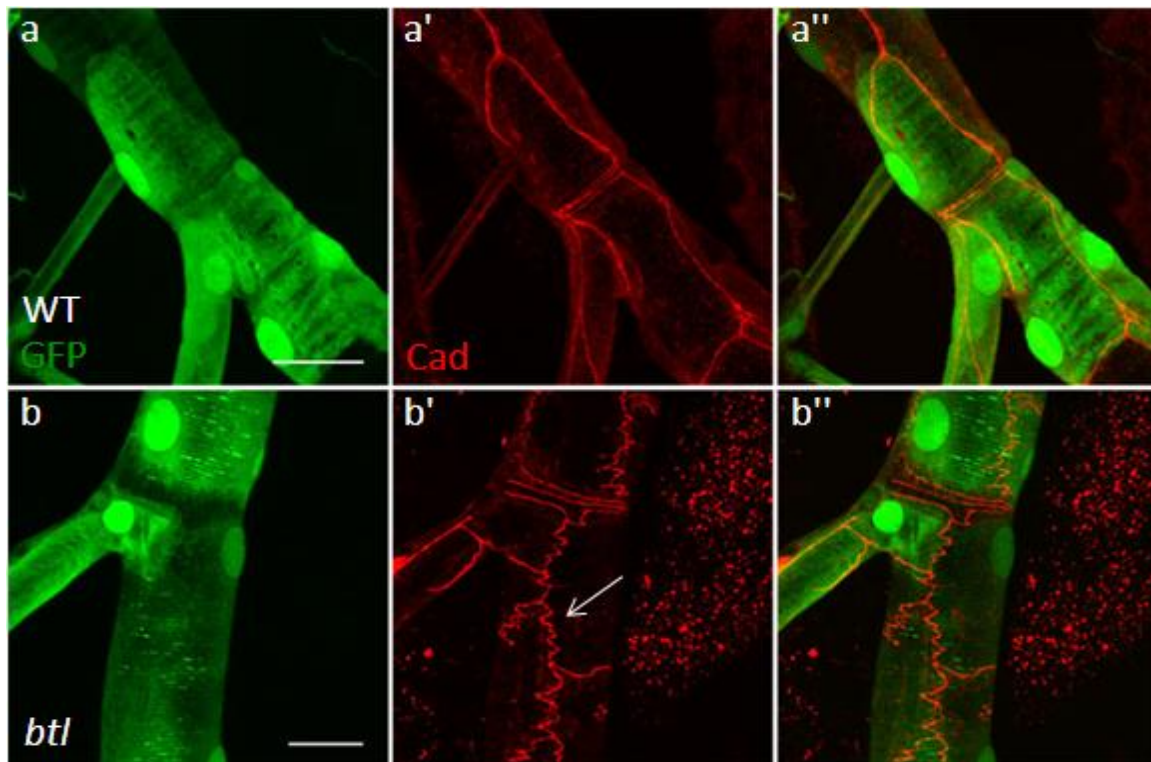
Figure 39: Effect of *btl* RNAi on the dorsal trunk
Dorsal trunk from larvae of the genotypes **(a-a'')** wild type; **(b-b'')** *btl* RNAi, visualised by tracheal specific cytoplasmic GFP (green) and antibodies specific for E-Cadherin (red). The cells that constitute the dorsal trunk in *btl* RNAi larvae showed abnormal morphology, the cell outlines were irregular in comparison to the wild type cells. E-Cad outlines the cell membrane as it is expressed at points of cell-cell contact (marked by arrow). Scale - 25 µm.

3.9.2 Knockdown of *Ras* disrupts branching in terminal cells

Ras is an important effector of FGF signalling. Ras transduces the signal from Btl to activate the MAPK signalling. Ras binds the serine/threonine kinase Raf and targets it to the membrane, which then leads to the activation of Raf, a step preceding MAPK induction in the tracheal system.

Knockdown for *Ras* was performed using the line NIG 9375-2. This line has no potential off-targets. *Ras* RNAi constructs were expressed along with UAS-GFP and UAS-dicer at 29°C. Expression of the *Ras* RNAi constructs in the tracheal system resulted in terminal cell branching defects similar to that of *slik* knockdown and *btl* knockdown discussed above. Branching in terminal cells was reduced compared to the wild type (Fig.40), albeit the phenotype was not as severe as with *btl* knockdown. *Ras* RNAi resulted in terminal cells with

branch counts ranging between 2 to 10 branches per cell. These results confirmed that tracheal branching morphogenesis was affected by knocking down components of the RTK-MAPK signalling pathway.
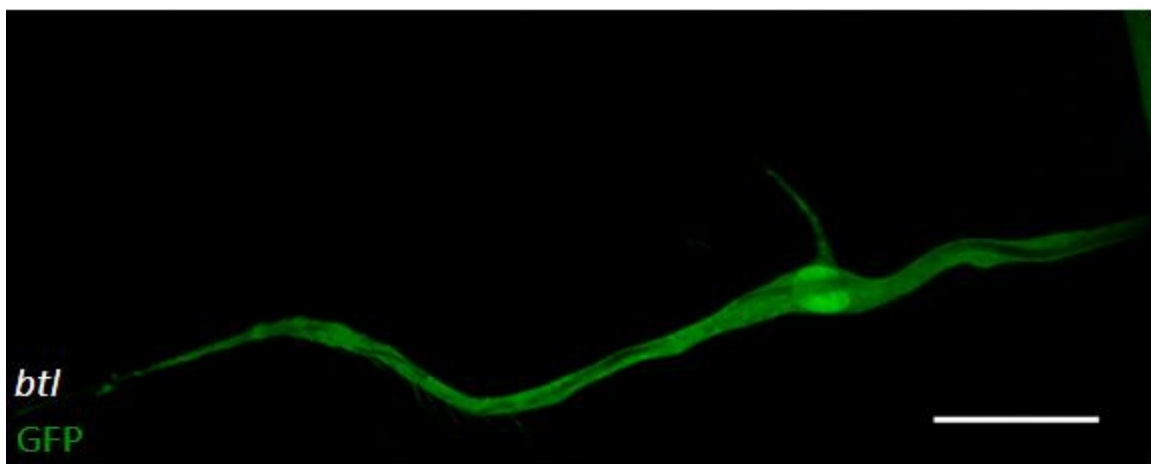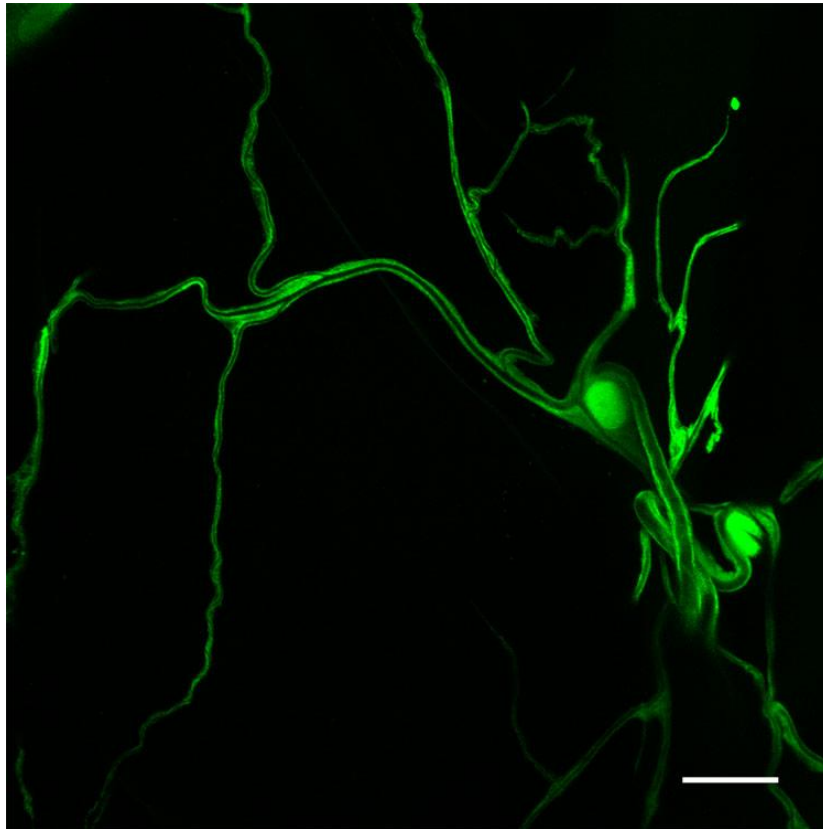

Figure 40: Effect of *Ras* RNAi in terminal cell branching
A terminal cell from a *Ras* RNAi larva. Terminal cells were visualised by the tracheal specific expression of cytoplasmic GFP using *btl*Gal4. Knockdown of *Ras* caused a moderate reduction in terminal branching. Scale - 25 µm.

3.9.3 Effect of *raf* RNAi on terminal cell development

Knockdown for *raf* was performed as described in section 3.8.2.

3.9.3.1 Knockdown of *raf* branching in terminal cells

raf RNAi resulted in various tracheal defects. The most prominent phenotype was reduction in terminal cell branching as with other members of the RTK pathway, *btl* and *Ras* or *slik*. Knockdown of *raf* resulted in terminal branches with approximately 4-10 branches per cell (Fig.41). This phenotype was fully penetrant and therefore observed in all terminal cells of

the knockdown larvae. Also, the knockdown induced lethality at pupal stages. However, the branching phenotype observed was not as severe as observed with the *btl* knockdown. In addition, *raf* knockdown presented additional phenotypes which are described below.
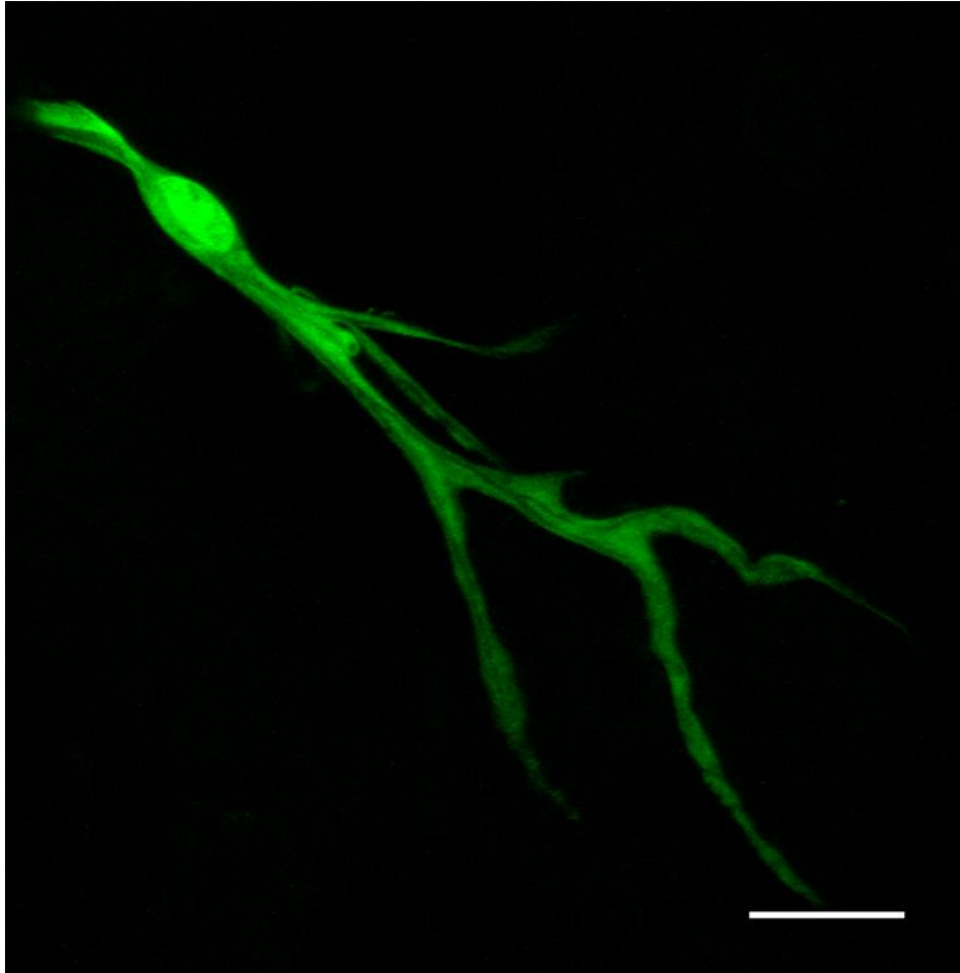
Figure 41: Tracheal specific *raf* RNAi reduces terminal branching in terminal cells
Terminal cell from a *raf* knockdown third instar larva, expressing cytoplasmic GFP in the tracheal system. *raf* RNAi results in reduced branching in terminal cells. Scale - 25 μm

3.9.3.2 Knockdown of *raf* results in cystic lumen within terminal cells

In addition to the branching defects induced upon *raf* RNAi, the terminal cells showed another. Though not a completely penetrant phenotype, I observed the presence of cystic lumen within the terminal branches. The cystic lumen phenotype is best described as a bubble-like expansion of lumen at random intervals in the branch (Fig.42). The cystic lumen phenotype was observed as a sole phenotype or in combination with the reduced branching

phenotype or even the multilumen phenotype described in the next section. This is a distinct phenotype and previously unobserved in any knockdowns of the other members of RTK-MAPK pathway.
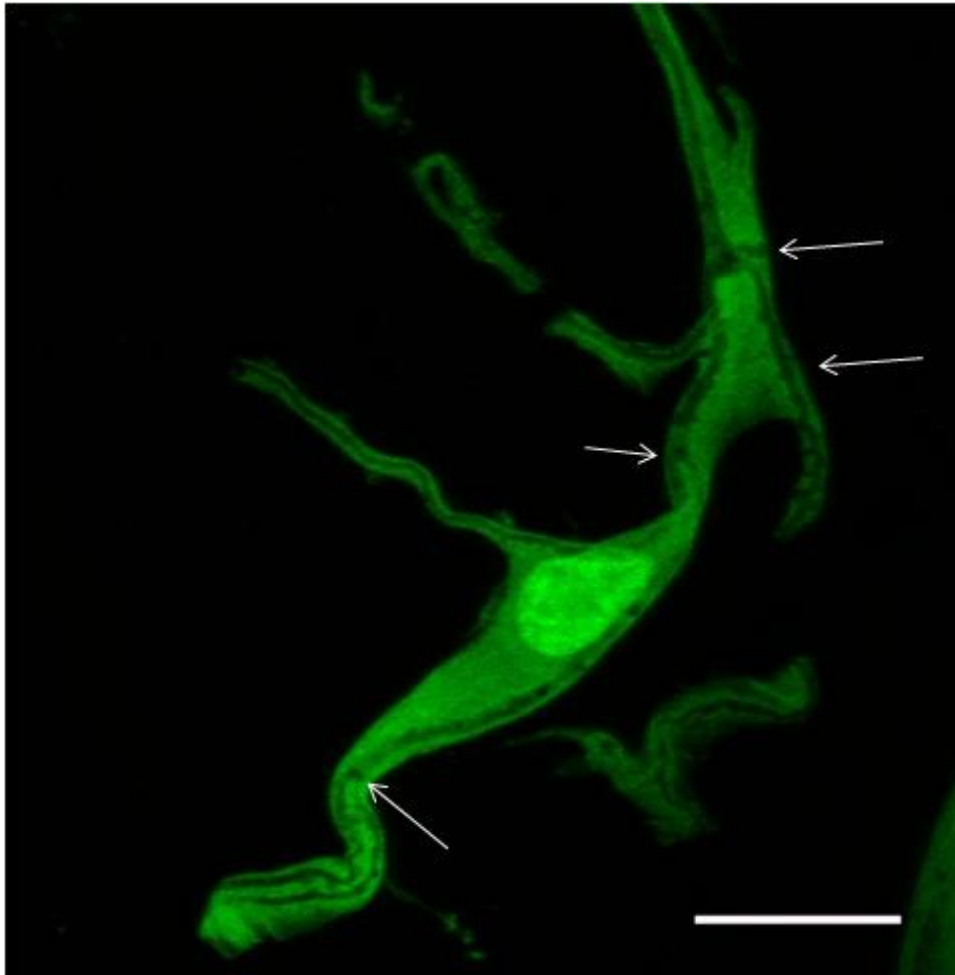
Figure 42: Tracheal specific *raf* RNAi in results cystic lumen within terminal cell
Terminal cell from a *raf* knockdown third instar larvae were imaged. The larval trachea is visualised by the expression of cytoplasmic GFP by *btl*Gal4. In addition to the branching phenotype the knockdown also resulted in luminal phenotypes, cystic lumen (marked by arrow) phenotype. Scale - 25 μm.

3.9.3.3 Knockdown of *raf* results in multilumen phenotype in terminal cells

A third phenotype commonly observed in the tracheal system of *raf* RNAi larvae was the multilumen phenotype. The terminal cells showed the occurrence of multiple tubes within a branch with or without additional phenotypes (Fig.43).
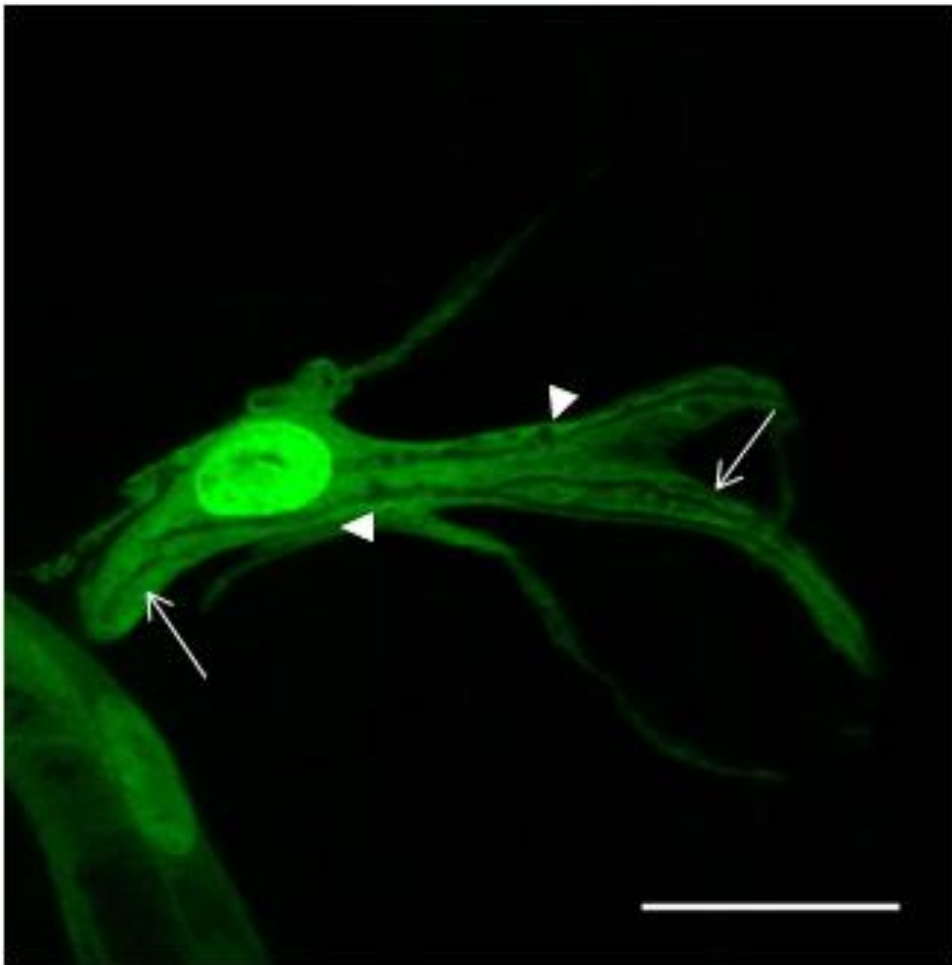
Figure 43: *raf* RNAi in terminal cells results in the multilumen phenotype
The terminal cells were visualised by expression of cytoplasmic GFP using the *btl*Gal4 driver. Upon *raf* RNAi terminal cells often resulted displayed in the multilumen phenotype (marked by arrows). Sometimes the multilumen phenotype was observed in combination with other phenotypes; here multilumen phenotype is present along with the cystic lumen phenotype (marked by arrow head). Scale - 25 μm.

3.9.4 Knockdown of *srf* disrupts branching in terminal cells

srf is a target of the FGF-MAPK signalling and a transcription factor that is critical in terminal cell development. *srf* mutants have abnormal terminal branching (GUILLEMIN *et al.* 1996). In order to make a phenotypic comparison between *slik* and *srf* mutant phenotypes I performed *srf* RNAi in the tracheal system. Srf in the tracheal system was depleted using RNAi constructs for *srf* expressed using *btl*Gal4 along with the expression of UAS-GFP and UAS-dicer constructs. The line used was VDRC 100609, which had no predicted off-targets and the RNAi was performed at 29°C. The knockdown resulted in animals with reduced body size. Third instar larvae from the knockdown experiment were dissected and imaged.

Analysis of the mutant larvae showed abnormal tracheal development. Branching was affected in almost all terminal cells of the knockdown larvae (Fig.44). The phenotype was similar to that observed with *btl* knockdown and any other members of the Btl/MAPK signalling pathway. The phenotype was also consistent with previously published data on *srf* mutants (AFFOLTER 1994; GUILLEMIN *et al.* 1996). In addition, the knockdown larvae did not progress to pupal stages.
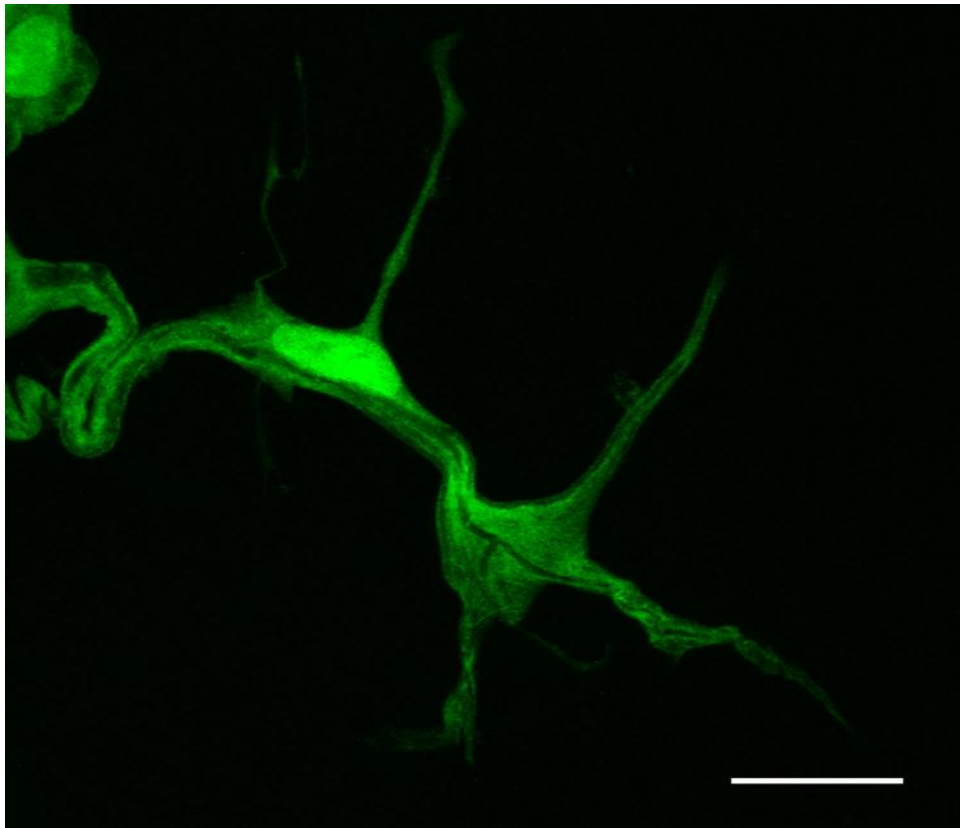
Figure 44: Effect of s*rf* RNAi on terminal cell branching
A terminal cell from a third instar larva upon *srf* knockdown, also expressing cytoplasmic GFP in the tracheal system. The knockdown resulted in severe reduction in terminal branching. Scale - 25 μm.

3.9.5 Knockdown of *egfr* disrupts branching in terminal cells

In addition to the RTK Btl, I also studied the effect of knockdown of the other functional RTK in the tracheal system; viz. *egfr*. Egfr plays an important role in tracheal placode invagination and migration of primary branches. To examine the role of EGFR in terminal cell development I performed *egfr* RNAi using the line VDRC 107130.

Knockdown of *egfr* resulted in a moderate reduction of branching in terminal cells (Fig.45). *egfr* knockdown animals entered pupal phases of development but did not eclose. The terminal cells showed a reduction in branch numbers but no other phenotypes were observed.
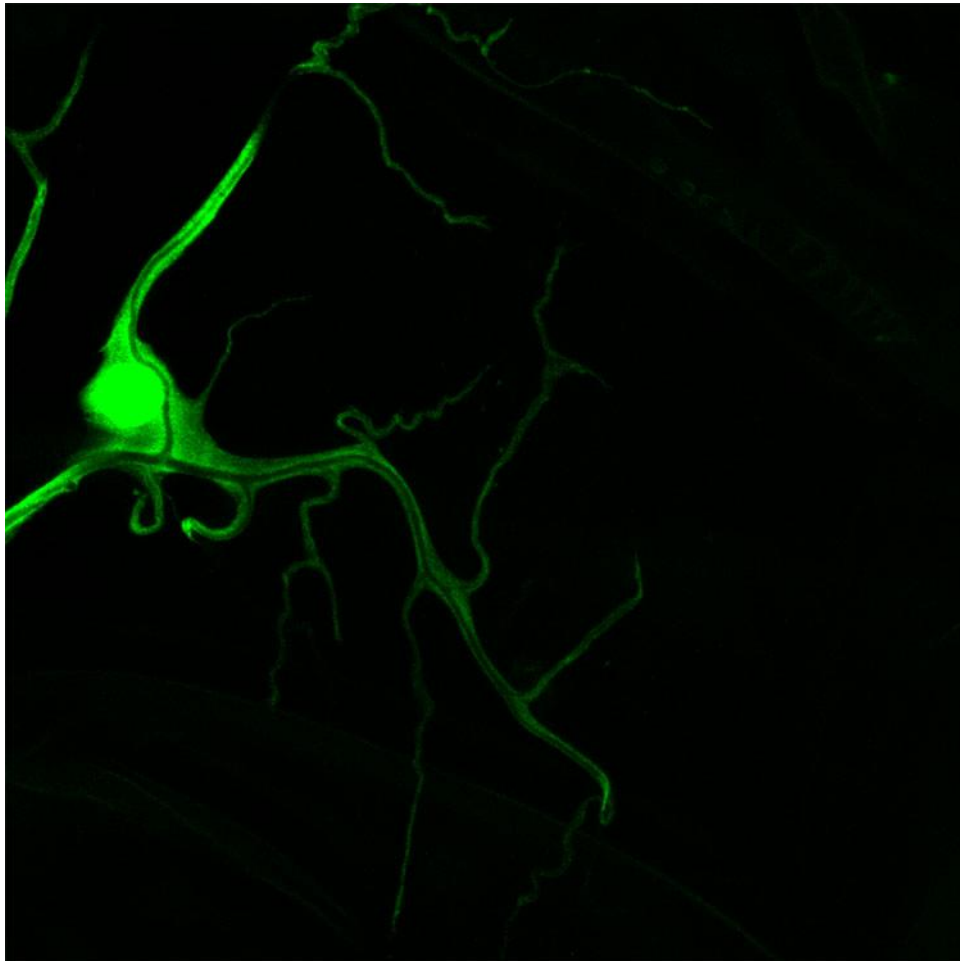
Figure 45: Knockdown of *egfr* in the tracheal system affects terminal branching
egfr knockdown was performed specifically in the tracheal system with RNAi constructs expressed using *btl*Gal4. Also expressed in the trachea were UAS-dicer and UAS-GFP, the latter was used to help visualise the tracheal system. The RNAi resulted in a moderate reduction of terminal branch numbers. Scale - 25 µm.

3.9.6 Evaluation of branching phenotype in mutants of RTK and downstream components

As described in the previous sections, knockdowns for *slik, Ras, raf, srf, btl and egfr* all resulted in a branching phenotype. To evaluate and derive a phenotypic correlation between individual knockdowns for the branching phenotype I counted branches from terminal cells from each of the knockdowns. For this purpose, terminal branches from a specific subset of

terminal cells called the dorsal terminal cells were counted. Dorsal terminal cells are the two terminal cells found at the region of dorsal branch fusion (Fig.46). Branching points were counted in dorsal terminal cells from the tracheal segments tr3- tr5 (Fig.21a). These segments were identified by the presence of the tracheal stem cell cluster, the tracheoblasts (Fig.21b). A branching point was scored when the branch in question contained a lumen within and that the lumen was continuous with the lumen from the preceding branch (Fig.47). Cytoplasmic extensions from an existing branch bearing no lumen within were not scored for. Terminal cell branch count was performed on an average of 5-6 larvae, as often only 1-2 intact dorsal terminal cells from tr3-tr5 were obtained after dissection, partly due to the difficulty in dissection of small-sized animals resulting from knockdown.
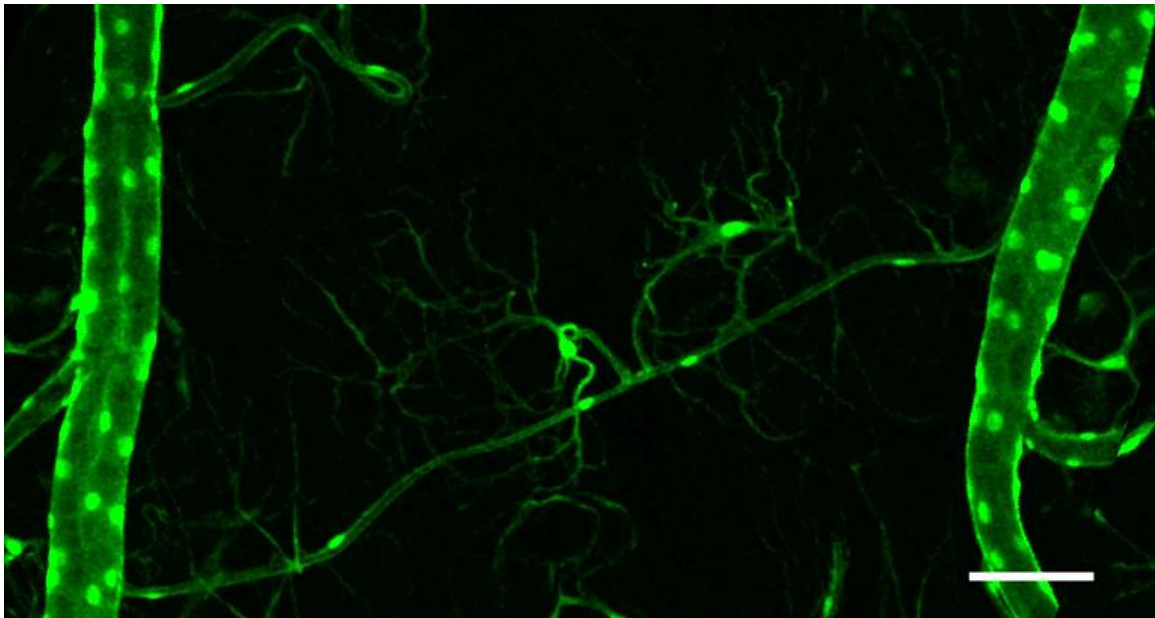
Figure 46: Overview of the dorsal terminal cells in the third instar larva
The tracheal system is visualised by the expression of cytoplasmic GFP in a tracheal specific manner using *btl*Gal4. Visible here are the two dorsal trunks in a segment of the larva, from each of which arise a dorsal branch directed to the midline of the animal. The dorsal branches fuse with each other at the body midline and project two terminal cells beyond this fusion point. These terminal cells arising beyond the point of the fusion cells are called referred to as the dorsal terminal cells. Scale - 100 µm.
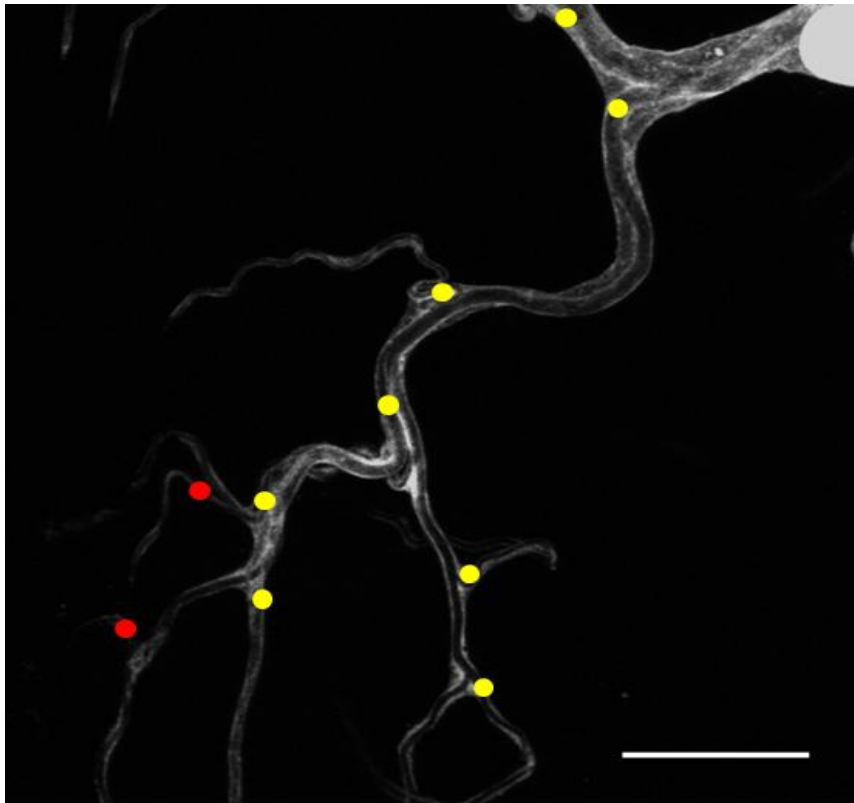
Figure 47: A terminal cell from a third instar wild type larva
A branching point is considered so when the tube within the branch is connected to the tube from the preceding branch (yellow dots). Cytoplasmic extensions that do not contain a tube within are not considered as branching points (red dots). Scale - 25 μm.
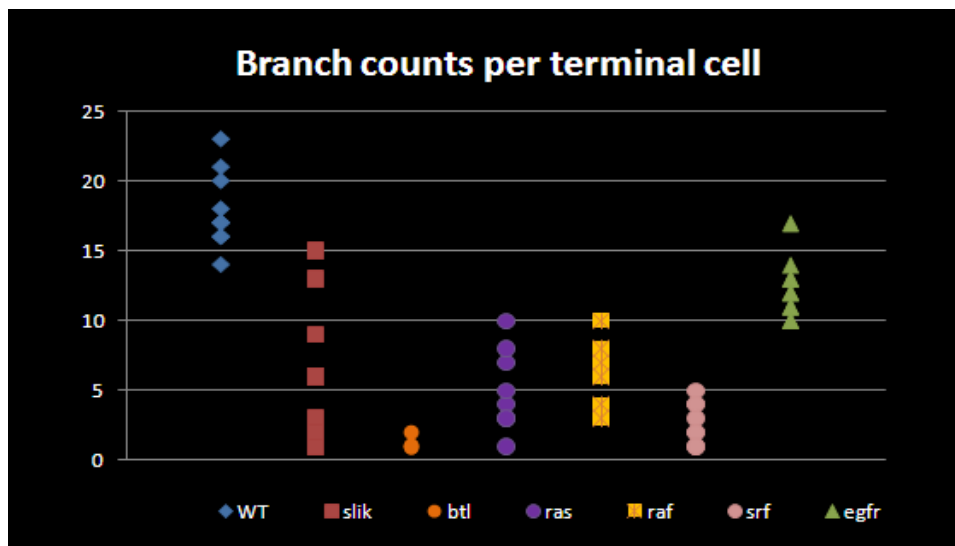
Figure 48: Number of branches in dorsal terminal cells from wild type and mutant larvae
Number of branching points was counted for dorsal terminal cells in wild type, *slik, btl, Ras, srf, and egfr* knockdowns. To visualise terminal cells cytoplasmic GFP was expressed in the tracheal system using *btl*Gal4, third instar larvae were filleted and the terminal cells were analysed. Numbers of branching points are plotted as dots; each dot represents the number of branching points for one cell, a total of 10 terminal cells were counted per genotype (*n=10*). The following were the average number of branches per cell along with their p-values from a Student's t-test: wild type 17.95 ± 2.69, *slik* 6.3 ± 4.76, p=2.72×10^{-6}, btl 1.1 ± 0.32, p= *btl* 1.75×10^{-14}, *Ras*

4.3 ± 3.16, p= $5.1\text{x}10^{-9}$, *raf* 5.9 ± 2.51, p=$5.5\text{x}10^{-9}$, *srf* 2 .7± 1.34, p= $4.35\text{x}10^{-12}$ and *egfr* 12.3 ± 2.11, p= $6.25\text{x}10^{-5}$

Branch counting was performed in the tracheal knockdowns for *slik, btl, egfr, Ras, raf, srf* along with wild type as control. Branches from individual terminal cells were counted and plotted on a scatter plot. Branch counts form 10 dorsal terminal cells were analysed. Each dot on the scatter plot represents the number of branches in a single dorsal terminal cell (Fig.48). Branch counting in wild type terminal cells showed that average branch numbers in these cells were about 17.95 ± 2.69 (*n=10*). Branch counting from the knockdown animals showed that all knockdowns influenced terminal cells branch numbers but to different degrees (Fig.48, values in Appendix Fig.52). Branch counts revealed an overall reduction in the number of branches per cell. A Student's t-test was also done to calculate the p-values for the branch numbers. The p-values obtained were highly significant with all p values being p <0.001. These results confirmed that branching is indeed perturbed in knockdowns of *slik,* its interaction partner *raf* and members of the RTK-MAPK signalling and its target, *srf.*

4. DISCUSSION

The *Drosophila* tracheal system is commonly used as a model to study the molecular and cellular basis of tube morphogenesis. Although several studies have focussed on understanding tracheal patterning and tube formation, the events that lead to the tracheal development in larval phases remain largely unexplored. Our interest in the tracheal system focuses on the development of the terminal cells, the cells that deliver oxygen to the target tissues. Of particular interest is the mechanism of terminal branch development and lumen formation. Very little is known about the molecular and cellular aspects of terminal cell development. Earlier studies in the larval tracheal system have shown that tube formation within terminal cells is ensued by tube stabilisation. Only a handful of candidate genes have been identified with respect to fulfilling these functions. Tube stabilisation has been shown to require talin (*rhea*) and integrins (*mew, if, mys*) (LEVI *et al.* 2006), while the lumen formation requires the apical polarity complex Baz/Par6/aPKC, Crumbs, Btsz, Ikkε, Dlis-1 (Jayan N. Nair, PhD thesis) (GERVAIS and CASANOVA 2010; OSHIMA *et al.* 2006). It is understood that Moesin, by regulating actin organisation at the apical membrane, is essential for terminal branching and tube development (POLESELLO *et al.* 2002) (Jayan N. Nair, PhD thesis). While it is known that Moesin is essential for tube formation, it is not clear whether Moesin regulates the process of tube formation or whether it is required subsequent to tube formation in order to stabilise the newly formed tube. Moesin is a well characterised membrane anchor for the actin cytoskeleton and studies have shown that activation of Moesin through phosphorylation is a prerequisite for this function. Until recently, the kinase that activates Moesin was unknown, studies in wing imaginal discs identified Slik (a member of the Sterile-20 kinase family) as the activation factor (HIPFNER and COHEN 2003; HIPFNER *et al.* 2004). This study demonstrates the functional relevance of Slik in the development and maintenance of the larval tracheal system.

4.1 Persistent Slik expression in all stages of tracheal development

Slik is known to regulate both Moesin and Merlin through phosphorylation leading to distinct effects. Phosphorylation activates Moesin, which then binds to F-actin and stabilises the actin cytoskeleton (POLESELLO *et al.* 2002). However, in case of Merlin, phosphorylation results in

the loss of its tumour suppressor function (HUGHES and FEHON 2006). In addition, Slik genetically and physically interacts with Raf in a kinase independent manner to promote growth and cell survival (HIPFNER and COHEN 2003). Previous works showed that both Slik and Moesin are enriched at the apical membrane of the wing disc epithelium and that the loss of Slik results in loss of p-Moesin (HIPFNER and COHEN 2003; HIPFNER *et al.* 2004).

My experiments to investigate Slik expression and localisation in the tracheal system showed that that Slik is indeed expressed in the tracheal system. Slik showed enriched apical localisation from the very first stage of embryonic tracheal development, which then persisted through the entire embryonic tracheal development. Interestingly, the apical enrichment of Slik in the embryonic trachea is also mirrored by F-actin distribution in the tracheal cells (Appendix Fig.54) (LLIMARGAS and CASANOVA 1999). This suggests a possible role for Slik in regulating Moesin for actin stabilisation during the tracheal development. Stainings in larvae showed that Slik was also enriched at the apical membrane within terminal cells i.e. the membrane facing the tracheal lumen. Further, coimmunostainings for Slik and E-Cad in fusion cell of the dorsal trunk demonstrated that Slik localises more apically than the E-Cad labelled adherens junctions. These finding are consistent with the previously reported distribution pattern of Slik in the wing disc epithelium (HIPFNER *et al.* 2004). Further, coimmunostainings for Slik and p-Moesin in the larval trachea showed that in addition to the enrichment of activated Moesin at the apical membrane, Moesin also colocalised with Slik in the terminal cells.

4.2 Slik is important for tracheal development in Drosophila

Earlier reports have implicated Slik in the proliferation and growth of cells in the wing imaginal disc through regulation of Moesin and Raf (HIPFNER and COHEN 2003; HIPFNER *et al.* 2004). Tracheal specific knockdown of *slik* disrupted the normal terminal cell development. The knockdown also resulted in reduced larval sizes along with perturbing further development from the larval stages. The reduced body size in larvae could be an indirect consequence of lowered metabolism due to lack of oxygenation. These results suggest that Slik's function in the tracheal system is required not only for the terminal cell

development but also for the overall development in *Drosophila*. The observed phenotypes are consistent with *slik¹* mutants and MARCM clone phenotypes. However, unlike in wing discs where *slik* mutant cells undergo apoptosis *slik* RNAi does not reduced terminal cell numbers. Careful analysis revealed branching/growth and tube formation defects in *slik* compromised terminal cells. Further, immunostainings showed that loss of Slik leads to a complete loss of activated Moesin (p-Moesin) at the apical membrane of terminal cells. This is consistent with previously published data that Slik phosphorylates Moesin and specifically at the amino acid residue Threonine[556].

4.3 Moesin is essential for tube formation and stability in terminal cells

In addition to the loss of p-Moesin, knockdown of *slik* also resulted in tube formation and branching defects within terminal cells. Most of the mutant cells showed a significant reduction in branching, as well as the multilumen phenotype. Moreover, the multilumen phenotype observed in *slik* mutant terminal cells is similar to the previously observed *moesin* knockdown phenotype (Jayan N. Nair, PhD thesis), indicating a possible link between the status of activated Moesin and the observed phenotypes. Since Slik has been shown to phosphorylate Moesin in other tissues (CARRENO *et al.* 2008; HIPFNER and COHEN 2003; HIPFNER *et al.* 2004; HUGHES *et al.* 2010), the similarity of the phenotypes between the loss of Moesin and Slik in the terminal cells, might be expected.

Further evidence for the regulation and activation of Moesin at the apical membrane in terminal branches comes from studies in our lab. Terminal cells of *bitesize* (*btsz*) mutants as well as RNAi larvae showed tube formation and branching defects (unpublished data, Jayan N. Nair, Appendix Fig.50). *btsz* was previously identified as one of the membrane anchors of Moesin at the apical membrane in the embryonic epithelium (PILOT *et al.* 2006). Additionally, mutant alleles of *talin, α-integrins and β -integrins* also showed multiple lumens in terminal branches (Fig.6)(LEVI *et al.* 2006). The talin-integrin complex positioned at the basal membrane acts as an anchor for terminal branches to connect to the underlying tissues. This positioning is thought to occur through the interaction of the actin cytoskeleton with the talin-integrin complex leading to stabilisation of the tube in terminal branches. Since activated Moesin, which localises at the apical membrane in terminal branches, is an anchor

for F-actin it could stabilise the actin cytoskeleton at the apical membrane and thereby regulate terminal branching and tube formation.

4.4 Kinase activity of Slik is essential for its function in terminal cells

We know from earlier work that Slik's kinase function is important for maintaining the epithelial integrity of wing imaginal discs (HIPFNER and COHEN 2003). Comparable terminal cell phenotypes in *slik* and *moesin* RNAi and the loss of p-Moesin enrichment at the apical membrane in *slik* mutants indicated that Slik's kinase activity is essential for its function in terminal cells. To confirm this aspect, I tested the effects of expression of Slik variants in terminal cells. Overexpression of wild type Slik did not result in any phenotypes in the tracheal system. Overexpression of the kinase dead form of Slik (Slik^{kd}) resulted in multilumen phenotype indicating that the kinase activity of Slik is indispensible in tracheal development. An explanation to this phenotype is that the Slik kinase dead construct acts as a dominant negative. The Slik^{kd} construct is a point mutation in the kinase subdomain of the protein and therefore the construct is likely to retain its kinase independent functions. This would allow other Slik interacting proteins to still associate with the kinase dead form. One such protein is Sip1 which is the *Drosophila* homologue of the mammalian *EBP50/NHERF1*. Sip1 is a scaffold protein which regulates several transmembrane receptors as well as downstream signal transduction activity. Sip1 functions as a scaffold for Slik at the apical membrane (HUGHES *et al.* 2010). Slik^{kd} could still interact with Sip1 and occupy postions at membrane and at the same time bind to Moesin. However, despite the interaction Slik^{kd} would be unable to phosphorylate Moesin and thus deplete pools of p-Moesin available to act as crosslinkers of F-actin to the apical membrane, leading to destabilised tubes and hence the multilumen phenotype.

On the other hand, expression of Slik^{kin} has shown to increase levels of p-Moesin and cause relocalisation of p-Moesin from the apical surface (HIPFNER *et al.* 2004). Slik^{kin} has intact kinase domain but lacks the remaining domains, therefore cannot interact with Sip1 leading to loss of apical localisation. Unanchored Slik (Slik^{kin}) perhaps activates Moesin at regions other than the apical membrane. Stabilisation of F-actin at random positions within the cells could lead to a disorganised cytoskeleton and thus the multilumen phenotype. This is

consistent with phenotype associated with overexpression of phosphomimetic form of Moesin in the tracheal system. Work from our lab showed that overexpression of Moesin^{TD556} (phosphomimetic form) in the trachea resulted in abnormal lumen phenotypes (Jayan N Nair, PhD thesis, Appendix Fig.52)

Further evidence to support the idea that *slik* stabilises the cytoskeleton through Moesin can be obtained from *slik^1* mutant animals. Dorsal trunks of *slik^1* mutant larvae have smaller lumen when compared with wild type dorsal trunks of similar sizes. Lumen formation is determined by several factors, one of them is the arrangement of F-actin core at luminal site (OSHIMA *et al.* 2006). Also lumen expansion requires rearrangement of the actin cytoskeleton. Actin rearrangement and stabilisation requires the function of crosslinkers such as Moesin to anchor to the membrane. Loss of Slik in the dorsal branches affect levels of activated Moesin and this could lead to defects in actin organisation resulting in failure of lumen expansion. The severity of the phenotype is perhaps attenuated by the presence of the maternally expressed Slik which allows development of the trachea in escapers. To exclude the maternal contribution of Slik, analysis of the trachea from germline clone of *slik^1* have to be performed.

To address the question if anchorage of Moesin to the membrane is a prerequisite to phosphorylation, further experiments have to be implemented. Mutations in two residues at the N-terminus of Moesin have been shown to inhibit binding to Phosphatidylinositol 4,5-bisphosphate (PtdIns(4,5)P$_2$) (ROCH *et al.* 2010). Experiments to rescue *slik* mutant phenotype with Moesin^{TD556} and Moesin^{TD556} with additional PtdIns(4,5)P$_2$ binding mutations should address the question .

4.5 FGF/RTK Breathless regulates Moesin in trachea

Results from RNAi experiments demonstrated that in addition to Slik, Btl also contributes to the phosphorylation of Moesin. Stainings to detect pan-Moesin and Slik in the *btl* RNAi terminal cells showed levels of these remained unchanged. Further, knockdown of downstream signalling component of the Btl/MAPK pathway *raf,* did not affect levels of p-Moesin in the terminal cells. These results imply that both Slik and Btl are equally important

for activation of Moesin. Further, my studies suggests that Btl mediated regulation of Moesin is at post-translational level and not at transcriptional level. p-Moesin staining in larvae of *egfr* knockdowns showed that distribution of p-Moesin was unaffected in the tracheal system (unpublished data Jayan N. Nair Appendix Fig.53). This confirmed that regulation of p-Moesin was specific to just one of the RTKs expressed in the tracheal system, namely *btl.*

It is clear from the results that activation of Moesin through phosphorylation at T^{556} in the tracheal system requires the function of both Btl and Slik. Btl mediated regulation of Moesin is a novel finding from this study. The contribution of Btl in the phosphorylation of Moesin may be either direct or indirect. The possibility that an RTK phosphorylates ERM protein is not unfounded. Substantial amount of evidence show that RTK phosphorylates ERM proteins directly or indirectly. First, Btl is a Receptor Tyrosine Kinases (RTK) with proven kinase activity (LEE *et al.* 1996). Direct phosphorylation of ERM proteins by RTK has been long established. Studies in mammalian systems have shown Ezrin the homologue of Moesin to the phosphorylated at N-terminal positions by EGFR (KRIEG and HUNTER 1992). Perhaps, Btl phosphorylates Moesin at N-terminal regions permitting subsequent phosphorylation by Slik at T^{556}. A second possibility is that Slik itself needs to be activated to perform its kinase function in the trachea, the prerequisite being activation by Btl. Finally, recent work in mammalian cell culture systems showed that Nik (Nck interacting kinase/ *Misshapen* (*Msn*) in *Drosophila*), a Sterile 20 kinase induced phosphorylation of ERM proteins in response to EGF stimulation. Also, Moesin was shown to physically interact with Nik via its N-terminus and also to be directly phosphorylated at amino acid residue T^{558} by the NIK domain (BAUMGARTNER *et al.* 2006). It is probable the relation between Btl and Slik is similar to that described above for EGFR and NIK. Moreover, previous work has not biochemically proven that Slik directly phosphorylates Moesin (HIPFNER and COHEN 2003; HIPFNER *et al.* 2004) therefore one cannot exclude the possibility that one of the two kinase (Slik or Btl) activates an unknown protein that would phosphorylate the later allowing activation of Moesin.

In order to determine how the two kinases Slik and Btl regulate and activate Moesin further studies are required. A kinase assay should reveal if Slik directly phosphorylates Moesin or whether it requires the coordinated action of Btl. It would also be interesting to know if Slik

is phosphorylated by Btl. Finally it would be important to look at p-Moesin level is an *msn* RNAi background to test if this also contributes to the activation of Moesin.

4.6 Possible function of Merlin in terminal cell development

In addition to the regulating Moesin through its kinase activity Slik also regulates Merlin function, hence it is imperative to investigate the function of Merlin in tracheal development. The role of Merlin in tracheal development is unexplored. The large amounts of cytoplasmic material seen in terminal cells of *Merlin* knockdown animals can be attributed to the loss of the tumour suppressor function of Merlin. Loss of Merlin in mice have been to show to result in uncontrolled growth of tissues leading to enormous sized organs (YI and KISSIL 2010). Another possible factor contributing to size of terminal cells is the sustained expression of signalling molecules. Experiments in wing discs have showed Merlin to localise to both membrane and cytoplasmic compartment of the cell. The functional form of Merlin, i.e. the non-phosphorylated form showed a clear enrichment in the cytoplasm and often colocalised to endocytic compartments. Merlin and Expanded have been shown to regulate steady-state levels of signalling receptors (EGFR, Notch, Smoothened, and Patched) as well as adhesion molecules (E-cad, Fat). Loss of these proteins can cause hyperactivation of associated signalling pathways. In addition, *Merlin;ex* double mutant cells show that the receptor levels are upregulated at the plasma membrane as a result of defect in receptor clearance. Consistent with this, knockdown of *Merlin* would result in the failure of receptor endocytosis. EGFR is an important factor in tracheal development and also upregulates E-cad to maintain epithelial integrity of the migrating tracheal tubes. EGFR also promotes invagination of the tracheal placode (LLIMARGAS and CASANOVA 1999) as well primary branching (WAPPNER *et al.* 1997). Perhaps sustained expression of some of these or other factors in the tracheal system results in the growth phenotype. Finally, as *Merlin* RNAi was not performed in combination with *expanded*, the activity of the functionally redundant protein/ interaction partner of Merlin cannot be disregarded unless a *Mer/ex* double knockdown is performed.

4.7 Does Slik modulate the MAPK pathway to regulate growth of terminal cells?

Previous studies have shown that Slik-Raf mediated signalling in wing disc is independent of the canonical MAPK signalling and also independent of Silk's kinase function. Slik-Raf interaction promotes cell proliferation and provides survival cues to cells of the wing disc epithelium (HIPFNER and COHEN 2003; HIPFNER *et al.* 2004). I wished to determine if the branching defect resulted from the loss of Moesin function or kinase independent Slik-Raf signalling events.

However, *raf* is also an integral component of the Btl/MAPK signalling which is indispensable for tracheal development. Btl/MAPK signalling positively regulates expression of Srf, the transcription factor absolutely essential for terminal cell development. To test the hypothesis that Slik-Raf interaction modulated the Btl/MAPK pathway in the tracheal system, growth of terminal cells in Btl/MAPK and *slik* RNAi were compared by evaluating the number of branches in the knockdown terminal cells. Knockdown of members of the Btl/MAPK pathway and *srf* resulted in branching phenotypes. The phenotypes resulting from the knockdowns were comparable to those of *slik* RNAi larvae, with all knockdowns resulting in a significant reduction in branches. The results suggest a possible input into the Btl/MAPK signalling pathway via the Slik-Raf interaction, but these results still do not exclude the possibility that the Slik-Raf interaction may contribute to terminal branch development via a yet unknown pathway.

To understand the dynamics of Slik-Raf interaction and its input into the Btl/MAPK signalling, further experiments are required. Since Slik and Raf interact genetically an epistatic experiment rescuing *slik* RNAi phenotype with Raf^{gof} should restore branching in terminal cells. An alternate assay would be to analyse if the phenotypes from Raf^{gof} is an attenuated by *slik* RNAi. A distinction between the Slik-Raf input into the Btl/MAPK and to the yet unknown pathway needs to be assessed through a few epistatic experiments such as rescue of *slik* branching phenotype by the expression of *rolled/erk,* or *srf.* Additionally,

immunostaining for dpERK in trachea of s*lik* knockdown larvae should reveal if *slik* contributes to Btl/MAPK signalling to promote terminal cell development.
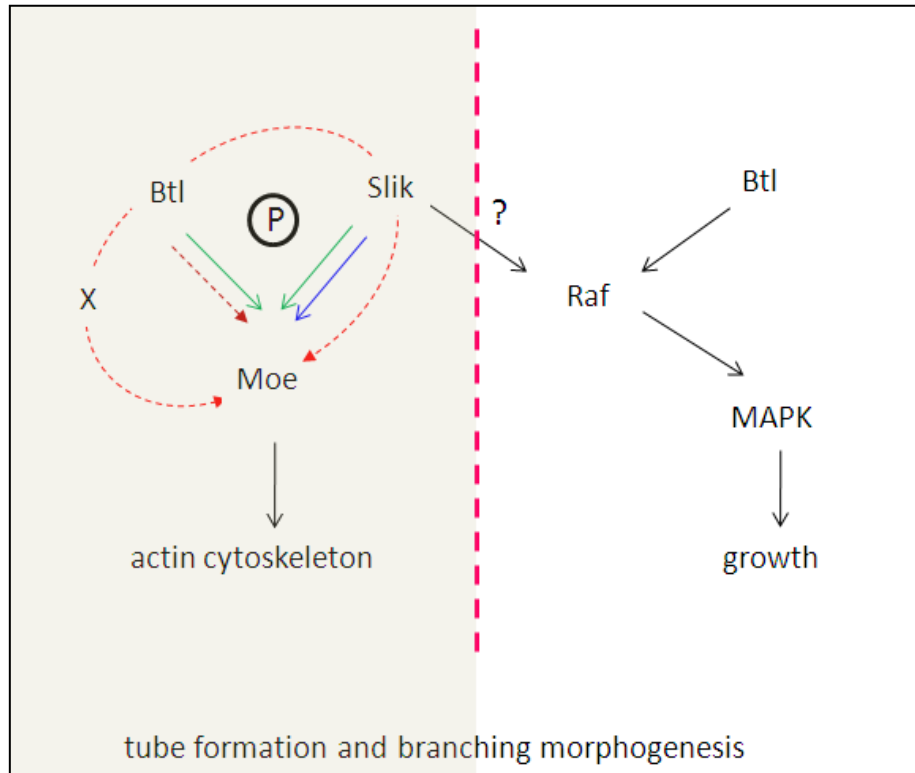
Figure 48: Schematic representation of the Silk's role in terminal cell development
Slik contributes to both tube and branch formation in terminal cells through two different pathways. Previous studies have showed that Slik regulates Moesin function by phosphorylation (P) (denoted by blue). This works shows that both Breathless and Slik phosphorylate Moesin to activate it (denoted by green arrows). Activation of Moesin stabilises F-actin and in turn positions the tube within the terminal branch. The exact mechanism of how Breathless phosphorylates Moesin is yet unknown and could be achieved through any of the three mechanisms indicated (a) direct, (b) through regulation of *slik* and (c) through an unknown factor (denoted by red arrows). Slik's input in to the Btl/MAPK signalling pathway is yet to be ascertained.

From results so far, I can conclude that Slik is essential for normal tracheal development and in particular for tube formation and branching in the terminal cells (Fig.48). Further, my work shows that Moesin is a crucial effector downstream of Slik. In addition to Slik-mediated regulation of Moesin, this works shows that Btl is also involved in Moesin regulation. The mechanism by which Btl mediates regulation of Moesin is yet to be elucidated. Finally, in addition to tube formation, Slik may contribute to the branch formation in terminal cells through providing signalling input in to the Btl/MAPK pathway through the Slik-Raf interaction.

5. REFERENCES

AFFOLTER, M. M., J. WALLDORF, U. GROPPE, J. KLOTER, U. LAROSA, M. GEHRING, W.J., 1994 The Drosophila SRF homolog is expressed in a subset of tracheal cells and maps within a genomic region required for tracheal development. Development **120:** 743-753.

BAER, M. M., A. BILSTEIN and M. LEPTIN, 2007 A clonal genetic screen for mutants causing defects in larval tracheal morphogenesis in Drosophila. Genetics **176:** 2279-2291.

BAUMGARTNER, M., A. L. SILLMAN, E. M. BLACKWOOD, J. SRIVASTAVA, N. MADSON *et al.*, 2006 The Nck-interacting kinase phosphorylates ERM proteins for formation of lamellipodium by growth factors. Proc Natl Acad Sci U S A **103:** 13391-13396.

BEITEL, G. J., and M. A. KRASNOW, 2000 Genetic control of epithelial tube size in the Drosophila tracheal system. Development **127:** 3271-3282.

BRETSCHER, A., K. EDWARDS and R. G. FEHON, 2002 ERM proteins and merlin: integrators at the cell cortex. Nat Rev Mol Cell Biol **3:** 586-599.

CARRENO, S., I. KOURANTI, E. S. GLUSMAN, M. T. FULLER, A. ECHARD *et al.*, 2008 Moesin and its activating kinase Slik are required for cortical stability and microtubule organization in mitotic cells. J Cell Biol **180:** 739-746.

CASANOVA, J., 2007 The emergence of shape: notions from the study of the Drosophila tracheal system. EMBO Rep **8:** 335-339.

CELA, C., and M. LLIMARGAS, 2006 Egfr is essential for maintaining epithelial integrity during tracheal remodelling in Drosophila. Development **133:** 3115-3125.

FOLKMAN, J., and C. HAUDENSCHILD, 1980 Angiogenesis in vitro. Nature **288:** 551-556.

GERVAIS, L., and J. CASANOVA, 2010 In Vivo Coupling of Cell Elongation and Lumen Formation in a Single Cell. Current Biology **20:** 359-366.

GHABRIAL, A., S. LUSCHNIG, M. M. METZSTEIN and M. A. KRASNOW, 2003 Branching morphogenesis of the Drosophila tracheal system. Annu Rev Cell Dev Biol **19:** 623-647.

GLAZER, L., and B. Z. SHILO, 1991 The Drosophila FGF-R homolog is expressed in the embryonic tracheal system and appears to be required for directed tracheal cell extension. Genes Dev **5:** 697-705.

GUILLEMIN, K., J. GROPPE, K. DUCKER, R. TREISMAN, E. HAFEN *et al.*, 1996 The pruned gene encodes the Drosophila serum response factor and regulates cytoplasmic outgrowth during terminal branching of the tracheal system. Development **122:** 1353-1362.

HIPFNER, D. R., and S. M. COHEN, 2003 The Drosophila sterile-20 kinase slik controls cell proliferation and apoptosis during imaginal disc development. PLoS Biol **1:** E35.

HIPFNER, D. R., N. KELLER and S. M. COHEN, 2004 Slik Sterile-20 kinase regulates Moesin activity to promote epithelial integrity during tissue growth. Genes Dev **18:** 2243-2248.

HIPFNER, D. R., K. WEIGMANN and S. M. COHEN, 2002 The bantam gene regulates Drosophila growth. Genetics **161:** 1527-1537.

HUGHES, S. C., and R. G. FEHON, 2006 Phosphorylation and activity of the tumor suppressor Merlin and the ERM protein Moesin are coordinately regulated by the Slik kinase. J Cell Biol **175:** 305-313.

HUGHES, S. C., E. FORMSTECHER and R. G. FEHON, 2010 Sip1, the Drosophila orthologue of EBP50/NHERF1, functions with the sterile 20 family kinase Slik to regulate Moesin activity. J Cell Sci **123:** 1099-1107.

JANKOVICS, F., R. SINKA, T. LUKACSOVICH and M. ERDELYI, 2002 MOESIN crosslinks actin and cell membrane in Drosophila oocytes and is required for OSKAR anchoring. Curr Biol **12:** 2060-2065.

JARECKI, J., E. JOHNSON and M. A. KRASNOW, 1999 Oxygen Regulation of Airway Branching in Drosophila Is Mediated by Branchless FGF. Cell **99:** 211-220.

KARAGIOSIS, S. A., and D. F. READY, 2004 Moesin contributes an essential structural role in Drosophila photoreceptor morphogenesis. Development **131:** 725-732.

KEISTER, M. L., 1948 The morphogenesis of the tracheal system of Sciara. Journal of Morphology **83:** 373-423.

KLÄMBT, C., L. GLAZER and B. Z. SHILO, 1992 breathless, a Drosophila FGF receptor homolog, is essential for migration of tracheal and specific midline glial cells. Genes & Development **6:** 1668-1678.

KRIEG, J., and T. HUNTER, 1992 Identification of the two major epidermal growth factor-induced tyrosine phosphorylation sites in the microvillar core protein ezrin. Journal of Biological Chemistry **267:** 19258-19265.

KUNDA, P., A. E. PELLING, T. LIU and B. BAUM, 2008 Moesin controls cortical rigidity, cell rounding, and spindle morphogenesis during mitosis. Curr Biol **18:** 91-101.

LAVISTA-LLANOS, S., L. CENTANIN, M. IRISARRI, D. M. RUSSO, J. M. GLEADLE *et al.*, 2002 Control of the Hypoxic Response in Drosophila melanogaster by the Basic Helix-Loop-Helix PAS Protein Similar. Mol. Cell. Biol. **22:** 6842-6853.

LEE, T., N. HACOHEN, M. KRASNOW and D. J. MONTELL, 1996 Regulated Breathless receptor tyrosine kinase activity required to pattern cell migration and branching in the Drosophila tracheal system. Genes Dev **10:** 2912-2921.

LEVI, B. P., A. S. GHABRIAL and M. A. KRASNOW, 2006 Drosophila talin and integrin genes are required for maintenance of tracheal terminal branches and luminal organization. Development **133:** 2383-2393.

LLIMARGAS, M., and J. CASANOVA, 1999 EGF signalling regulates cell invagination as well as cell migration during formation of tracheal system in <i>Drosophila</i>. Development Genes and Evolution **209:** 174-179.

LUBARSKY, B., and M. A. KRASNOW, 2003 Tube morphogenesis: making and shaping biological tubes. Cell **112:** 19-28.

MAITRA, S., R. M. KULIKAUSKAS, H. GAVILAN and R. G. FEHON, 2006 The tumor suppressors Merlin and Expanded function cooperatively to modulate receptor endocytosis and signaling. Curr Biol **16:** 702-709.

MANNING, G. K., M.A., 1993 *Development of the Drosophila tracheal system*. Cold Spring Harbor Press (Cold Spring Harbor, New York)

MARAIS, R., J. WYNNE and R. TREISMAN, 1993 The SRF accessory protein Elk-1 contains a growth factor-regulated transcriptional activation domain. Cell **73:** 381-393.

MCCARTNEY, B. M., and R. G. FEHON, 1996 Distinct cellular and subcellular patterns of expression imply distinct functions for the Drosophila homologues of moesin and the neurofibromatosis 2 tumor suppressor, merlin. J Cell Biol **133:** 843-852.

MCCARTNEY, B. M., R. M. KULIKAUSKAS, D. R. LAJEUNESSE and R. G. FEHON, 2000 The neurofibromatosis-2 homologue, Merlin, and the tumor suppressor expanded function together in Drosophila to regulate cell proliferation and differentiation. Development **127:** 1315-1324.

MEDINA, E., J. WILLIAMS, E. KLIPFELL, D. ZARNESCU, G. THOMAS *et al.*, 2002 Crumbs interacts with moesin and beta(Heavy)-spectrin in the apical membrane skeleton of Drosophila. J Cell Biol **158:** 941-951.

METZGER, R. J. A. K., M. A., 1999 Genetic control of branching morphogenesis. Science **284:** 1635-1639.

NAKAMURA, F., L. HUANG, K. PESTONJAMASP, E. J. LUNA and H. FURTHMAYR, 1999 Regulation of F-Actin Binding to Platelet Moesin In Vitro by Both Phosphorylation of Threonine 558 and Polyphosphatidylinositides. Mol. Biol. Cell **10:** 2669-2685.

OSHIMA, K., M. TAKEDA, E. KURANAGA, R. UEDA, T. AIGAKI *et al.*, 2006 IKK[var epsilon] Regulates F Actin Assembly and Interacts with Drosophila IAP1 in Cellular Morphogenesis. Current Biology **16:** 1531-1537.

PILOT, F., J. M. PHILIPPE, C. LEMMERS and T. LECUIT, 2006 Spatial control of actin organization at adherens junctions by a synaptotagmin-like protein Btsz. Nature **442:** 580-584.

POLESELLO, C., I. DELON, P. VALENTI, P. FERRER and F. PAYRE, 2002 Dmoesin controls actin-based cell shape and polarity during Drosophila melanogaster oogenesis. Nat Cell Biol **4:** 782-789.

REICHMAN-FRIED, M., B. DICKSON, E. HAFEN and B. Z. SHILO, 1994 Elucidation of the role of breathless, a Drosophila FGF receptor homolog, in tracheal cell migration. Genes & Development **8:** 428-439.

REICHMAN-FRIED, M., and B.-Z. SHILO, 1995 Breathless, a Drosophila FGF receptor homolog, is required for the onset of tracheal cell migration and tracheole formation. Mechanisms of Development **52:** 265-273.

ROCH, F., C. POLESELLO, C. ROUBINET, M. MARTIN, C. ROY *et al.*, 2010 Differential roles of PtdIns(4,5)P2 and phosphorylation in moesin activation during Drosophila development. J Cell Sci **123:** 2058-2067.

ROULEAU, G. A., P. MEREL, M. LUTCHMAN, M. SANSON, J. ZUCMAN *et al.*, 1993 Alteration in a new gene encoding a putative membrane-organizing protein causes neuro-fibromatosis type 2. Nature **363:** 515-521.

SABOURIN, L. A., K. TAMAI, P. SEALE, J. WAGNER and M. A. RUDNICKI, 2000 Caspase 3 cleavage of the Ste20-related kinase SLK releases and activates an apoptosis-inducing kinase domain and an actin-disassembling region. Mol Cell Biol **20:** 684-696.

SAMAKOVLIS, C., N. HACOHEN, G. MANNING, D. C. SUTHERLAND, K. GUILLEMIN *et al.*, 1996 Development of the Drosophila tracheal system occurs by a series of morphologically distinct but genetically coupled branching events. Development **122:** 1395-1407.

SATO, M. A. K., T. B., 2002 FGF is an essential mitogen and chemoattractant for the air sacs of the Drosophila tracheal system. . Dev Cell 195-207.

SHAFIQ, S. A., 1963 Electron Microscopy of the Development of Tracheoles in Drosophila Melanogaster. Quarterly Journal of Microscopical Science **s3-104:** 135-140.

SKAER, H., 1997 Morphogenesis: FGF branches out. Curr Biol**:** 238-241.

SPECK, O., S. C. HUGHES, N. K. NOREN, R. M. KULIKAUSKAS and R. G. FEHON, 2003 Moesin functions antagonistically to the Rho pathway to maintain epithelial integrity. Nature **421:** 83-87.

SUTHERLAND, D., C. SAMAKOVLIS and M. A. KRASNOW, 1996 branchless Encodes a Drosophila FGF Homolog That Controls Tracheal Cell Migration and the Pattern of Branching. **87:** 1091-1101.

TREISMAN, R., 1994 Ternary complex factors: growth factor regulated transcriptional activators. Current Opinion in Genetics & Development **4:** 96-101.

UV, A., R. CANTERA and C. SAMAKOVLIS, 2003 Drosophila tracheal morphogenesis: intricate cellular solutions to basic plumbing problems. Trends in Cell Biology **13:** 301-309.

VINCENT, S., R. WILSON, C. COELHO, M. AFFOLTER and M. LEPTIN, 1998 The Drosophila protein Dof is specifically required for FGF signaling. Mol Cell **2:** 515-525.

WAPPNER, P., L. GABAY and B. Z. SHILO, 1997 Interactions between the EGF receptor and DPP pathways establish distinct cell fates in the tracheal placodes. Development **124:** 4707-4716.

WIGGLESWORTH, V. B., 1954 Growth and Regeneration in the Tracheal System of an Insect, Rhodnius prolixus(Hemiptera). Quarterly Journal of Microscopical Science **s3-95:** 115-137.

YI, C., and J. L. KISSIL, 2010 Merlin in organ size control and tumorigenesis: Hippo versus EGFR? Genes Dev **24:** 1673-1679.

6. APPENDIX

6.1 Terminal cell counts from tracheal segments tr3-5 from wild type and *slik* RNAi larvae

	wt	*slik*
L1	32	32
L2	25	29
L3	29	34
L4	31	34
L5	29	27
Avg.	29.2	31
St.dev	2.68	3.082

Figure 50: Terminal cell counts from wild type and *slik* RNAi

L1-10 represents five different animals from which terminal cells were counted. Terminal cells were counted from the tracheal segments tr3-tr5 in both wild type and *slik* RNAi larvae. The average and standard deviation of both the data sets are shown in red

6.2 Knockdown of *btsz* leads to lumen formation and branching defects in terminal cells
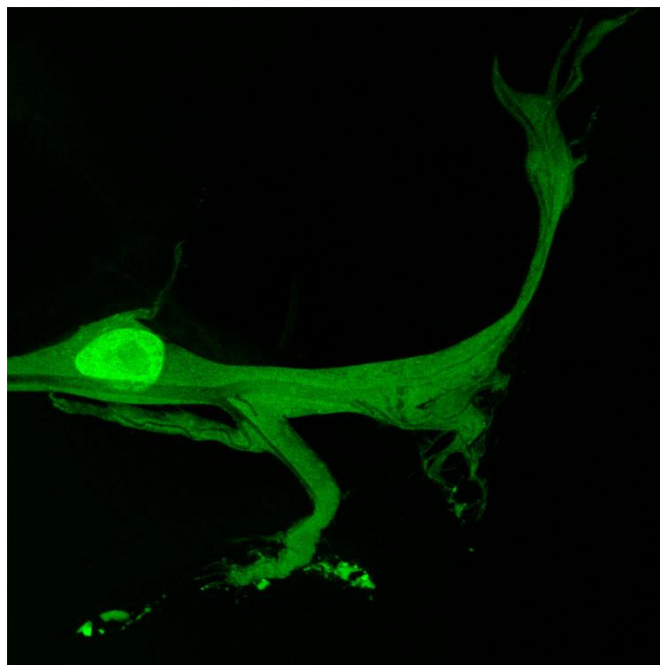

Figure 51: *btsz* knockdown in terminal cell affect branching
Terminal cells from *btsz* RNAi larva al cell were visualised by the tracheal specific expression of cytoplasmic GFP using *btl*Gal4. Depletion of *btl* severely affects growth of terminal branches. Scale - 25µm

6.3 Branch counts from various knockdowns in the tracheal system

	wt	*slik*	*btl*	*Ras*	*raf*	*srf*	*egfr*
TC1	20	3	1	10	10	4	10
TC2	16	6	1	7	8	3	17
TC3	17	1	1	1	3	3	12
TC4	17	2	1	1	3	2	11
TC5	18	6	1	1	3	2	11
TC6	21	2	2	3	7	1	13
TC7	23	15	1	8	8	2	14
TC8	16	6	1	4	4	1	10
TC9	17	13	1	5	7	5	13
TC10	14	9	1	3	6	4	12
avg.	17.9	6.3	1.1	4.3	5.9	2.7	12.3
st.dv	2.685351	4.762	0.316228	3.16403	2.514403	1.33749	2.110819

Fig 52: Branch counts in terminal cells upon RNAi of *slik, btl, Ras, raf, srf, egr*

TC 1-10 represents 10 differenct terminal cells from which measurement was taken. The average and standard deviation of dboth the data sets are shown in red

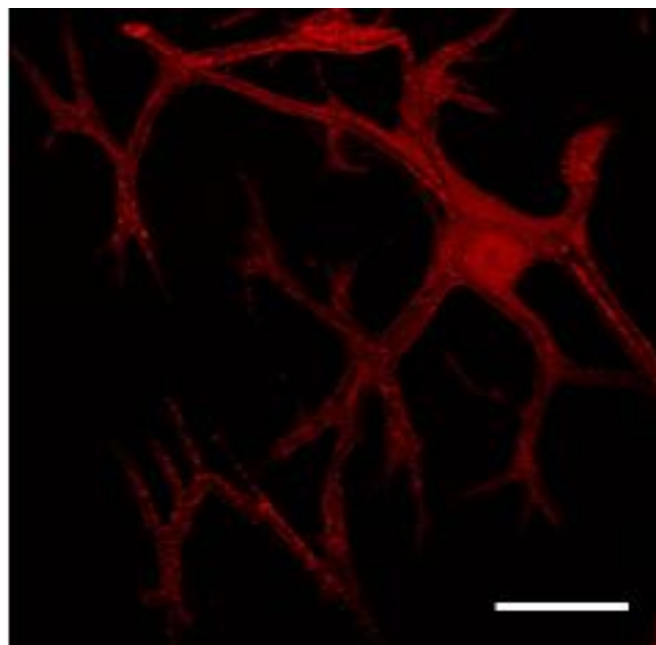## 6.4 Overexpression of phosphomimetic form of Moesin in the tracheal system

Figure 53: Overexpression of MoeTD[559] (phosphomimetic form) in the terminal cells affect branching
Terminal cells were visualised by the tracheal specific expression of DS-Red along with the MoeTD[559] using *btl*Gal4. Depletion of *btl* severely affects growth of terminal branches and tube formation within the branches. Scale - 25µm

6.5 Knockdown of *egfr* does not affect p-Moesin localisation in terminal cells
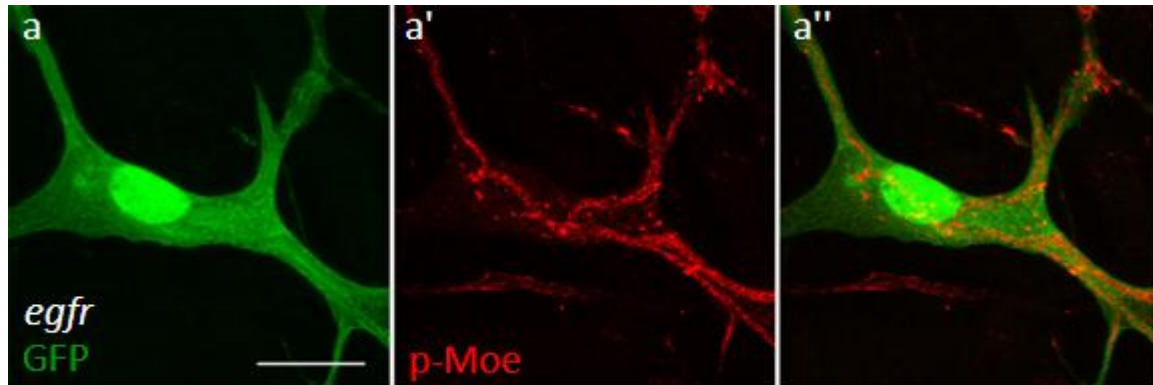

Figure 54: Effect of *egfr* knockdown on p-Moesin localisation in the terminal cell
Terminal cell from a *egfr* knockdown third instar larva **(a-a'')**. **(a)** Terminal cell is visualised by tracheal specific cytoplasmic GFP (green) and **(a')** p-Moesin (red). p-Moesin expression is undisturbed upon *egfr* knockdown. p-Moesin expressed in surrounding tissues is also detected. Scale - 25µm (Unpublished data, Jayan N.Nair)

6.6 Localisation of F-actin in developing embryonic tracheal system
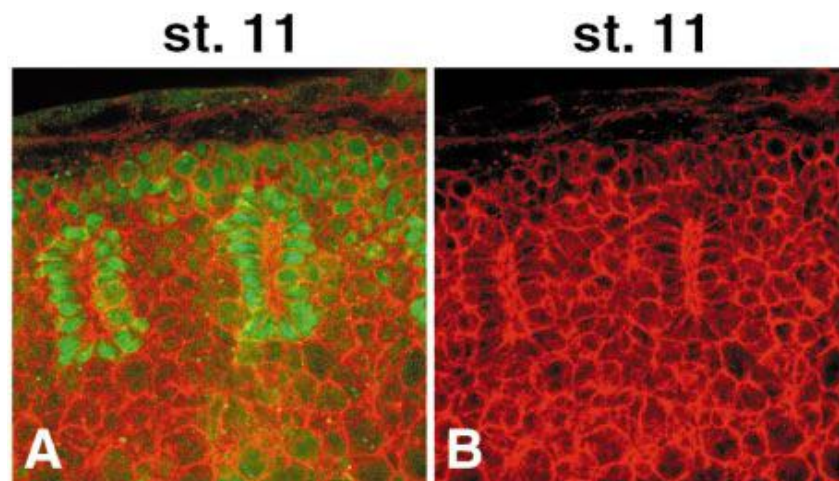
Figure 55: F-actin distribution in tracheal placodes of wild type stage 11 embryos
Single confocal sections of embryos stained with anti-Vvl to visualise the tracheal cells (*green*) and incubated with phalloidin-Texas red to visualise actin distribution (*red*). Each image shows two metameres; anterior is to the *left* and dorsal is *up*. First panel shows a merged image of actin distribution and anti-Vvl to visualise the tracheal cells; the single image of the actin distribution is also shown in the next panel. **A, B** In wildtype embryos actin accumulates in the centre of the tracheal pit, outlining the point of invagination. (LLIMARGAS and CASANOVA 1999)

ABBREVIATIONS

bp   base pairs

BSA   Bovine Serum Albumen

btl   *breathless*

btsz   *bitesize*

dNTP   deoxy nucleotide tri phosphate

dof   *Downstream of FGF*

egfr   *Epidermal growth factor receptor*

ERM   Ezrin-Radixin-Moesin

ERK   Extracellular-signal-Regulated Kinase (MAPK)

FGF   Fibroblast growth factor

FLP   yeast Flp recombinase

FRT   Flp recombinase target site

GFP   Green fluorescent protein

if   *inflated*

Kb   Kilo base

M   mol per litre

m   milli

MAPK   Mitogen Activated Protein Kinase

MEK   Mitogen-activated protein kinase/extracellular signal-regulated kinase kinase

Mer   *Merlin*

mew	*multiple edematous wings*
moe	*moesin*
mys	*myospheroid*
µ	Micro
ng	Nanogram
PCR	Polymerase Chain Reaction
RTK	Receptor Tyrosine Kinase
slik	*SLK and LOK like kinase*
srf	*Serum response factor*
UAS	Upstream activating sequence
VDRC	Vienna Drosophila Research Center

ABSTRACT

The *Drosophila* Sterile20 like kinase Slik is involved in maintaining epithelial integrity and promotes tissue growth during development. It regulates activity of members of the band 4.1/Ezrin/Radixin/Moesin (ERM) superfamily proteins through phosphorylation. Apart from its kinase activity, Slik also interacts with Raf to promote cell survival and growth. Raf is an important downstream effector of the Bnl/Btl RTK pathway crucial for tracheal development. An immediate target of the RTK-MAPK signalling is SRF (serum response factor), a transcription factor known to be indispensible for terminal cell development. Here, I show that Slik contributes to tracheal terminal cell development through both its kinase-dependent and independent functions. Both Slik and activated Moesin (p-Moesin) are enriched at the apical membrane in terminal cells. *slik* mutant or knockdown terminal cells show branching defects and destabilised tubes similar to the phenotype of *moesin* mutants, suggesting that *slik* is an essential factor in terminal cell growth and development. This is further supported by the effect of expressing a kinase-dead form of *slik,* which causes a multilumen phenotype similar as the one seen in *slik* mutant cells. In addition, *slik* depletion results in the loss of p-Moesin at the apical membrane in the terminal cells indicating that Slik through its kinase dependent function towards Moesin regulates tracheal terminal cell development. This study also reports a novel regulator of Moesin; I have identified Btl as an important factor that post-translationally regulates the phosphorylation of Moesin.

Apart from the luminal defects, *slik* depletion also resulted in reduced branching of terminal cells. The same phenotype is observed upon knockdown of *raf.* As Raf is thought not be a kinase substrate of Slik but rather a binding partner, the results suggest an additional, kinase independent function of Slik in tracheal development. The disruption of the downstream target of the Bnl/Btl signalling pathway *srf*, the signalling transducer *Ras*, or the receptor *btl* itself also resulted in similar branching defects. We propose that *slik* acts in the development of terminal cells through activation of Moesin at the apical membrane and a possible regulation of the Bnl/Btl RTK pathway through its interaction with Raf.

ZUSAMMENFASSUNG

Die *Drosophila* Sterile 20 like kinase Slik ist sowohl am Erhalt der epithelialen Integrität als auch an der Förderung des Gewebewachstums während der Entwicklung beteiligt. Sie reguliert die Aktivität von Proteinen der Band 4.1/Ezrin/Radixin/Moesin (ERM) Proteinfamilie durch Phosphorylierung. Zusätzlich zur Kinaseaktivität interagiert Slik mit Raf und wirkt dadurch positiv auf die Überlebensrate und das Wachstum von Zellen ein. Raf ist ein wichtiger Faktor im Bnl/Btl RTK Signaltransduktionsweg, der unverzichtbar für die Tracheenentwicklung ist. Ein direktes Zielgen des RTK-MAPK Signalwegs ist *srf* (serum response factor), ein Transkriptionsfaktor der für die Entwicklung der Terminalzellen unentbehrlich ist. In der vorliegenden Arbeit zeige ich, dass Slik auf zwei unterschiedlichen Wegen zur Tracheenentwicklung beiträgt; durch eine Kinase-abhängige als auch eine Kinase-unabhängige Funktion. Sowohl Slik als auch aktiviertes Moesin (p-Moesin) liegen an der apikalen Membran der Terminalzelle angereichert vor. Terminalzellen, in denen die Funktion von *slik* entweder durch eine Mutation oder durch einen RNAi induzierten Knockdown gestört ist, zeigen Defekte in der Verästelung sowie eine Destabilisierung der intrazellulären Röhre. Dieser Phänotyp gleicht dem von *moesin* Mutanten und indiziert eine essentielle Funktion von *slik* im Wachstum und der Entwicklung der Terminalzellen. Der Effekt der Überexpression einer Kinase-defizienten Form von Slik unterstützt diese Annahme: es wird ein Multilumen-Phänotyp beobachtet, wie er auch in *slik* mutanten Zellen zu finden ist. Desweiteren resultiert die Reduktion von Slik in einem Verlust von p-Moesin an der apikalen Membran in Terminalzellen. Dies deutet darauf hin, dass Slik durch seine Kinase-Aktivität gegenüber Moesin die Entwicklung der trachealen Terminalzellen reguliert. In dieser Studie konnte ich überdies einen neuen Regulator von Moesin nachweisen: es zeigte sich, dass Btl die post-translationelle Phosphorylierung von Moesin reguliert.

Zusätzlich zu den luminalen Defekten resultierte die Reduktion von Slik auch in einer geringeren Verästelung der Terminalzellen. Der Knockdown von Raf erzeugt denselben Phänotyp. Da Raf kein direktes Substrat der Slik Kinase zu sein scheint, sondern ein Interaktionspartner, legen diese Ergebnisse eine zweite, Kinase-unabhängige Funktion von

Slik in der Tracheenentwicklung nahe. Die Unterbrechung des Bnl/Btl Signaltransduktionsweges durch Knockdown des Zielgens *srf*, des Signalmoleküls *ras* oder des Rezeptors *btl* resultierte in ähnlichen Verästelungsdefekten. Zusammenfassend postulieren wir folgendes Modell: Slik reguliert die Entwicklung der Terminalzellen durch die Aktivierung von Moesin an der apikalen Membran und beeinflusst den Bnl/Btl RTK Signaltransduktionsweg über die direkte Interaktion mit Raf.

EIDESSTATTLICHE ERKLÄRUNG

Ich versichere, daß ich die von mir vorgelegte Dissertation selbständig angefertigt, die benutzten Quellen und Hilfsmittel vollständig angegeben und die Stellen der Arbeit - einschließlich Tabellen, Karten und Abbildungen -, die anderen Werken im Wortlaut oder dem Sinn nach entnommen sind, in jedem Einzelfall als Entlehnung kenntlich gemacht habe; daß diese Dissertation noch keiner anderen Fakultät oder Universität zur Prüfung vorgelegen hat; daß sie - abgesehen von unten angegebenen Teilpublikationen - noch nicht veröffentlicht worden ist sowie, daß ich eine solche Veröffentlichung vor Abschluß des Promotionsverfahrens nicht vornehmen werde. Die Bestimmungen dieser Promotionsordnung sind mir bekannt. Die von mir vorgelegte Dissertation ist von Prof. Dr. Maria Leptin betreut worden.

Keine Teilpublikationen

Köln,

Februar 2011   **Fiona Paul Ukken**

LEBENSLAUF

Name: Fiona Paul Ukken

Geburtsdatum: 04.06.1982

Geburtsort: Cochin, Indien

Staatsangehörigkeit: Indisch

1998-2000   Gymnasium,St.John's English School and Junior College, Chennai,
                                      Indien

2000-2003   Bachelor of Science (B.Sc), University of Madras, Chennai, Indien

2003-2005   Master of Science (M.Sc), University of Madras, Chennai, Indien

2005-2006   Project assistant
                                      Centre for DNA Fingerprinting and Diagnostics, Hyderabad, Indien

2006-2010   Doktorarbeit bei Prof. Dr. Maria Leptin am
                                      Institut fuer Genetik, Universitaet zu Koeln und
                                      am EMBl, Heidelberg
                                      Titel: "Functional characterisation of the Sterile 20 like kinase Slik in
                                      tracheal morphogenesis in *Drosophila melanogaster*"

Köln
Februar 2011   Unterschrift